WHAT IS INTERESTING ABOUT THE REGION OF SMALL MOMENTUM TRANSFERS AT HIGH ENERGIES?

Ya.I. Azimov, E.M. Levin, M.G. Ryskin, V.A. Khoze

Translated by kind permission of the editor, from the Proceedings of the 9th Winter School of the Leningrad Nuclear Physics Institute on Nuclear and Elementary Particle Physics, 15-26 Feb. 1974. Leningrad, Akademiya Nauk SSSR, 1974, pp. 5-161.

Translated at CERN by B. Hodge
(Original: Russian)
Not revised by the Translation Service

(CERN Trans. 74-8)

Geneva

December 1974

WHAT IS INTERESTING ABOUT THE REGION OF SMALL MOMENTUM TRANSFERS AT HIGH ENERGIES?

Ya.I. Azimov, E.M. Levin, M.G. Ryskin, V.A. Khoze*)

---

*) V.N. Gribov participated actively in the discussions of all fundamental questions discussed in this paper.

WHAT IS INTERESTING ABOUT THE REGION OF SMALL MOMENTUM TRANSFERS AT HIGH ENERGIES?

By Ya. I. Azimov, E. M. Levin, M. G. Ryskin and V. A. Khoze *

A B S T R A C T

In these papers, an attempt is made to make a complete review of those experiments at small momentum transfers and high energies ($E_{lab.}$ = 50-1000 GeV), the setting up of which would enable answers to be given to the most interesting questions posed by the modern theory of hadron scattering at high energies. The basis of these is as follows : is it not possible at the achievable energies to ~~discover~~ determine the characteristic consequences for the hadron scattering processes resulting from the ~~fact~~ hypothesis of constant cross-sections ~~for an~~ at asymptotic energy? Specifically, this means: the disappearance of quasi-elastic processes at zero momentum transfers, the vanishing of all vertices of vacuum Reggeon emission and of particle emission from a vacuum Reggeon, if crossed by a zero momentum. The papers examine precisely the behaviour of the cross-sections of the various reactions to which the above-mentioned features of asymptotic scattering lead, at real energies. Inspite of the fact that such examinations are of a particularly

---

*V. N. Gribov participated actively in the discussions of all fundamental questions discussed in this paper.

estimatory nature, the authors consider that as a result of difficult, but in principle feasible experiments at small t and in a wide energy range, the asymptotic theory may be verified.

Furthermore, the papers examine in detail questions of a more specific interest, such as the behaviour of $\rho = \frac{\mathrm{Re}A}{\mathrm{Im}A}$ for high energies, the kink in the slope of the diffraction cone at $t \approx -0.1\ (\mathrm{GeV}/c)^2$, hadron scattering on a deuteron target etc.

The first part of the papers may be considered as an attempt to enumerate the fundamental qualitative results of the theory of complex angular momenta, which are necessary for an understanding of the whole of this series of papers.

I. INTRODUCTION

Basically, this series of papers is devoted to a review of those experiments at small momentum transfers and high energies (>50 GeV), the setting up of which would enable the following question to be answered: are the present-day concepts on hadron interactions at high energies reasonable or unreasonable? In discussing the possibility of one type of measurement or another, we were guided towards the set-up used in the LNPI [1] for those questions relating to accuracy, the range of accessible momentum transfers etc. First of all let us dwell on a theoretical description of hadron interaction at high energies. The only consistent

theoretical foundation for studying strong interactions at high energy as a whole (and not individual reactions) is now the theory of complex angular momenta and the parton (multi-peripheral) picture of interactions which is closely related with it. Unfortunately, the theory of complex momenta was not discussed in detail at the winter schools at LNPI (an intelligible exposition of the fundamental arguments and results of this theory is given in [2]), but the space-time picture of interaction, occurring in the parton (multiperipheral) model, has been examined on several occasions at these schools [3] (and in particular detail at the last of these [4,5]). Here we shall not discuss in detail the theory of complex angular momenta but shall rather enumerate the fundamental consequences of it which must be known in order to understand these papers, and we shall also dwell on the basic experimental data which confirm it.

REGGEONS

I. Dependence of scattering amplitude on energy. In the theory of complex angular momenta a fundamental contribution to the amplitude of hadron interaction at high energies is the exchange of a particle or group of particles with a variable spin $\alpha(t)$ ($t = (P_a - P_{a'})^2$ - momentum transfer, see Fig. 1.1a). Such a particle (group of particles) is referred to as a Regge pole or Reggeon. Reggeon exchange leads to an ~~exponential~~ power-law dependence of amplitude on energy $S^{\alpha(t)}$ ($S = (P_a + P_b)^2$, see Fig. 1.1a) and corresponds to a definite feature (related to the pole) of the partial amplitudes ($f_j(t)$) of the t-

channel angular momentum (j) (i.e. $f_j(t) = \frac{z}{j - \alpha(t)}$). The link between the asymptotic form of $S^{\alpha(t)}$ with the spin of a particle participating in the exchange is shown in Fig. 1.1b, where the amplitudes are given for the exchange of vector and scalar particles. In this case a contribution is given by the t-channel partial amplitudes $f_1(t)$ and $f_0(t)$, respectively. Comparing drawings 1.1a and 1.1b, we see that Reggeon exchange may in fact be looked on as an exchange of a particle with a spin $\alpha(t)$. $\alpha(t)$ is referred to as the trajectory of the Reggeon.

2. Link between a Reggeon and particles with high spins. This link is established by the fact that for $t > 0$, when $\sqrt{t}$ is the energy and the process must be regarded as shown in Fig. 1.1c, the real part of the trajectory $\alpha(t)$ ($Re\,\alpha(t)$) equals integer values ~~changes into a whole number~~ $(n)(Re\alpha(t_n) = n)$ for values of $t = t_n$, corresponding to the masses ($t_n = M^2$) of resonances with a spin $n\,(j = n)$. The width of the resonances is expressed by $Im\,\alpha(t_n)$, namely : $M\Gamma = \frac{Im\alpha(t_n)}{\alpha'}$, where $Re\alpha(t) \approx \alpha(t_n) + \alpha'(t - t_n)$. It is recalled that the contribution of resonance to the reaction is written in the usual form :

$$B(s,t) = -\frac{\pi\sqrt{s}}{\rho}(2j+1)\frac{M\Gamma^{el}}{s - M^2 + iM\Gamma}P_j(z),$$

where M, j, Γ and Γ^{el} are equal to the, # mass, spin total and elastic width of the resonance, $P_j(z)$ = a Legendre polynomial, z = the cosine of the scattering angle, ρ = the momentum in the cms system. In this way, once the resonance spectrum is known, it is possible to establish a picture of the dependence of $\alpha(t)$ on t . The

surprising thing is that all known resonances lie on linear trajectories, which have the form $\alpha(t)=\alpha(0)+\alpha' t$ (see drawing 1.2). This fact enables us to predict the energy dependence of the amplitude of the interaction of two particles at high energy, which is determined by the same d (t) (see Fig. 1.1a).

3. Space - time picture of interaction. The basic idea of the parton model /4,6/ is that a fast hadron (moving with a momentum of p) may be regarded as consisting of a large number ($\sim \ln p$) of point particles (partons) which can be described in the usual quantum-mechanical manner by means of a wave function. But in what manner does the interaction with the target take place in this model? As the interaction cross-section of point particles is not greater than $\pi \lambda^2 \sim 1/s_{12}$, where s_{12} is the pair energy of two particles (1 and 2 in Fig. 1.3a), it will only be the slow partons which will interact with the target at rest, as is shown in Fig. 1.3a. The process of elastic scattering expressed in this way will be that when a slow parton interacts with the target it is scattered at a very small angle. In this case there will be a probability (not small for small momentum transfers) that the partons will collect in a hadron similar to the initial one (elastic scattering), or in a hadron with other quantum numbers (quasi-elastic scattering) see Fig. 1.3b). It is natural that the probability of such collection will rapidly fall as the momentum transfer increases, roughly in accordance with $e^{-R^2(t)}$ R = radius of the parton (hadron) system, i.e. substantial distances in a plane perpendicular to the direction of the flight of a particle

a, on which slow partons may be found. As was explained in detail in /4/, these distances are $\sim\sqrt{\alpha' \ln S}$. In this way the amplitude of elastic scattering will be $\sim e^{-R^2(t)} = e^{-\alpha' \ln S(t)} = S^{\alpha' t}$. In other words, the basic contribution to the cross-section in this picture will be given by the processes of the multiperipheral type, which differ kinematically from the others in that the relative energies of any two neighbouring particles (i and $i+1$ in Fig. 1.3c) or otherwise their square of the mass $S_{i,i+1} = M^2_{i,i+1} = (q_i + q_{i+1})^2$, are limited and do not increase with a rise in the total energy of the colliding particles. Finally, in accordance with the optical theorem $S\sigma = \mathrm{Im}\, A$, where A is the amplitude of elastic scattering, and, consequently the equality shown in Fig. 1.3c must be satisfied; later, we shall use this to a very great extent.

4. Quantum numbers. As all resonances must lie on Reggeon trajectories at $t>0 (\mathrm{Re}\,\alpha(M^2) = j$; (M and j = mass and spin of the resonance), it is clear that the Reggeons are characterized by the same quantum numbers as the resonances. In other words, each Reggeon has a definite isotopic spin (I), strangeness (S), parity (P) etc. Table 1 shows the quantum numbers and parameters of the trajectories, and also those particles which lie on these trajectories for all of the most important Reggeons. It is necessary to pay attention to the fact that in the theory of complex angular moments a new quantum ~~figure~~ number appears - ~~a~~ the signature which characterizes the change in the Reggeon contribution (R (S, t)) during the substitution S → -S. For Reggeons with a positive signature (σ = + 1 in Table 1) R (S, t) = R (-S, t), for Reggeons with a negative signature $R(s,t) = -R(-S,t)$. It should

be noted that if $R(S,t)$ equals the Reggeon contribution to the reaction $a + b \to a + b$, then for high S $R(-S,t)$ equals the contribution of the same Reggeon to the crossing-symmetrical reaction $\bar{a} + b \to \bar{a} + b$, consequently the signature forms a link between the scattering of a particle („a") and an anti-particle („$\bar{a}$")on a target („b"). On the other hand, the signature characterizes the parity of the spins (j) of those resonances which lie on a given trajectory (for baryons the parity is $j-\frac{1}{2}$). The trajectories with a positive signature pass through resonances with spins of ~~equal~~ even parity (see Table 1 for trajectories f, A_2, π), whilst trajectories with a negative signature pass through resonances with spins having an odd parity (see ρ, ω - trajectories in Table 1 and Fig. 1.2). For the characteristic of the trajectories we shall subsequently find convenient the quantum number $P_\tau = P\cdot\sigma = P(-1)^n$, where P and σ are equal to the parity and signature of the trajectory, n the spin of j for a boson and $j-\frac{1}{2}$ for baryons. If $P_\tau = +1$ particles 0^+, 1^-, 2^+ lie on the trajectory, i.e. particles which are described by scalar, vector and tensor wave functions (particles with a natural parity $P=(-1)^j$, j = spin resonance). If $P_\tau = -1$, then on the trajectory lie resonances 0^-, 1^+, 2^-, and for such particles we must use pseudo-scalar, axial-vector and pseudo-tensor wave functions (particles with non-natural parity $P = -(-1)^j$). On completing a summary examination of the quantum numbers of Reggeons, we note that for all known Reggeons with $\alpha(0) \geq 0$, one simple relation between quantum numbers is fulfilled:

$$\sigma G\cdot(-1)^I = +1 , \qquad (1.1)$$

For the convenience of the reader, ~~Fig.~~ Table 2 enumerates the most interesting reactions and shows which Reggeons contribute to them and how they do this.

5. ~~Exponential~~ Power-law dependence of amplitudes on energy. Let us go into greater detail on the basic consequences of the fact that at high energies a contribution is given to the hadron scattering amplitude (A) by Reggeon exchange, i.e. $A \sim S^{\alpha(t)}$. Above all, the differential cross-section for a fixed t should fall ~~exponentially~~ as a power in S with the increase in energy. In effect,

$$\frac{d\sigma}{dt} = \frac{1}{16\pi S^2}|A|^2 \sim S^{2(\alpha(t)-1)}. \qquad (1.2)$$

It is obvious that the ~~exponential~~ power-law character of the fall is maintained also for the total cross-sections of this process, if we disregard their additional logarithmic fall as S increases.

$$\int \frac{d\sigma}{dt} dt \sim S^{2(\alpha(0)-1)} \frac{1}{R_0^2 + \alpha' \ln S}. \qquad (1.3)$$

In this way, all cross-sections should behave according to $\sigma = AS^{-n}$, where „ n " may be calculated by $\alpha(0)$ of the corresponding Reggeon. It will be immediately seen that the cross-sections of the elastic reactions and diffraction dissociation, to which the basic contribution is given by the exchange of a vacuum pole (P, $\alpha_P(0) = 1$, see Table 1), should be almost constant. For the reactions in which there is an exchange of isotopic spin in the t-channel (for example $\pi^- p \to \pi^0 n$) $n = -2(\alpha_\rho(0) - 1) = +1$. For reactions with an exchange of strangeness (for example $K^- p \to \pi^0 \Sigma^0$) $n = -2(\alpha_{K^*}(0) - 1) = 1.34$; with an exchange of a baryon number $n = -2(\alpha_N(0) - 1) = 2.8$ etc.

Table 3 shows the experimental /7/ and theoretical values of "n" for many reactions. It will be seen that the ~~exponential~~ power-law drop in cross-sections agrees well with experiment and the values of "n", calculated by the Reggeon trajectories, at least qualitatively agree with the experimentally observed dependence of cross-section on energy.

6. ~~Narrowing~~ Shrinkage of the diffraction cone. As follows from (1.2),

$$\frac{d\sigma}{dt} \sim s^{2(\alpha(0)-1)} e^{-2\alpha'|t|\ln s} g_a^2(t) g_b^2(t) = g_a^2(0) g_b^2(0) e^{-2(R_0^2+\alpha'\ln s)|t|} \cdot s^{2(\alpha(0)-1)}, \qquad (1.4)$$

where $g_a(t)$ and $g_b(t)$ are taken, for simplicity, in the form $g(t) = g(0)\, e^{-\frac{R_0^2|t|}{2}}$. It will be seen from (1.4) that the slope of the cross-section ("b" in expression $\frac{d\sigma}{dt} = Ae^{-b|t|}$) must increase with a rise in s ($b = 2(R_0^2 + \alpha' \ln s)$). This ~~narrow-~~ shrinkage ~~ing~~ of the diffraction cone is observed for those reactions in which a contribution is given only by one Reggeon (for example the reaction $\pi^- p \to \pi^0 n$ takes place owing to the exchange of only the ρ-Reggeon), or in the case where the reaction is measured right up to the high energies, for which only the contribution of a Reggeon with the highest $\alpha(0)$ survives (see Fig. 1.4, 1.5, 1.6). For some reactions, however, "b" does not depend on S (see for example * $\pi^- p$ and $K^- p$ in Fig. 1.6, whereas in other cases (see $\bar{p}p$ in Fig. 1.6) the diffraction cone is widened as S increases ("b" falls with a rise in S). The usual explanation of this fact is that in these reactions the contribution is given by the exchanges of many Reggeons

---

*There is an indication that when there is a limitation of the range to $|t| < 0.1$ and energies to $S > 40$ GeV^2 in these reactions the cone also will ~~be narrowed~~ shrink /8/.

(see Table 2) and, at an energy which is not too high, they are all substantial, and an asymptotic narrowing of the cone does not develop. In reality, let

$$\frac{d\sigma}{dt} = \tau_1 e^{2(R_1^2+\alpha_\rho' \ln S)t} + \frac{\tau_2}{\sqrt{S}} e^{2(R_2^2+\alpha_f' \ln S)t} \qquad (1.5)$$

The first term corresponds to the contribution of the vacuum Reggeon, the second to interferences with all non-vacuum Reggeons of type ρ the A_2, ω, f, $\alpha(0)$ of which are close to 1/2 (see Table 1). If $\frac{d\sigma}{dt}$ is represented in the form $A e^{bt}$, b for (1.5) is equal to

$$b(t) = \frac{d^2\sigma}{dt^2} \Big/ \frac{d\sigma}{dt} = 2\,\frac{\tau_1(R_1^2+\alpha_\rho' \ln S) + \frac{\tau_2}{\sqrt{S}}(R_2^2+\alpha_f' \ln S)}{\tau_1 + \frac{\tau_2}{\sqrt{S/S_0}}} =$$

If we take $\tau_2/\tau_1 = 2$ (which corresponds to an identical contribution of ρ and f to the amplitude) and

$$= 2\left(R_1^2+\alpha_\rho' \ln S + \frac{\tau_2}{\tau_1\sqrt{\frac{S}{S_0}}}(R_2^2+\alpha_f' \ln S)\right)\left(1+\frac{\tau_2}{\tau_1\sqrt{S/S_0}}\right)^{-1} \qquad (I.6)$$

then the variation in „b" as S increases from 10 to 100 GeV^2 is equal to 1. Let us note that „b" for P (first term in (1.5)) varies by $\Delta b = 2$. It is clear that by selecting R_1^2, R_2^2, τ_2/τ_1, etc., it is not difficult to arrive at a coincidence with experiment. (Let us note that for large energies the cone must ~~be shortened~~ shrink in all reactions, including also $\pi^- p$ - and $K^- p$ -scattering). In this language the ~~shortening~~ shrinkage of the cone in pp and $K^+ p$ occurs, beginning with comparatively small energies, because the contributions of the poles ρ, A_2, ω and f, which generally speaking may

exist in these processes, ~~are shortened~~ shrink. In this way the experimental data show a ~~shortening~~ shrinkage of the diffraction cone in accordance with the theoretical predictions.

7. Factorization. Reggeon exchange, like particle exchange, has a factorization feature which consists in the fact that the Reggeon contribution (see Fig. 1.1 a) is of the form :

$$A(s,t) = g_a(t)\, g_b(t)\, s^{\alpha(t)} \qquad (1.7)$$

(i.e. the dependence on the sorts of particles, which are exchanged with a Reggeon, is separated out in the form of separate ~~multipliers~~ factors $g_a(t)$ and $g_b(t)$). It follows in particular from (1.7) that if only the exchange of one Reggeon is important, then

$$\frac{\sigma(aA \to aA)}{\sigma(bA \to bA)} = \frac{g_a(0)}{g_b(0)} \qquad (1.8)$$

irrespective of the type of target A. For example, ~~they should be equal to~~ we have the equality

$$R_1 = R_2 = R_3 = R_4, \qquad (1.9)$$

where

$$R_1 = \frac{\sigma(\pi^- p \to \pi^- p)}{\sigma(pp \to pp)}\,;\quad R_2 = \frac{\sigma(\pi^- p \to \pi^-(p\pi^0)}{\sigma(pp \to p(p\pi))}\,;$$

$$R_3 = \frac{\sigma(\pi p \to \pi(p\pi^+\pi^-))}{\sigma(pp \to p(p\pi^+\pi^-))}\,;\quad R_4 = \frac{\sigma(\pi p \to \pi(p\pi\pi))}{\sigma(pp \to p(p\pi\pi\pi))}\,. \qquad (1.10)$$

The brackets denote systems of particles travelling with similar momenta (see Fig. 1.7 which graphically elucidates relation (1.9)).

Table 4 shows the values of R_1, R_2, R_3 and R_4, taken from /9/. It will be seen that within the limits of experimental error (which, however, are great) the relation (1.9) agrees with experiment. Naturally, factorized relations exist only when there is an exchange of one Regge pole, consequently their fulfilment should be improved as the energy increases, since at high energies a basic contribution is given by the exchange of the Reggeon with the biggest $\alpha(0)$. (For the reactions enumerated in Tables 4 and 5 the vacuum pole P is given in Table 1). Table 5 shows the values for the ratios

$$R_1 = \frac{\sigma(\gamma p \to \rho^0 p)}{\sigma(\gamma p \to \rho^0(p\pi^+\pi^-))} \; ; \; R_2 = \frac{\sigma(pp \to pp)}{\sigma(pp \to p(p\pi^+\pi^-))} ;$$

$$R_3 = \frac{\sigma(\pi p \to \pi p)}{\sigma(\pi^+ p \to \pi^+(p\pi^+\pi^-))} ,$$

which should also be equal to each other ($R_1 = R_2 = R_3$). It will be seen that this equality improves as the energy rises and is fulfilled with an accuracy of 10%. The overall totals for the verification of the factorization lie in the fact that factorization takes place with an accuracy of 10-20%.

8. Dependence of Reggeon contribution on the spin of scattered particles. Hitherto we have not taken into account the spin of scattered particles, and expression (1.7) for Reggeon contribution has, in essence, been written for scalar particles. In this case when particles have a spin, the vertices are $g_a(t)$ and $g_b(t)$, generally speaking, will depend on the polarization vectors of the particles a and b. There is a simple rule for writing this dependence /10/, namely: the vertices g_{a_i} (see Fig. 1.8) are

constructed from the polarization vectors forming part of the vertex of the particles (e_a , e_b) of the vectors p_a and p_b , $q^\perp$ and q'' , where $q^\perp$ is a component of momentum transfer, directed perpendicularly to the plane formed by the vectors p_a and p_b of the initial particles in the reaction a + b → c + d (see Fig. 1.8), q'' = the component of momentum transfer lying in the plane p_a and p_b . From the polarization vectors q'' and q' , a four-dimensional scalar is constructed if the product P_r of the particles and the Reggeon entering the vertex is equal to +1 ($P_r^a P_r^c P_r^d$ for the vertex acd on Fig. 1.8) and a pseudo-scalar, if the product is -1. P_r for a particle is $P(-1)^j$, where j is the spin, and P is the internal parity.

For example π changes ~~to~~ into A_1 (1^+) and A_2 (2^+) ~~owing to~~ through the exchange of a Reggeon with $P_r = +1$. The P_r of a π -meson is -1 , A_1 (1^+) is -1 and A_2 (2^+) is +1. In this way the vertex $\pi \to A_1$ is a scalar, equal to $g_1(e_{A_1} q'') + g_2(e_{A_1} q^1)$, whereas the vertex $\pi_\alpha \to A_2$ must be pseudo-scalar, i.e.

$$g_1 e_{\mu\nu\lambda\sigma} p_{a_\mu} q''_\nu q^\perp_\lambda e_{\sigma\delta} q^\perp_\sigma + g_2 e_{\mu\nu\lambda\sigma} p_{a_\mu} q''_\nu q^\perp_\lambda e_{\sigma\delta} q''_\delta .$$

From this it will be seen that the reaction amplitude with production of A_2 (for example $\pi p \to A_2 p$) vanishes when $q_\perp \to 0$ (for a zero angle), whilst A_1 may be produced at a zero angle.

9. Complex nature of Reggeon contribution. The Reggeon exchange amplitude, unlike particle exchange, generally speaking, is complex. This can be seen if only from the space-time picture of the Reggeon, since the imaginary part of the Reggeon contribution corresponds to the fact that multi-particle production processes

contribute to Reggeon exchange. The complex nature of the Reggeon is determined by the so-called signature ~~multiplier~~ factor (n) , which is

$$\eta = \begin{cases} -ctg\,\frac{\pi\alpha(t)}{2} + i & \text{For a positive signature} \\ -tg\,\frac{\pi\alpha(t)}{2} - i & \text{For a negative signature} \end{cases} \qquad (1.11)$$

In this way, finally the contribution of the Reggeon to the scattering amplitude a + b → a + b is equal to

$$R(s,t) = \eta(\alpha(t))\, g_a(t)\, g_b(t)\, s^{\alpha(t)} \qquad (1.12)$$

Let us note that η has a graphic physical meaning. In reality, if $t > 0$ and $Re\,\alpha(t_0) = 0$,

then, when $t \to t_0$

$$R(s,t) \underset{t\to t_0}{\to} \frac{g_a g_b s^{\alpha(t_0)}}{\sin\frac{\pi\alpha(t)}{2}} = \frac{g_a g_b}{\frac{\pi}{2}\alpha'(t-t_0) + i\,Im\,\alpha(t_0)} \qquad (1.13)$$

$$= \frac{C}{t - t_0 + i\frac{Im\,\alpha(t_0)}{\alpha'}},$$

i.e. the signature ~~multiplior~~ factor ensures precisely the necessary correlation between Reggeon exchange and resonances, to which reference was made above. Of course, in the example analyzed above, it was only the amplitude with a positive signature which possessed the pole, when $t \to t_0$. In the negative signature, there is no pole when $t \to t_0$. This is reflected by the fact that particles with an even spin parity lie on trajectories with a positive signature. The direct consequence of the theory is

that for reactions to which only one Reggeon contribute, inspite of the fact that the amplitude is complex, the polarization must be equal to zero. This is due to the fact that the amplitude with and without spin-flip in this case has an identical phase, whilst the polarization $\mathcal{P} \sim Im A^{++} A^{*+-} = 0$. However the probability of spin-flip should, generally speaking, be great. One of the simplest examples is as follows: the polarization in $\pi^- p \to \pi^0 n$ (exchange of only a ρ Reggeon) must be small, which corresponds with the new experiment /II/ (Fig. 1.9 a). Since the interference of the two Reggeons contributes to the polarization, then, for example, it should fall roughly in accordance with $1/\sqrt{s}$ for the reactions $pp \to pp, \pi p \to \pi p$ i.e.

$$\mathcal{P} = \frac{Im R R^*}{R^2 + R^2} \sim \frac{1}{\sqrt{s}}, \qquad (1.14)$$

R designates any non-vacuum Reggeon $\alpha(0) = \frac{1}{2}$, i.e. ρ , A_2, f and ω .

The dependence (1.14) corresponds to the experimental results (Fig. 1.9 b, in which are given the polarization values as a function of S , the continuous line is the dependence $1/\sqrt{s}$).

REGGE CUTS

We have seen that the exchange of Reggeons, which occurred naturally in the theory of complex moments, explains many characteristic features of scattering at high energies. However, it appears that it is not possible to confine oneself only to the contributions of Reggeon exchanges to the scattering amplitude at high energy. The fact is that the exchange of two, three etc. Reggeons, generally speaking, produces a contribution which is not small. For example, the contribution of the exchange of two Reggeons (α_1 and α_2 in Fig. 1.10) is of the form : /12/

$$R_c^{(2)}(s,t) = \frac{i}{3}\int \frac{d^2K}{(2\pi)^2} R_{\alpha_1}(s,t) R_{\alpha_2}(s,t) N_1(\alpha_1,\alpha_2,K^2,(q-K)^2) \cdot$$
$$\cdot N_2(\alpha_1,\alpha_2,K^2,(q-K)^2) =$$
$$= i\, s^{\alpha_1(0)+\alpha_2(0)-1}\int e^{-(\alpha_1' K^2+\alpha_2'(q-K)^2)} d_2 S \cdot \qquad (1.15)$$
$$\cdot \varrho(\alpha_1)\varrho(\alpha_2)\cdot N_1(\alpha_1,\alpha_2,K^2,(q-K)^2) N_2(\alpha_1,\alpha_2,K^2,(q-K)^2)\frac{d^2K}{(2\pi)^2} .$$

Let us examine briefly the basic characteristics of this type of exchange which corresponds to more complex ones than the pole features of the partial amplitude of the cross-over channel (f_j) in the plane of complex angular moments (j) (the so-called ~~branching points~~ Regge cuts). In concrete terms, the graph of Fig. 1.10 corresponds to

$$f_j \sim \ln\left(j-\alpha_1(0)-\alpha_2(0)+1-\frac{\alpha_1'\alpha_2'}{\alpha_1'+\alpha_2'}t\right) .$$

I. The quantum numbers of cuts. The quantum numbers, such as isotopic spin, strangeness, the baryon number, G -parity for ~~branching~~ cuts, are obtained in the same way from the quantum numbers of the Reggeons as for the quantum numbers of the two, three etc. particle systems. For example, the isotopic spin of two-Reggeon

~~branching~~ cut $(I^{(2)})$ (see Fig. 1.10) can pass through values extending from $I_1 + I_2$ to $I_1 - I_2$, where I_1 and I_2 are the isotopic spins of Reggeons α_1 and $\alpha_2 (I_1 \geqslant I_2)$, the ~~branching~~ cut strangeness is $S^{(2)} = S_1 + S_2$, the G-parity is $G^{(2)} = G_1 G_2$ etc.

It is necessary, in particular, to dwell on two important features of ~~branching~~ cut quantum numbers.

a) The signature of n-Reggeon exchange $(\sigma^{(n)})$ is equal to the product of the Reggeon signatures $\sigma^{(n)} = \sigma_1 \ldots \sigma_n$ (for graph Fig. 1.10 $\sigma^{(2)} = \sigma_1 \sigma_2$).

b) The parity of a system of many Reggeons is not fixed. In effect, for the very same reason as the two-particle system, which may have both positive and negative parities depending on their relative orbital movement. In this way the P_n of the corresponding ~~branching~~ cut point is also not fixed. This is a very characteristic feature of ~~branching~~ cuts, and below we shall give some examples of processes in which this feature is developed.

c) An exception is the system of two equal (identical) Reggeons (for example the exchange of two ρ-Reggeons), which has only one (positive) parity. This can be explained in the same way as the fact that the system of two identical scalar neutral bosons can have only even orbital moments, i.e. their wave function must be symmetrical ...

2. Energy dependence. From the simple expression (1.15) it would be seen that the exchange of two Reggeons generally speaking leads to an ~~exponential~~ power-law dependence $S^{\alpha_1(0)+\alpha_2(0)-1}$, whilst for all

Reggeons in which $\alpha_1(0), \alpha_2(0) < 1$, these corrections are small in comparison with the exchange of a Reggeon $\alpha_1(s^{\alpha_1(0)})$ or $\alpha_2(s^{\alpha_2(0)})$. Only in the case when one of the Reggeons is a vacuum-Reggeon, i.e. $\alpha_1 = \alpha_P(0) = 1$, does ~~branching~~ the cut give a contribution of $\sim s^{\alpha_2(0)}$, i.e. of the same order as the contribution of one Reggeon. However the ~~branching~~ cut shown in Fig. 1.11 (or 1.10), has in this case too a small value in comparison with the contribution of the pole, but this small value is only logarithmic. In reality, we shall disregard the dependence of N_1 and N_2 on K^2 in comparison with the rapid (~~exponential~~ power-law) dependence (this can be done if $\alpha'_P \ln s \gg \langle k^2 \rangle^{-1}$ where $\langle k^2 \rangle$ is the characteristic momentum transfer in N_1 and N_2), then the integral for d^2K^1 can be taken, and it is of the order $1/(\alpha_1' + \alpha_2') \ln s$.

From the view point of the space - time description, the ~~branching~~ cut (see for example Fig. 1.10) corresponds to the process shown in Fig. 1.12. This diagram shows two fluctuations, which began at slightly different moments in time, but each produced a slow particle which corresponds with a target at rest. The smallness of this process can easily be evaluated from the fact that both slow particles must have an identical impact parameter (ρ), coinciding with the impact parameter of the target. As the substantial ρ^{α} in each fluctuation $\sim \frac{1}{m^2} \ln s$, this smallness is of the order

$$1/m^2 / 1/m^2 \ln s \sim 1/\ln s$$

(for more details, see /3-5/).

The graph of the type in Fig. 1.11 shows a smallness $\sim (\alpha'_P \ln s)^{-n}$. In this way, for large energies the scattering amplitude can be represented in the following form

$$A(s,t) = \sum_i s^{\alpha_i(t)} \varphi_i(t, \alpha'_P \ln s), \qquad (1.16)$$

where $\varphi_i(t, \alpha' p \ln S)$ takes into account the contribution of all ~~branching~~ cuts of the type in Fig. 1.11 when $\alpha = \alpha_i$. For large $\alpha' p \ln S$ we have $\varphi(t, \ln S) \to g_a(t) g_b(t)$, where $g_a(t)$ and $g_b(t)$ are residues of the Reggeon α_i .

3. Dependence on t. It can easily be seen that the ~~branching~~ cut gives a slower reduction in amplitude as the momentum transfer increases $|t|$. In reality, at high energies (let $\alpha_2(0) = 1$)

$$R_c^{(2)}(s,t) \sim s^{\alpha_1(0)} e^{+\frac{\alpha' p \alpha' i}{\alpha' i + \alpha' p} \cdot t \ln s} \qquad (1.17)$$

and even when $\alpha_1' = \alpha' p$, the slope of the cone is obtained $b_c = \frac{\alpha' p}{2} \ln S$, which is twice as small as the slope owing to the exchange of one Reggeon. It is necessary to note that even at energies which are not too high, the assertion that the contribution of ~~branching~~ the cut falls slowly as $|t|$ increases, remains applicable, in any case this is visible from two examples :

a) A weakly-coupled system of the deuteron type. The exchange of one Reggeon gives a dependence of (see Fig. 1.13 a) $S^2(t) s^{\alpha(t)}$ where S (t) is the electromagnetic form factor of the deuteron, and the exchange of two is of the form :

$$s^{\alpha(0)} \int S^2(4\kappa^2) d\kappa^2 e^{-(\alpha' p (\frac{q}{2} - \kappa)^2 + \alpha' i (\frac{q}{2} + \kappa)^2) \ln s} ,$$

i.e. it falls ~~extremely~~ very slowly as t increases (see Fig. 1.13 b). It is clear that a qualitatively similar character in the dependence on t will exist in any model where the hadron is represented as a weakly coupled system of quarks, partons etc.

b) Eikonal. In N, account is taken only of the graphs of the type shown in Fig. 1.14. Unlike the case of the previous examination, the hadron is represented as a strongly coupled system. If we take $g(t) = g(0)e^{-\frac{R_0^2(t)}{2}}$, we have for the graph of Fig. 1.14 the answer (for Fig. 1.10 $\alpha_1 = \alpha_2 = \alpha_p$):

$$R_c^{(2)} = \frac{g_a^2(0) g_s^2(0)}{32\pi(R_0^2 + \alpha'_p \ln s)} e^{\frac{(R_0^2 + \alpha'_p \ln s)t}{2}}, \qquad (1.18)$$

i.e. in this approximation the ~~branching~~ cut slope is twice as small as that of the pole.

4. ~~Complexity~~ Phase and sign of ~~branching~~ cut contributions. The ~~entire~~ ~~complexity~~ phase of the ~~branching~~ cut contribution (for example, the second one - see Fig. 1.10) is determined entirely by the ~~multiplier~~ factor $i\eta(\alpha_1(t))\eta(\alpha_2(t))$. For example, let $\alpha_2(t) = \alpha_p(t)$, then

$$\eta(\alpha_p(t)) = i - ctg\frac{\pi\alpha_p(t)}{2} = i - \frac{\pi}{2}\alpha'_p t$$

for small t and, consequently, the phase of the cut contribution is given by

$$-\varphi(\alpha_1(t)) - \frac{\pi}{2}\alpha'_p t \, i\varphi(\alpha_1(t)), \qquad (1.19)$$

It can be seen from (1.19) that :

a) For small t (i.e. everywhere in (1.15) we take out from the integral) the ~~branching~~ cut contribution has the same ~~complexity~~ phase as the pole, but the ~~branching~~ cut contribution is negative. The overall contribution of the pole and ~~branching~~ cut of the type shown in Fig. 1.10 is of the form (~~when~~ at t = 0) :

$$\varphi(\alpha(0)) \cdot s^{\alpha(0)} \cdot \left[1 - \frac{c}{R^2 + \alpha' \ln s}\right], \qquad (1.20)$$

where $c = \frac{g_a^2(0)\, g_b^2(0)}{16\pi}$ in the eikonal approximation. Let us note that the contribution of the exchange of (n+1) Reggeons has a sign $(-1)^n$, and consequently in formula (1.20) generally speaking, there are also positive terms but they are smaller (logarithmically) at high energies. (The contribution „$n+1$" of ~~branching~~ the cut is of the order $(-1)^n \frac{C_n}{(\alpha' \rho \ln S)^n}$).

b) When taking into account the following corrections for small t, the ~~branching complexity~~ cut phase differs from the Reggeon ~~complexity~~ phase. For example: let us examine the exchange of two vacuum Reggeons (P, see Table 1) ~~where~~ at t = 0. The pole gives a purely imaginary contribution (i S) of ~~branching~~ the cut (see expression (1.15)).

$$-S\int\left(i-\frac{\pi}{2}\alpha_\rho'(\kappa_1^2+\kappa_2^2)\right) S^{-2\alpha_\rho'\kappa^2} N_1 N_2 \frac{d\kappa^2}{(2\pi)^2} =$$
$$= S\left(-i+\frac{\pi}{2}\frac{\partial}{\partial \ln S}\right)\int e^{-2\alpha_\rho'\kappa^2 \ln S} N_1 N_2 \frac{d\kappa^2}{(2\pi)^2}. \qquad (1.21)$$

It is clear that the expression (1.21) can be rewritten in another way, namely:

$$Re\, R_c^{(2)}(s,t) = s\frac{\pi}{2}\frac{\partial}{\partial \ln s}\left(\frac{Im\, R_c^{(2)}(s,t)}{s}\right). \qquad (1.22)$$

It is interesting to note that the relation (1.22) is true not only for the simplest exchange (see Fig. 1.11), but also when taking into account all vacuum ~~branching~~ cuts. Consequently, when examining high energies, at which a contribution is given only by the vacuum pole, and coupled with the exchange of many vacuum poles ~~of branching~~ of cuts, we can write the ~~coupling~~ relation between $ReA(s,t)$ and $ImA(s,t)$ (or the total cross-section) as:

$$ReA(s,0) = \frac{\pi}{2} s \frac{\partial}{\partial \ln s}\frac{ImA(s,0)}{s} = \frac{\pi}{2} s \frac{\partial}{\partial \ln s}\sigma(s), \qquad (1.23)$$

where $\sigma(s)$ is the total cross-section. Formula (1.23) establishes the link between the rate of variation in the total cross-sections on the energy and $\mathrm{Re}A(s,0)$.

The fact that the cut has a phase which is different from that of the pole may manifest itself in various phenomena, in particular, it may serve as a ~~source~~ cause of polarization in those reactions where a contribution is given by the exchange of one Reggeon (for example, in $\pi^- p \to \pi^0 n$).

5. The coupling of the cuts with particles carrying a spin. Multi-Reggeon amplitudes (N in formula (1.15) can be constructed for the case where the external particles a and b have spins, in accordance with the same rules as for constructing the vertex of the coupling of one Reggeon, but only in the system of vectors from which it is necessary to construct N, it is necessary to include, in addition to the polarization vectors of particles a and b (e_a and e_b), q'' and $q^{\perp}$, also the vectors $K_1^{\perp} \dots K_n^{\perp}$ /10/. In this connection let us point out that P_2 of the cut ~~branching~~ is not fixed and therefore it is necessary to construct from all these factors both a scalar and a pseudo-scalar.

Examples :

a) $\pi^- p \to A_2 p \cdot \left.\frac{d\sigma}{dt}\right/_{t=0}$ is determined only by the contribution of the cut ~~branching~~ (see Fig. 1.15 a) with a negative P_r /13/. For N_1 it is possible to write $n_1 \varepsilon^{A_2}_{\mu\nu} q''_\mu q''_\nu$, which corresponds to $P_r = -1$ for a system of Reggeons (production of $P_{r_2} \pi P_{r_2} A_2 P_r$ (cut ~~branching~~) = +1). This contribution does not disappear for $q^{\perp} \to 0$ and determines $\left.\frac{d\sigma}{dt}\right/_{t=0}$ (the pole contribution tends to zero at $t \to 0$ see above).

b) $pp \to pp$ the spin-spin term in the scattering amplitude (type $b(\sigma_1\sigma_2)$ for $t\to 0$ cannot appear owing to the Reggeon exchange with $P_r = +1$. In reality the coupling vertex of this Reggeon with P is of the form (it is necessary to construct the scalar):

$$\bar{u}(p_2)(g_1 + g_2\hat{q}^{\perp})u(p_1') \quad \text{or in the two dimensional form}$$
$$\bar{g}_1 + \bar{g}_2([\bar{\sigma}\bar{q}^{\perp}]\bar{n}), \tag{1.24}$$

where $\vec{n}$ is the direction of the colliding particles (the remaining designations are shown in Fig. 1.15 a), for $q^{\perp}\to 0$ in (1.24) there remains only the contribution which is not dependent on the spins. For the exchange of two Reggeons, the vertex $N^{(2)}$ is of the form

$$\bar{u}(p_2)(n_1 + n_2(\hat{K}_1^{\perp} + \hat{K}_2^{\perp}))u(p_1'). \tag{1.25}$$

Equation (1.25) takes into account that the two Reggeons are identical and consequently N must be a symmetrical function of K_1 and K_2. It is clear that for $q^{\perp}\to 0\ K_1^{\perp} = -K_2^{\perp}$ and (1.25) disappear. In this way the ~~branching~~ cut gives a contribution to the spin-spin interaction, only beginning from the exchange of three Reggeons, where $N^{(3)}$ must have the form

$$N^{(3)} = n^{(3)}\bar{u}(p_2)\{(K_1^2 + K_2^2)\hat{K}_3 + (K_1^2 + K_3^2)\hat{K}_2 + (K_1^2 + K_2^2)\hat{K}_3\}u(p_1'). \tag{1.26}$$

For $q_{\perp}\to 0$ the contribution of three-Reggeon exchange will be proportional to

$$\int e^{-\alpha'((K_1^{\perp}+K_2^{\perp})^2 + (K_1^{\perp})^2 + (K_2^{\perp})^2)} e^{\eta} s\, N^{(3)}N^{(2)} d^2K_1^{\perp} d^2K_2^{\perp}, \tag{1.27}$$

Since $(N^{(3)})^2 \sim (K^{\perp})^6$, then after integration for $K_1^{\perp}$ and $K_2^{\perp}$ we have a contribution of the order of $1/(\alpha' p \ln s)^5$ i.e. the spin-spin terms should fall rapidly as the energy rises.

What is the effect of the presence of ~~branching~~ the cut on the asymptotic nature at high energies?

I. Behaviour of total cross-sections. As has already been pointed out in (see (1.20)) the total cross-sections for $S \to \infty$ approach their maximum value from below (this fact was predicted in /14/ a long time before the acquisition of experimental data demonstrating the increase of the total cross-sections - a psychological plus to the advantage of the concept under examination). This conclusion is based on the fact that the exchange of two vacuum Reggeons is of a screening character (has a negative contribution). Experimentally, at the present time the increase in the total cross-sections has been revealed for K^+p and pp -scattering (detailed discussions of the experimental data are given in /15/). Let us note that the simple eikonal evaluation for (1.15) gives an increase in $\sigma(K^+p)$ which corresponds with experiment, and a slightly lower increase in comparison with the experimental values in the case of $\sigma(pp)$ /16/. Naturally, the eikonal is not a strict result and the behaviour which is predicted by this type of formula can be accepted only as a rough estimate. In particular, in the models of the "brittle" hadron the behaviour

$$\sigma_{tot} = \sigma_{\infty} - \frac{c}{\bar{R}_0^2 + \alpha' \ln S}$$

will be determined by $\bar{R}_0^2$, which is linked with the slope in the diffraction cone (in this model it is determined by $S(t)$, see Fig. 1.13 a). $\bar{R}^2$ is significantly smaller than the characteristic distances over which there is a variation in $S(t)$, consequently in this type of model the increase in cross-section will be faster than for the simple eikonal estimates.

2. The real part of the scattering amplitude must be positive when $S \to \infty$ /14/. This can also be seen from (1.22). Consequently if experimentally $ReA < 0$, then for ~~any~~ higher values of S it ~~may~~ should tend to zero. From (1.22) it follows that this point corresponds to the minimum of the total cross-section. Experimentally, $\rho = \frac{ReA}{ImA}$ tends to zero for pp -scattering at $S \sim 500$ (GeV)^2 /17/ (see Fig. 1.16).

3. Crossover: The phenomenon known as "crossover" is that the differential cross-sections $\frac{d\sigma}{dt}(\pi^- p), \frac{d\sigma}{dt}(K^- p), \frac{d\sigma}{dt}(pp)$ at which t $(t = t_0,\ t_0 \sim 0.1 - 0.2$ (GeV/c)$^2)$ cross over (see Fig. 1.17) with $\frac{d\sigma}{dt}(\pi^+ p), \frac{d\sigma}{dt}(K^+ p), \frac{d\sigma}{dt}(pp)$, respectively. The explanation of this is as follows : the difference in cross-sections $\Delta(ab) = \frac{d\sigma}{dt}(ab) - \frac{d\sigma}{dt}(\bar{a}b)$ is determined by the interference of the contributions of Reggeons of a positive and negative signature (the first give an identical contribution to the scattering cross-section of particles and anti-particles, the contributions of the second are distinguished by the sign).

This is

$$\Delta(ab) = Re\, P(s,t) R^*(s,t), \tag{1.27}$$

where P(S,t) is the contribution of the vacuum Reggeon (P) and the vacuum ~~branching~~ cut (the contribution of the remaining Reggeons can be disregarded for sufficiently large S). R(S,t) is the contribution of non-vacuum Reggeons with a negative signature (ρ for $\Delta(\pi^\pm p)$ and basically for $\Delta(K^\pm p)$ and $\Delta(p^\pm p)$) and of the ~~branching~~ cut points of the type in Fig. 1.11, where α is the non-vacuum Reggeon. The tendency to zero of $\Delta(ab)$ at $t = t_0$ is due to the fact that $R(S,t_0) = 0$ owing to compensation of the Reggeon contribution and first ~~branching~~ cut /18/, i.e. compensation of the contributions of the diagrams

shown in the figures type 1.18. As the graph 1.18 b falls more slowly with an increase in small t than graph 1.18 a, it is clear that for a certain small t this compensation is possible. It follows from the condition that this occurs at $t_0 \sim 0.1 - 0.2$ (GeV/c)^2, that the contribution of the diagram of Fig. 1.18 b must be increased approximately twice in comparison with the eikonal contribution, i.e. it must be approximately 50-60% of the contribution of the Reggeon for S = 100 GeV^2.

4. Dips. A negative ~~branching~~ cut contribution and the different dependence on t of the exchange of a Reggeon and ~~branching~~ cut leads to the fact that the differential cross-section must have a minimum ("dip") at a certain value of small t. These "dips" are in fact observed (see Fig. 1.19 a, b and Table 2). An explanation of the minimum in the reactions $\pi^{\pm}p$, $K^{-}p$, $\bar{p}p$ for $t \sim -0.6$ (GeV/c)^2 (which disappears at high energies) consists in the fact that the contribution of $R^{-}(S,t)$ (see above) tends to zero in this point owing to compensation of the graphs 1.18 a and 1.18 b. The fact that this occurs in a slightly different point for small t, is due to the fact that this minimum occurs in an amplitude with a reversal of helicity. Let us note that in those reactions where the contribution of non-vacuum poles is ~~shortened~~ small ($K^{+}p$ and pp, for example), such type of minimum does not exist (see, for example, /19/ and Table 2) and on the contrary in those reactions where only the exchange of a non-vacuum Reggeon is possible it is present (see $\pi^{-}p \to \pi^{0}n$ in Fig. 1.19 a). The minimum at t = -1.3 (GeV/c)^2 in the pp -scattering can be explained by the fact that there is ~~a mutual reduction of~~ cancellation between the contributions of the pomeron and ~~of~~ the ~~branching~~ cut due to the exchange of two P. The correct position of the minimum is obtained from an eikonal estimate

of the contribution of ~~branching~~ the cut (i.e. 10-15% for $t = 0$). However this evaluation cannot reproduce the trend of the differential cross-section.

5. The cut gives a contribution for $t = 0$ /13/ in such reactions as $\pi p \to A_2 p$, $\pi p \to \rho p$, i.e. in the reactions of type $0^- N \to 1^-(2^+) N\ (0^-, 1^-, 2^+ \ldots P)$. As has already been pointed out, the contribution of all known Reggeons tends to zero at $t = 0$ in these reactions. In addition in such reactions as $pp \to \pi^+ n$, $pn \to np$ and others one can clearly see from experiment a peak linked with the exchange of a π-meson (characteristic $\Delta t \sim m_\pi^2$). However the contribution of the π-exchange must disappear in these reactions at $t \to 0$ (since the ~~deduction~~ contribution of the π-meson in the $N\bar{N}$ system diminishes as when) ~~at~~ $t \to 0$). Consequently, the absence of a minimum $\bar{u}\gamma_5 u \sim \sqrt{-t}$ at $t = 0$ in these reactions may be explained only by ~~branching~~ cut of the type πP (P = vacuum pole, see Table I), which may have a different parity and not tend to zero at $t \to 0$. In this case, the ~~branching~~ cut contribution must be taken to be 1.5 - 2 times greater than for the eikonal estimate /20/.

6. One of the most interesting predictions linked with the presence of ~~branching~~ cuts is that in studying the production cross-section σ_n as function of the number of particles n we should observe for large energies characteristic minima for n = N, 2N, 3N etc. /21,22/ (see Fig. 1.20 a, N = multiplicity of the particles in the fluctuation corresponding to one Reggeon). In reality the graph of Fig. 1.10 corresponds to the fluctuation of Fig. 1.12 in which on the average 2N particles are produced etc. If in each fluctuation the particles are distributed according to Poisson's law, then the dependence of Fig. 1.20 a

is obtained. For present-day energies the peaks overlap (since $N \leq \sqrt{2N}$, where $\sqrt{2N}$ is the width of the peak), and consequently the ~~branching~~ cuts must lead to a dependence of σ_n on n which is wider than for the Poisson distribution. Such a widening is observed in fact in the experiments /23/, and for its explanation it is sufficient to suppose the ~~branching~~ cuts contribution obtained from the eikonal estimate /24/.

7. The cut leads to a strong dependence of the average number of π-mesons ($\langle n_0 \rangle^-$) for a given number of $\pi^-(n_-)$ on n_-, even if in one fluctuation (one Reggeon) π and π^0 are produced independently /25/. In reality in each fluctuation the average number of π^0 is equal to the average number of π^- (see Fig. 1.20 c), but the average number of π^0, produced by q fluctuations, is equal to $\frac{q}{2}N$, because the function $\langle n_0 \rangle^-$ will have small steps in the regions of $n = \frac{q}{2}N$. For present-day energies the dependence will be $\langle n_0 \rangle = n_-$ up to the time when all of the peaks in σ_n are overlapping. The experimental results can be explained if use is made of the eikonal /25/ for estimating the ~~branching~~ cut contribution.

8. If we consider the reactions of the inclusive type (for example $p + p \to p$ + ~~all the remainder~~ anything), whilst measuring the protons with longitudinal momenta, close to the momentum of an incident particle ($x = \frac{q_\parallel}{p} \to 1$, $q_\parallel$ = longitudinal momentum of the particle being recorded, p is the pulse of the incident hadron), then for an increase in the longitudinal momentum of the recorded particle the multiplicity of all particles produced in this reaction should increase /26/. In reality if for small $q^\perp$ a contribution is given to this process by the graph of 1.21 a, then, as $q^\perp$ increases the contribution of the ~~branching~~ cuts

~~points~~ increases (their contribution falls more slowly as $q_\perp$ increases) and the graphs of type Fig. 1.21 b and c become substantial. However the number of particles which correspond to these is equal to 2N and 3N etc. $N = a \ln s'$ is the multiplicity of particles in the processes of Fig. 1.21 a.

To sum up, we may say that a sufficiently large number of characteristic features of the processes at high energies are linked with the presence of multi-Reggeon exchange and, if we speak of figures, the correct evaluation of the value of this exchange is given by the eikonal multiplied by a coefficient of 1-2. In other words, the contribution of the graphs of type Fig. 1.11 is small at high energies.

Results of the latest development of the theory [22,27]

It is a well known fact that the total ~~interaction~~ cross-sections of hadrons at comparatively small energies fall rapidly as the energy increases, whilst at large energies the total cross-sections are practically independent of energy (in any case, the drop or increase of total cross-sections at $S > 50\ (\text{GeV})^2$ is ~~of a~~ much slower ~~nature~~ than their decrease at $S \lesssim 50\ (\text{GeV})^2$. The problem of the ~~stability~~ constancy of total cross-sections at high energies is one of the most interesting problems in the theory of complex angular momenta. At first sight it is solved very simply: for this one has only to assume that there exists a Reggeon with $\alpha(0) = 1$ (the vacuum Reggeon or Pomeranchuk pole). However a Reggeon introduced in this manner has certain characteristics which are not at all simple. First of all there are no particles (more precisely, no particles have yet been found), which would lie on a trajectory corresponding to this Reggeon. Indeed the trajectory itself is somewhat unusual, in any case, $\alpha' p \sim 0.2 - 0.3\ (\text{GeV}/c)^{-2}$, whilst α' of all remaining Reggeons is of the order of $0.6 - 1\ (\text{GeV}/c)^2$. We are certain that all the remaining trajectories exist, since if the resonances with high spins did not lie on these trajectories (i.e. if their spin did not depend on the momentum transfer small t), then the exchange of a resonance would lead to an increase in cross-section (S^{j-1}, where j is the resonance spin) which would be faster than follows from the Froissard ~~limitation~~ bound ($\sigma \leq \ln^2 S$). For the vacuum trajectory such an argument does not (probably) exist. In this way the vacuum trajectory has been introduced only to explain the constancy of the cross-sections. But it has turned out that it is not so easy to ensure the constancy of the cross-sections, even if it is assumed that a Pomeranchuk pole exists. Already ten years ago it was shown

that the emission of particles from a vacuum Reggeon leads to an increasing section in contradiction with the Froissard condition /28/. The only solution was to assume that the vertex of hadron emission from P disappears at $(K_i^{\perp})^2 \to 0$ (see γ in Fig. 1.22 a). In this way it was clear that the constancy of cross-sections imposed many conditions on the interaction of particles and Reggeons, and right up to recent times it was not clear what this full list of conditions was. By all appearances, these conditions have now been formulated /2-7/. However before enumerating them, let us dwell on the so-called "~~reinforced~~ enhanced" graphs (see for example Fig. 1.22 b). To this, corresponds a fluctuation of the type shown in Fig.1.22 c, in which the second "bunch" of partons is emitted by a particle which is slow in comparison with the incident particle. These graphs provide basically a contribution which, as before, has a factorization characteristic, and they determine the true behaviour of the scattering amplitude at large S, which differs from $S^{\alpha_P(t)}$ /12,29/. The results of works /22,27/ can be formulated in the following manner. To ensure that the total hadron cross-sections at high energies are constant, it is essential that :

1) the cross-sections of all hadrons are equal to each other at $S \to \infty$. This means, for example, that $\sigma_{\pi p} = \sigma_{pp} = \sigma_{pd}$ must be equal and so on. This condition provides a theoretical criterion, as to the energies at which the asymptotic nature occurs.

2) The processes of diffraction dissociation, i.e. the processes in which a resonance or group of particles is produced (see Fig. 1.23 a) owing to the exchange of a vacuum pole, should ~~disappear~~ vanish at $q^{\perp} \to 0$, generally speaking, in accordance with $(q^{\perp}\vec{e})$, where $\vec{e}$ is a vector

(tensor) of polarization of the resonance (of the group of particles), and in accordance with $(q^{\perp})^2$ for emission of a particle with zero spin. The cause of this ~~reduction to zero~~ vanishing can easily be understood ~~on~~ from the parton diagram, since the particles "a" and "c" are described by different wave functions, which are orthogonal to each other at $q^{\perp} \to 0$. This occurs in a similar manner to the disappearance of the ~~disintegration~~ break-up cross-section of the deuteron at $q^{\perp} \to 0$ (see Fig. 1.23 c), since it is proportional to

$$\int d(\vec{\xi}_1 - \vec{\xi}_2)\psi_d(\vec{\xi}_1 - \vec{\xi}_2) e^{i\vec{q}(\vec{\xi}_1 - \vec{\xi}_2)} \psi_{pp}(\vec{\xi}_1 - \vec{\xi}_2) =$$
$$\underset{q_\perp \to 0}{=} \int \psi_d(\vec{\xi}_1 - \vec{\xi}_2)\psi_{pp}(\vec{\xi}_1 - \vec{\xi}_2) d(\vec{\xi}_1 - \vec{\xi}_2) = 0,$$

ψ_{pp}, ψ_d are the wave functions of two free nucleons coupled in the deuteron.

3) All the vertices of emission of a vacuum Reggeon from other Reggeons of type $nP \to mP$, $nP + R \to mP + kR$, $nR \to mP + kR (k \neq 0)$ etc. (see Fig. 1.24) must disappear at $K^{\perp} \to 0$ (K^1 is the momentum over the vacuum Reggeon, P designates a vacuum Reggeon, R is a non-vacuum Reggeon). For example $\gamma_{PPP} = g_{PPP}(k_1^{\perp}, K_2^{\perp})$, $\gamma_{RPR} = g_{RPR}(k_1^{\perp}, k_2^{\perp})$ etc.

4) As has already been pointed out, the vertex of emission of any hadron from a vacuum pole should be vanishing when $K_i^{\perp} \to 0$. For example j_{12} in drawing 1.22 a should be proportional to $(K_1^{\perp} K_2^{\perp})$

In this way, the vacuum pole should have such a high symmetry that at zero momenta it should not interact with anything, except for the

vertices of type $aa \to P$ and $RR \to P$ (a is a particle) - see Fig. 1.24 f, g, i.e. it will provide a contribution only to the processes of elastic particle-and Reggeon-scattering.

The purpose of the following chapters is to discuss how it is possible to prove experimentally that all the above-mentioned consequences are accomplished. As present-day energies are far from asymptotic ($\sigma_{\pi p} \neq \sigma_{pp}$), the question of an experimental separation of the various contributions is not so easy and unambiguous. Subsequently we shall examine in greater detail how the asymptotic characteristics of the vacuum pole can develop at the attainable energies. It is clear that clarification of this question is the most important problem from the standpoint of the present-day theory of hadron interaction at high energies.

pp 54 - 63 (part)

II. Elastic scattering in the region of Coulomb interference and the diffraction peak

It is a well known fact that the measurement of the dependence of the elastic differential cross-section on t in the region of Coulomb interference enables a determination to be made of the real part of the forward scattering amplitude. Consequently this discussion here will concern only the reason why these results are interesting.

The contribution of a pomeron to the forward scattering amplitude is purely imaginary, but the exchange of several pomerons produces in the amplitude also a real part. At high energies the contribution of pomeron ~~branching~~ cuts to the value of $\rho = \frac{Re\,A(0)}{Im\,A(0)}$ is approximately equal to

$$\rho \approx \frac{\pi}{2} \cdot \frac{1}{\sigma_t} \frac{d\sigma_t}{d\ln s} . \qquad (2.I)$$

In the derivation of expression (2.I) use has been made only of the fact that both the pomeron and all pomeron ~~branching~~ cuts have a positive signature and are located, at $t = 0$, a point $j = I$. It is also assumed that the contributions of other features to σ_t and to ρ are not substantial. As has already been mentioned, at a high energy σ_t should increase, approaching a constant maximum (see introduction). In accordance with (2.I), $\rho > 0$ actually diminishes.

For a finite energy, there are corrections to (2.I), which take into account the detailed structure of multi-pomeron exchanges, and

not only the position of ~~branching~~ the cut in the j - plane. In addition, there are the contributions of the non-pomeron exchanges. These, apparently, contribute substantially to ρ for pp- scattering in the energy region 10 - 30 GeV. In any case, in this region $\rho_{pp} < 0$, and ~~exponentially~~ as a power in s tends to zero as the energy increases. However, already at the Serpukhov energies (E < 60 GeV) departures occur from this simple dependence /30/ and a tendency arises for ρ_{pp} to pass through zero at a finite energy (Fig. I.16). Passing through zero ~~appears to be~~ is essential, since at E < 70 GeV $\rho_{pp} < 0$ ~~is smaller than 0~~, and in the asymptotic region $\rho > 0$. However, generally speaking it is difficult to say at precisely what energy $\rho = 0$ and in what manner ρ behaves in the vicinity of this energy. The answers to these questions depend on the structure of the contributions of the various pomeron ~~branchings~~ cuts, and on the relationship of the value of these contributions and of the contributions of the non-pomeron features. Experiments on the CERN colliding beams /31/ indicate that ρ_{pp} passes through zero at E_{lab} = 250 GeV. Recent measurements by the Soviet/American group in Batavia /17/ show that ρ_{pp} increases from -0.156 ± 0.012 at E_{lab} = 51.5 GeV to $+0.039 \pm 0.012$ at E_{lab} = 393 GeV and passes through zero at $E_{lab} = 280 \pm 60$ GeV (Fig. I.16). If the dispersion relations are correct and the Pomeranchuk theorem is right, these results confirm the increase in $\sigma_t(pp)$ discovered at CERN, at least up to 2000 GeV, and contradict the constant nature of $\sigma_t(p\bar{p})$, starting from 120 GeV. Figure 2.I shows also the values of ρ_{pn} at E < 70 GeV /32/. It is obvious that these agree well with ρ_{pp}.

It appears that the measurements of ρ for $\bar{p}p$ - scattering are no less interesting, even at E $\lesssim$ 60 GeV. The reason is as follows. If we judge from the energy behaviour of $\sigma_t(pp)$ and $\sigma_t(\bar{p}p)$, are/then among the non-pomeron contributions to the amplitude of pp and $\bar{p}p$ - scattering the greatest contributions are those of the ω - Reggeon and ρ' - Reggeon, coupled with an f - meson (see Table 1). At $t=0$ $\alpha_\omega(0) \approx \alpha_{\rho'}(0) \approx -\frac{1}{2}$ (here $\alpha(t)$ is the Reggeon trajectory). The ~~residues~~ signs of the of these Reggeons, apparently, are such that their contributions to $\sigma_t(pp)$ ~~are reduced~~ subtract each other, whilst ~~the~~ their contributions to $\sigma_t(\bar{p}p)$ ~~accumulate~~ add. The equality of the residues of ρ' and ω - Reggeons is one of the consequences of the hypothesis of exchange degeneration (see for example [19]), in accordance with which the trajectories and residues of Regge poles of various signatures are equal to each other. The signature of ρ' is positive also in accordance with (I.11) $\eta_{\rho'}(t=0) = i-1$, whereas ω is negative and $\eta_\omega = i+1$ (in this it has been ~~computed~~ considered that $\alpha_\omega(0) = \alpha_{\rho'}(0) = \frac{1}{2}$). Consequently in the case of the pp - interaction, which contains the remainder of $\rho'-\omega$ (see Table II), the imaginary part of the non-pomeron contributions is zero, whereas for $\bar{p}p$ - scattering, which contains the sum of $\rho'+\omega$, the non-pomeron contribution to the imaginary part is great. It is precisely this which explains that in the interval E = 10 - 70 GeV $\sigma_t(pp) = \text{const}$, whereas $\sigma_t(\bar{p}p)$ varies very significantly. But then in the real part of the amplitude of forward scattering, the situation is the reverse: the contributions of ω and ρ' to ρ_{pp} ~~accumulate~~ add, and the contributions to $\rho_{\bar{p}p}$ are reduced. Consequently it may be expected that the contribution of pomeron ~~branching~~ cuts to $\rho_{\bar{p}p}$ will be of significance at energies lower than ρ_{pp}. A measurement at 11.9 GeV/c gives $\rho_{\bar{p}p} = -0.006 \pm 0.034$ with a systematic

error of $\pm$ 0.06 /33/.

In the case of $K^{\pm}$ p -scattering, the situation is very similar to that of pp - and $\bar{p}p$ -scattering. Here also the non-pomeron contributions to $\sigma_t(K^{\pm}p)$, ~~are reduced~~ subtract each other, and we may expect their ~~reduction~~ mutual subtraction also in ρ_{K^-p}. The substantial differences ~~are~~ is that $\sigma_t(K^+p)$ begins to increase at a much earlier time than $\sigma_t(pp)$, and that there are very few data for $\rho_{K^{\pm}p}$ at high energies. Here it is interesting to note that the recent measurement of ρ_{K^-p} at p_{K^-} = 10 GeV/c /34/ shows that $\rho_{K^-p} > 0$ and apparently, depends weakly on the energy in the range p = 1 to 10 GeV/c (Fig. 2.2). It is precisely these features which are expected for the contribution of two-pomeron exchange. It should, incidentally, be noted that a recent measurement at 14 GeV/c, reported to the conference at Aix-en-Provence /35/, gave a value of $\rho_{K^-p} < 0$. Apparently the situation requires further experimental study. In order to demonstrate what value of ρ may be given by pomeron ~~branching~~ cuts, and what value by non-pomeron poles, Figures 1.16 a and 2.2 show the curves for the dependencies of ρ_{pp}, $\rho_{\bar{p}p}$ and ρ_{K^+p}, ρ_{K^-p} on S*. These curves have been computed in the simple model, where account has been taken of a pomeron, two-pomeron ~~branching~~ cut, ρ' and ω.

$$A(0,S) = i\,S\left(0 - \frac{c}{R^2 + \alpha'_P \ln S}\right) + (\rho_{P'} \mp \rho_\omega)\,\xi_\omega \sqrt{S} \,. \qquad (2.2)$$

---

* Similar curves for $\rho_{K^{\pm}p}$, $\rho_{K^{\pm}n}$ have been communicated in papers by K. A. Ter-Martirosyan /36/, where an examination was made of a more realistic model and during ~~processing~~ the fitting of the experimental results no conditions of exchange degeneration were imposed.

The contribution of ~~branching~~ the cuts (coefficient C) has been chosen in such a w as to describe the increase in pp (or $K^+ p$) -cross-sections (see Fig. 2.3) observed experimentally, at $S > 100$ GeV^2 ($S > 20$ GeV^2), the residue ρ' and ω was determined from the remainder of the cross-sections $\sigma(pp) - \sigma(\bar{p}p) = 2g_{\omega}\sqrt{s}$, $\sigma(K^-p) - \sigma(K^+p) = 2g_{\omega}\sqrt{s}$, whereas the real part of the forward scattering amplitude, occurring as a result of ~~branching~~ cuts, has been found by (2.1). As has already been stated, in the $\bar{p}p$ - and K^-n interactions, ReA(o) occurs only on account of ~~branching~~ cuts. Consequently $\rho_{\bar{p}p}$, ρ_{K^-p} are small (of the order of +0.04 - +0.03) and decrease slowly as S increases. At the same time ρ_{pp} and ρ_{K^+p} are negative right up to $S \sim 1000$ GeV^2, and are determined by the contribution of non-pomeron poles, which decreases ~~exponentially~~ as a power in S ($1/\sqrt{S}$) as the energy increases. As can be seen from drawings I.16 and 2.2 even such a simplified model agrees poorly with experiment (when $S > 20$ GeV^2). This is due to the fact that in the case where there is an exchange degeneration, the relation (2.1) unambiguously links $ReA(0,S)$ in $\bar{p}p$ (K^-p) -interactions with the speed of the increase in total pp (K^+p) -cross-sections (irrespective of the parametrization of the ~~branching~~ cut contribution). Of course, the curves given must not in any way be considered as precise quantitative predictions, but they give a representation of the scale of the real part occurring as a result of pomeron ~~branching~~ cuts, and of the ~~necessary~~ required accuracy when measuring it.

In the $\pi^{\pm}p$ -system the increase in total cross-sections has not yet been discovered*). It is possible that the measurements of

---

* Recent measurements carried out in the NAL bubble chamber (D. Bogert et al.) at 205 GeV/c give for $\sigma_t(\pi^-p)$, a value of 24 ± 0.5 mb.

$\rho_{\pi^{\pm}p}$ will make it possible to estimate the energy at which it ~~will~~ begin~~s~~. The ~~modern~~ present experimental situation is shown in Fig. 2.4.

To resume, it can be said that a precise measurement of the real part of the forward scattering amplitudes will enable our views of the multi-pomeron exchanges to be made clearer from the quantitative stand-point (and perhaps the qualitative stand-point). In particular, it will be possible to verify whether in fact $\sigma_t(pp)$ and $\sigma_t(K^+p)$ increase owing to a reduction in the ~~branching~~ cut contributions or in fact whether some other mechanism is at work.

In addition, it will be possible to verify in a more reliable manner the reduction in the contributions of ρ' and ω to $\sigma_t(pp)$ and to $\sigma_t(K^+p)$. The point is that ρ' and ω make a contribution to σ_t and to ρ of the same order, whereas the ~~branching~~ cuts contribution to ρ is less than to σ_t. If, therefore, the overall contribution of ρ' and ω to $\sigma_t(pp)$ and to $\sigma_t(K^+p)$ is in fact non-vanishing and is reduced ~~in~~ by the addition ~~with~~ of a ~~branching~~ cut contribution (such a reduction, of course, is possible only in a finite range of energies), then in ρ^-pp and in ρK^-p there will be no such additional reduction, at least at this energy. In this way, if ρ' and ω ~~are~~ do not completely ~~reduced~~ cancel each other, ρ^-pp and ρK^-p should contain negative terms which diminish like a power in S as the energy increases. The assumption of the total ~~reduction~~ cancellation of the contributions ~~of~~ from ρ' and ω is one of the consequences of the hypothesis of exchange degeneracy, which is closely linked with the idea of duality (see for example /19/. A verification of the extent to which exchange degeneracy is true ~~would be~~ is interesting for an understanding of the characteristics of many hadron processes.

Let us point out further, that although ρ and G_t are linked by a dispersion relation, in the conditions where only a limited energy range is accessible for study, measurements of ρ provide information independent of the measurements of G_t .

A further remark can be made in relation to the theoretical accuracy of the measurement of ρ . Usually the accuracy of determining ρ is generally restricted by the indeterminacy of the ~~beta~~ Bethe phase. In the difference of cross-sections of particles and anti-particles on the proton, many indeterminacies are eliminated /37/. The theoretical error for the real part of the crossing-symmetric amplitude, which precisely contains a contribution of pomeron ~~branching~~ cut, sharply diminishes.

In order to find ρ , as we know, it is sufficient to know only the dependence of the elastic cross-section on t in the range of Coulomb interference. Indeed a measurement of the absolute value of the differential cross-section of pp and $\bar{p}p$ -scattering in this field, as can be seen from the scattering example at low energies /38/, enables also the contribution of spin correlations to the cross-section of forward elastic scattering to be found.

Single-pomeron exchange does not give rise to correlations owing to the positive parity of the pomeron and factorization of its contribution. Two-pomeron exchange also does not give this contribution owing to the identicality of the pomerons. However, in the three-pomeron system (Fig. I.15 d) there are states which give a spin correlation, in forward scattering, of the type $(\vec{\sigma}_{1\perp}\,\vec{\sigma}_{2\perp})$, where the transversality

is determined in relation to the momenta of the initial fast particles. At a very high energy, the value of this spin correlation diminishes $\sim (\ln S)^{-5}$ in amplitude ($\sim (\ln S)^{-10}$ in cross-section - see Introduction for further details). As for the value of this at a finite energy, it is difficult to say anything definite. Probably at E $\gtrsim$ 10 GeV, it is less than the experimental error. But even a limitation to the contribution of spin correlation may be important for theory. Let us note that the contribution to spin correlation is given by another configuration of pomerons than to σ_t and ρ. Consequently the information which may be given by a measurement of this correlation is completely independent of the information obtained when measuring the total cross-section, and the real part of the amplitude of forward scattering.

Let us turn now to elastic scattering outside the region of Coulomb interference. Here one of the most interesting questions is the ~~narrowing~~ shrinkage of the diffraction cone. Single-pomeron exchange gives rise to universal ~~narrowing~~ shrinkage of the cone, identical for all reactions which contain it. An exchange of several pomerons as a result of non-factorizability complicates the picture and makes it non-universal. But it does not contribute any differences to the behaviour of the cone for particle and anti-particle scattering. If account is taken of the contribution of more distant, non-pomeron features, the behaviour of the cone becomes different for all reactions. However these contributions should diminish ~~exponentially~~ as a power in S as the energy increases.

Experimentally, a ~~narrowing~~ shrinkage of the cone is observed in pp- and K^+p -scattering. In π^+p -scattering the cone, apparently, also ~~narrows~~ shrinks, but much more slowly. In π^-p- and K^-p -scattering the ~~narrowing~~ shrinkage has not been detected, but in the $\bar{p}p$ the cone even widens out /II/. On the other hand, there are indications that also in π^-, K^-, $\bar{p}$ -scattering on the proton, it is possible to detect a ~~narrowing~~ shrinkage of the cone if we confine ourselves to an examination of fairly small t (for example $|t| \lesssim 0.1$ GeV^2) and sufficiently high energies $E \gtrsim 20 - 30$ GeV /8/. A comparison of elastic pp -scattering in conventional accelerators and colliding beams shows that the contribution of non-pomeron features to the differential cross-section apparently dies away (for small t) at $E \sim 30$-50 GeV. It may therefore be expected that at a high energy, the differential cross-sections of pp- and $\bar{p}p$ -interactions are similar, so that it will also be possible to detect a ~~narrowing~~ shrinkage of the cone in $\bar{p}p$ -scattering. In this way, a comparison of the behaviour of the diffraction cone in various reactions, particularly for particles and anti-particles, at $E > 30$ GeV, should provide important and interesting results.

Another interesting problem is the so-called kink in the diffraction peak, recently discovered in pp -scattering in colliding beams ($E_{lab} \gtrsim 250$ GeV) /39/. It is seen in the fact that at (t) ~ 0.13 GeV^2 there is a change in the progression of the differential peak, so that the slope in a peak measured at (t) < 0.13 GeV^2 , is approximately greater by 2 GeV^{-2} than the slope measured at (t)$>$ 0.13 GeV^2. The nature of the kink is not clear, although a great number of possible explanations have already been put forward. In effect, all of these explanations can be broken down into three groups. In one of these it is assumed that for some reasons or other the

reduction due to
~~deduction of~~ the vacuum Reggeon sharply changes the rate of the drop as the momentum transfer grows at $t \sim t_0 = -(0.1 - 0.15)$ $(GeV/c)^2$. In another, the variation in the slope is linked with a more complex dependence than the linear dependence of the trajectory of the vacuum pole on t (naturally, for explaining the experiment it is necessary that $\alpha(t)$ should change rapidly at $t \sim t_0$). The third group includes the attempts to explain the character of the behaviour of the differential cross-section by the ~~branching~~ cuts contribution. Let us go into greater detail into all of the above-mentioned possibilities. We shall first of all examine whether the behaviour of the residue should be in any way unusual, in order to explain the experimental data. It appears not. For this, it is sufficient to assume that the scattering amplitude

$$A(s,t) = G_p^2(t)\, e^{-\alpha' p \ln s/s_0 |t|} \cdot S, \qquad (2.3)$$

where $G_p(t)$ is the electrical form factor (Fig. 2.5). Let us note that the expression (2.3) arises in a natural manner, for example, in the quark model /40,41/. If the pp -scattering cross-section computed according to (2.3), is ~~processed~~ fitted with two exponents, as is done by the experimenters - see Fig. 2.6), the difference in their slopes is $\Delta b = 2.4$ (experimentally $\Delta b = 2$, see review /15/). However, for this it is necessary to assume $\alpha' p = 0.125$ (where $S_0 = 1\ GeV^2$), which is considerably less than the experimental value $\alpha' p \sim 0.3\ (GeV/c)^{-2}$. Of course we can pose $\alpha' p = 0.3\ (GeV/c)^{-2}$, but then in order to have agreement with the experiment it is necessary to consider $S_0 = 50\ GeV^2$. In this way the kink at $t_0 \sim -0.13\ (\frac{GeV}{c})^2$ appears strange only from the point of view of simple parametrization

$g(t) = e^{-R_0^2|t|}$. The basic qualitative consequence of this type of explanation is the fact that in other reactions, generally speaking, there will not be any kink in the diffraction cone or it will appear to be completely different from that in the pp . For example Fig. 2.7 shows

$$\frac{d\sigma(\pi p)}{dt} = G_\pi^2(t) G_p^2(t) e^{-2\alpha' p \ln S/t} , \qquad (2.4)$$

where the electromagnetic form factor of a π -meson $G_\pi(t)$ is taken in the form of $\sqrt{G_p(t)}$ (this behaviour of $G_\pi(t)$ agrees both with the simple considerations of the non-relativistic quark model, and with experimental data for $G_\pi(t)$ /42/). It can be seen from Fig. 2.7 that the kink in the diffraction peak at πp may be at $t = -0.22$ $(GeV/c)^2$, whilst $\Delta b = 1.7\ (GeV/c)^{-2}$. However the idea that only the behaviour of the residues is responsible for the kink which is observed contradicts the experimental data in respect of the dependence of the slope of the diffraction cone on energy. It is a known fact that the slope at small t ($|t| < 0.1\ (GeV/c)^2$) varies with an increase in $\ln S$ with $\alpha'_{p_1} = 0.28\ (GeV/c)^{-2}$, whereas at ~~great~~ intermediate ~~small t~~ t values $(0.15 \leq |t| \leq 0.5)\ \alpha'_{p_2} \sim 0.1\ (GeV/c)^{-2}$ (see for example /II/). On the contrary, it may be assumed that the entire kink is explained only by the variation in $\alpha' p$. In effect, $\Delta b = 2(\alpha'_{p_1} - \alpha'_{p_2}) \ln S = 2.4$ at the ISR energies. The idea why such a rapid variation in $\alpha_p(t)$ should be possible was proposed in /43/. It is that the large contribution to $\alpha' p(t)$ should be given by two- π -meson exchanges, which owing to the smallness of the mass of a pion lead to the small but quickly varying part in $\alpha'(t)$, the value of which depends only on the cross-section of $\sigma_{\pi\pi}$ at large energies. Computation of the graphs of the type shown in Fig. 2.8 a leads to /43/:

$$\alpha_p(t) = 1 + \alpha'_0 t - \frac{\sigma_{\pi\pi}}{32\pi^2} h_1(t),$$

where $$h_1(t) = -\frac{t}{\pi}\left[-\frac{8\mu^2}{t} - \left(1-\frac{4\mu^2}{t}\right)^{3/2} \ln \frac{\sqrt{1-\left(\frac{t}{4\mu^2}\right)^{-1}}+1}{\sqrt{1-\left(\frac{t}{4\mu^2}\right)^{-1}}-1} + \right. \qquad (2.5)$$

$$\left. - \ln \frac{m^2}{\mu^2}\right] = -\frac{t}{\pi} \cdot \begin{cases} \ln\left(-\frac{m^2}{t}\right) & (-t) \gg 4\mu^2 \\ \ln \frac{m^2}{\mu^2} - \frac{8}{3}, & (-t) \ll 4\mu^2, \end{cases}$$

μ is the mass of the pion, m is the nucleon mass. Fig. 2.9 shows the pp -scattering cross-section determined by $\alpha_P(t)$, calculated in accordance with (2.5) where $\sigma_{\pi\pi}$ was taken as 16 mb (Fig. 2.9 a) and 32 mb (Fig. 2.9 b), $\alpha'_0 = 0.21\ (\mathrm{GeV/c})^{-2}$, $b_0 = 7.44\ (\mathrm{GeV/c})^{-2}$. The cross-section $\frac{d\sigma}{dt} = Ae^{-b|t|}$, where $b = b_0 + 2\alpha'|t|\ln S$ in accordance with (2.5). The curve in Fig. 2.9 b quite well describes the experiment and gives $\Delta b = 1.75\ (\mathrm{GeV/c})^{-2}$, which is very close to that discovered in the experiment. However $\sigma_{\pi\pi}$ obtained from the factorized states ($\sigma_{\pi\pi} = \frac{\sigma^2_{\pi\pi}}{\sigma_{pp}}$) is 16 mb. Consequently it is quite possible that the nature of this characteristic behaviour of the cone consists in taking into account both effects: The exponential character of the behaviour of the residues and the presence of two - π -meson exchange in the trajectory of a vacuum Reggeon.

On the other hand, it appears more natural to explain the observed change in the slope of the diffraction cone by taking into account the contribution of ~~branching~~ cuts (i.e. the sum of the graphs in 2.8 b and 2.8 c). In effect, the contribution of ~~branching~~ cuts falls more slowly as t increases, than the contribution of the pole, and consequently at large t the slope should be smaller. Let

$$A(s,t) = g^2\left(e^{R^2t} - ce^{\frac{R^2t}{2}}\right), \qquad (2.6)$$

then $$\frac{\frac{d\sigma}{dt}}{\frac{d\sigma}{dt}\Big|_{t=0}} = \frac{1}{(1-c)^2}\left(e^{+R^2t} - ce^{+\frac{R^2t}{2}}\right)^2, \qquad (2.7)$$

whilst the slope $$b = \frac{d \ln \frac{d\sigma}{dt}}{dt} = \frac{2R^2\left(1-\frac{c}{2}e^{-R^2t/2}\right)}{\left(1-ce^{-R^2t/2}\right)} \qquad (2.8)$$

It can be seen from (2.8) that b increases as $|t|$ rises until the contribution of the pole and ~~branching~~ cuts are equal ($1 = c\ell^{\frac{-R^2 t_0}{2}}$ cuts), and then „b" begins to fall. In this way, allowance for ~~branching~~ cuts leads to an increase in the slope and only at large $|t|$ to a drop. Furthermore, ~~small~~ $t = t_0$ is usually linked with the position of a minimum in $\frac{d\sigma_{pp}}{dt}$ at $t = -1.3\ (\frac{GeV}{c})^2$ and therefore in the region of t which is of interest to us the contribution of ~~branching~~ cuts increases the slope /44/. However the latter argument only applies in the case if it is taken into consideration that ~~branching~~ the cut is of a non-~~amplified~~ enhanced character (i.e. the graphs of the type shown in Fig. 2.8 c). In effect, we know that at present day energies (for which $\sigma_{\pi p} \neq \sigma_{pp}$) the contribution of the ~~amplified~~ enhanced graphs should be great (see for example Fig. 2.8 d). But the ~~amplified~~ enhanced graphs fall rapidly as $|t|$ increases (faster than the non-~~amplified~~ enhanced graphs) and therefore cannot have an effect on the position of the minimum at $t = -1.3\ (GeV/c)^2$. For small t , the graphs of the type shown in Fig. 2.8 d are substantial, and they may lead to a reduction in the contribution of the pole at $(t_0) = 0.1\ (GeV/c)^2$. In this case it is easy to obtain agreement with experiment. For example the cross-section of the form

$$\frac{d\sigma}{dt}\Big/\frac{d\sigma}{dt}_{(t=0)} = \ell^{22t}\left[(1-0{,}58\cdot e^{-\frac{11}{2}t})^2 + 0{,}87\, e^{-11t}\right] \qquad (2.9)$$

satisfactorily describes all the qualitative changes in the experimental cross-section (see Fig. 2.10). Of course, in expression (2.9) the contribution of the real part or of other spin amplitudes is too great in comparison with the imaginary part of the amplitude (the first term in (2.9)). Nevertheless, the expression (2.9) shows that this explanation is also possible in principle. In this way, summing up,

it may be said that on the one hand the kink detected in the diffraction cone is not very surprising from the view point of present day views on the interaction of hadrons at high energies, and on the other hand the precise cause of it is still not known and additional measurements are necessary in various reactions and at different energies. We should also point out that if the kink is linked with $\alpha_p(t)$, then its character is identical in all reactions, whilst measurement of the slope difference Δb falls as the energy decreases (at $S = 52$ GeV^2 $\Delta b = 0.65$ (GeV/c)$^{-2}$ instead of $\Delta b = 1.75$ (GeV/c)^2 at ISR energies ($S = 2300$ GeV^2). Present day experimental information on this phenomenon is very scanty. It is known from experiment simply that there is a kink in pp -scattering at ISR energies, and that apparently it does not exist in π^-p -scattering at 14 GeV /15/ and that it does exist in K^-p -scattering at 10 GeV/c /34/c. At the present time there are no other experiments in which the scattering has been measured with sufficient accuracy either at $(t) < 0.1$ GeV^2, or at $(t) > 0.1$ GeV^2. A comparison of the results of the various experiments points, however, to a possible existence of a kink at other energies /46/.

In order to understand the nature of the kink it is necessary to ascertain to what extent it is universal (i.e. how it develops during the scattering of various particles) and how it behaves as the energy varies. For this purpose fairly accurate measurements of the elastic scatterings of different particles are required in an energy range of 30 - 400 GeV (between the previous accelerator energies and the ISR energies) and at (t) from ~ 0.05 GeV^2 to ~ 0.2 GeV^2, so that it would be possible to determine the slope at $(t) < 0.13$ GeV^2 and $(t) > 0.13$ GeV^2 with an accuracy of at least $\sim \pm 0.5$ GeV^{-2}.

III. Inclusive spectra in the three-Reggeon region

In recent years inclusive reactions have attracted an increasing attention from both theoreticians and experimenters. There are many reviews (for example [15]) containing discussions of experimental results and physics problems related to inclusive reactions. Here we shall discuss only those aspects which have a direct bearing on the proposed experiment to study the three-pomeron vertex. But first of all let us examine one kinematic relation.

Let there be two particles having momenta of p_1, p_2 and masses of m_1, m_2 which collide, forming two other particles (or groups of particles) having momenta of P_3, P_4 and masses of m_3, m_4 (Fig. 3.1). Let us examine this process in the rest system of particle I which we shall denote as the laboratory system. Then we can write the relations :

$$\begin{aligned} s &= (p_1+p_2)^2 = m_1^2 + m_2^2 + 2m_1E_2, \\ m_3^2 &= (p_1+q)^2 = m_1^2 + t + 2m_1q_0, \\ m_4^2 &= (p_2-q)^2 = m_2^2 + t - 2E_2q_0 + 2|\vec{p}_2|\cdot q_{\parallel}, \end{aligned} \tag{3.1}$$

where $q = p_3 - p_1 = p_2 - p_4$ is a four-momentum transfer, q_0 and $q_{\parallel}$ are the time and longitudinal (along $\vec{p}_2$) components, $t = Q^2$. For a large energy $E_2 \approx |\vec{p}_2|$ and $s \approx 2m_1E_2$ so that

$$\begin{aligned} q_0 &= \frac{m_3^2 - m_1^2 - t}{2m_1}, \\ q_{\parallel} - q_0 &\approx \frac{m_4^2 - m_2^2 - t}{2E_2} \approx \frac{m_4^2 - m_2^2 - t}{s}\cdot m_1 \end{aligned} \tag{3.2}$$

If t is fixed, then

$$t = q^2 = -(q_{\parallel} - q_0)(q_{\parallel} + q_0) - \vec{q}_{\perp}^{\,2} \approx -\vec{q}_{\perp}^{\,2} \quad (\text{при } m_{3,4}^2/s \ll 1). \tag{3.3}$$

Let us note that in the laboratory system

$$\vec{q}_\perp = \vec{p}_{3\perp},\ q_\parallel = p_{3\parallel},\ q_0 = T_3 + m_3 - m_2 \quad , \tag{3.4}$$

where T_3 is the kinetic energy of particle 3. Let us introduce also the value $x = \frac{2p_{3c\parallel}}{\sqrt{s}}$, where $p_{3c\parallel}$ is the longitudinal (in direction of $\vec{p}_{2c}$) component of the momentum of particle 3 in the centre-of-mass system. By carrying out the Lorentz transformation, it is easy to find that for a high energy

$$1 - x \approx \frac{q_\parallel}{m_1} - \frac{q_0}{m_1} + \frac{m_1^2 + m_3^2 - t}{s} \approx \frac{m_2^2 + m_3^2 - t}{s} \tag{3.5}$$

Frequently, use is also made of more precise relations:

$$t \simeq -q_\perp^2/|x| - (1-|x|)\left(\frac{m_3^2}{|x|} - m_1^2\right) \quad , \tag{3.3a}$$

$$1 - |x| \simeq \frac{m_2^2}{s} + \frac{2q_\perp^2}{|x|s} - \frac{m_3^2}{s}\left(1 - \frac{2}{|x|}\right) . \tag{3.5a}$$

We see that at a high energy the longitudinal and transverse components Q (or P_3) have a substantially different kinematic meaning. $q_\perp^2$ determine the value of t, since $q_\parallel$ and q_0 determines the masses of the final particles. It is clear (3.3) is correct in any frame of reference which moves with (or against) the momentum $\vec{p}_2$.

Let us now return to the inclusive processes. Let a fast initial particle A collide with a proton of the target which is stationary in the laboratory system, thus giving rise to a stream of fast particles, and that a recoil proton is emitted at a small momentum. We shall be interested in the kinematic configuration, when this process can be described by Reggeon exchange. The amplitude of this process is expressed by the diagram in Fig. 3.2.

In elastic or quasi-elastic scattering all large energies in the reactions have the same order of magnitude. The contribution of a Reggeon contains, as we know, the ~~multiplier~~ factor $\left(\frac{s}{s_0}\right)^{\alpha(t)}$, where $s_0 \approx$ I GeV^2. If, however, the invariant mass M of the stream of fast particles is great in comparison with the usual masses, than there are, in the reaction generally speaking several independent large energies, and the situation becomes complicated. A theoretical analysis shows in this case, that the single-Reggeon contribution to the amplitude contains the ~~multiplier~~ factor $\left(\frac{s}{M^2}\right)^{\alpha(-q_\perp^2)}$. Such a factor can be explained in various ways, for example, on the basis of representation of a multi peripheral model or by introducing complex angular momenta in multi-particle amplitudes. However, here we shall not go into the detail of the theory but shall use the result obtained.

In order, now, to obtain the cross-section of the inclusive reaction

$$A + p \longrightarrow p + \cdots \qquad (3.6)$$

we must summate the square of the amplitude modulus of Fig. 3.2 and integrate over the quantum numbers and momenta of the fast particles of the stream and summate over their number, which is shown schematically in Fig. 3.3a. It can easily be seen that the upper block in Fig. 3.2 can be considered as the interaction amplitude of particle A with Reggeon α with the formation of real particles. With this approach, the upper part of Fig. 3.3a contains the total cross-section of Reggeon interaction with particle A. The optical theorem links the total cross-section with the absorption part of the forward scattering amplitude, which corresponds to the diagram in Fig. 3.3b.

Generally speaking, the amplitude of the inclusive process may contain several different single-Reggeon contributions of the type in Fig. 3.2. In this case, there appear in the cross-section interference terms which correspond to the fact that the Reggeons in the left and right-hand sides of Fig. 3.3 a, b may be different.

Let us now note that the square of the mass of the stream M^2 plays the same part as the square of the total energy in the cms of S for the usual elastic amplitude. It is, therefore, natural to expect that at large $\frac{M^2}{S_0}$ the amplitudes of the interaction of Reggeons with a particle, in turn, are determined by the sum of the single-Reggeon exchanges. Then we come to diagram 3.3c , which is called the three-Reggeon diagram. Its contribution to the inclusive cross-section is described by formula /48/

$$\rho_{TR}^{\alpha\alpha\beta} \equiv \left(E\frac{d^3\sigma}{d^3p}\right)_{TR}^{\alpha\alpha\beta} = \frac{1}{16\pi^2}\cdot\frac{1}{S}\,a_\alpha^2(q_\perp^2)\cdot|\eta_\alpha(q_\perp^2)|^2\cdot\left(\frac{S}{M^2}\right)^{2\alpha(-q_\perp^2)} \times g_{\alpha\alpha\beta}(q_\perp^2)\cdot b_\beta(0)\cdot\left(\frac{M^2}{S_0}\right)^{\beta(0)}, \tag{3.7}$$

where E and p are the energy and recoil proton momentum, a_α and b_β are the vertices of Reggeon coupling with the particles, $\eta_\alpha(q_\perp^2)$ is the signature ~~multiplier.~~ factor The value $g_{\alpha\alpha\beta}$ describes a three-Reggeon vertex. The ~~multiplier~~ factor $\frac{1}{S}$ is linked with the flow of initial particles. The contributions of the interference terms, where all three Reggeons are different, also are of a form similar to (3.7). In expression (3.7) instead of $-q_\perp^2$ one often writes t . However, at $\frac{S}{M^2} \gg 1$, where this expression was in fact obtained, small t and $q_\perp^2$ practically coincide (see (3.3)), so that if their difference is taken into account, accuracy will be exceeded. If, however, we use (3.7) for the finite

values of $\frac{S}{M^2}$, then t contains the contribution of the longitudinal and time components and it becomes important as to which variable should be used. It is, however, clear that the question of how to write the asymptotic formula in the non-asymptotic region can only be answered on the basis of a more complete theory or experimental data. However, as has already been pointed out, the transverse and longitudinal components of the momentum transfer have, at a high energy, a substantially different meaning. This is once again shown in formula (3.7) where the trajectory and vertices at $S \gg M^2 \gg S_0$ depend on $q_\perp^2$, whereas $\frac{M^2}{S} \approx \frac{q_\parallel - q_0}{mp}$ (see (3.2)). In addition the permissible range of variation in t depends on M^2 and S ($t < t_{min}$). For an insufficiently high resolution this may lead to an erroneous reduction in the cross-sections at small t. Consequently we consider it more reasonable to use precisely $q_\perp^2$, and not t.

Using the variable x, equation (3.7) assumes the form (see (3.5)):

$$\rho_{TR}^{\alpha\alpha\beta} = \frac{1}{16\pi^2 S_0} \cdot g_{\alpha\alpha\beta}(q_1^2) \cdot \alpha^2(q_1^2) \cdot |g_\alpha(q_1^2)|^2 \cdot \varepsilon(0) \times \left(\frac{S}{S_0}\right)^{\beta(0)-1} (1+x)^{\beta(0)-2\alpha(-q_1^2)} \cdot \qquad (3.7a)$$

In this way, the energy dependence of the inclusive cross-section in the three-Reggeon region at x = const is determined by the sum of the Reggeon contributions (more precisely, the upper Reggeons in Fig. 3.3c). Here the non-pomeron contributions, for which $\beta(0) < 1$, decrease ~~exponentially with~~ as a power of the energy.

Formally equations (3.7) and (3.7a) can be used when

$$\frac{S}{M^2} \gg 1, \frac{M^2}{S_0} \gg 1, q_\perp^2 \approx m^2 \; ; \quad \text{i.e.} \; \frac{S}{S_0} \gg \frac{1}{1+x} \gg 1. \qquad (3.8)$$

We shall discuss the experimental situation below but it is already clear from (3.8) that in order to determine the three-Reggeon contribution to the inclusive cross-section much greater energies are required than for observing the Reggeon behaviour of two-particle amplitudes, where only $\frac{s}{s_0} \gg 1$ is required (let us recall that $S_0 \approx$ I GeV^2).

The conditions of (3.8) show also that in the three-Reggeon range, the value of x should be close to -1. $x \to -1$, the inclusive cross-section ~~behaves exponentially,~~ goes as a power and it may either decrease or increase. But even if the cross-section increases, it remains, of course, limited, since in the physical region $1 + x > \frac{2(m^2 + q_\perp^2)}{s}$.

Of special interest is the case where all three Reggeons are pomerons. In accordance with (3.7) the three-pomeron contribution to the inclusive cross-section is of the form :

$$\rho_{TP} = G(q_\perp^2) \cdot (1+x)^{-1+2\alpha' p q_\perp^2}, \qquad (3.9)$$

where use was made of the expansion of the trajectory of the pomeron $\alpha_P(-q_\perp^2) = 1 - \alpha' p q_\perp^2$ at small $q_\perp^2$.

In order to obtain the contribution of the inclusive three-pomeron cross-section to the total cross-section of interaction it is necessary to integrate ρ_{TP} in the three-Reggeon region over the recoil proton momenta. The invariant phase volume can be conveniently integrated over the azimuthal angle and expressed by the variables x and $q_\perp^2$ (at $|x| \approx 1$).

$$\int \frac{d^3p}{E} \approx \pi \int dx\, dq_\perp^2 .$$

If $G(0) \neq 0$, then at $S \to \infty$ the three-pomeron contribution to the total cross-section increases in accordance with $\sim G(0) \ln \ln S$. If the three-pomeron contribution remained ~~restricted~~ limited at $S \to \infty$, then its increase might have been compensated by the reduction in the contribution from other kinematic regions and the total cross-section might have remained constant. But since it increases in an ~~unrestricted~~ unlimited manner, it cannot in any way be compensated. In this way, if the total cross-section is asymptotically constant, then $G(0)=0$, i.e. $g_{ppp}(0)=0$, where g_{ppp} is the vertex of coupling of the three-pomeron. This result is important not only for the behaviour of inclusive cross-sections, but also for understanding the structure of pomeron ~~branching~~ cut and the trajectory of the pomeron /14/, since its verification is very interesting.

The study of the three-Reggeon region is generally very interesting since it provides substantially new information concerning the trajectories and other properties of Reggeons. But the study of the three-pomeron contribution is of particular importance. As has been explained, it is expected that $g_{ppp}(0) = 0$. However, pomeron ~~branching~~ cuts may imitate the effective three-pomeron coupling with $g^{ef}_{ppp}(0) \neq 0$. The three-pomeron region may prove responsible for the main part of the observed increase in the cross-sections of K^+p and pp -interaction /15,49,50/, and it may determine the energy behaviour of the correction in scattering on a deuteron /50,51/ etc. A more detailed discussion of the contribution of ~~branching~~ cuts will be found below .

Let us examine the experimental situation. The investigation of three-pomeron contribution has hitherto been made only in the

$p + p \to p+\ldots$ reaction on the CERN colliding beams and in $p+p \to p+x$ and $\pi^{\mp} p \to x + p$ at Batavia. At CERN the measurements of the inclusive cross-section have been carried out at four ISR energies $|t| \gg 0.15$ GeV^2 and $|x|$ up to unity, but with an error of $\Delta x \sim 0.01$-0.02 /52-54/. The measurements at Batavia were carried out by various groups with different methods /23,53,55-57/. They cover a wide range of S and t. The absolute calibration of the cross-sections in these measurements however is apparently of a preliminary nature (the error in the absolute normalization is $\lesssim 30\%$).

Figures 3.4 - 3.6 show the existing experimental data for proton spectra obtained at Batavia and CERN for small q_1^2. Here it should be noted that the drop in cross-section observed in Fig. 3.5f at $t \sim 0.03$-0.05 GeV^2, may obviously be linked with the fact that in this case, for a large part of the interval over M^2 there was the inequality $|t| \lesssim |t_{min}| = m^2 M^4/S_2$ (and such events were kinematically prohibited). This situation once again points to the fact that it is preferable to make the search for spectra at small transfers and non-asymptotic energies as a function of q_1^2 (which may be vanishing) and not as a function of t.

In order to describe the existing ISR spectra it was sufficient to take into account two Reggeons: the Pomeranchuk pole P with $\alpha_P(0) = 1$ and the Regge pole R with $\alpha_R(0) = 1/2$ /50,55/. This pole provides an effective description for the contributions of P', ω and other Reggeons, which it has not yet been possible to break down. The contribution of the terms which describe the interference of P and R is apparently small and it can be disregarded. In this way, in the inclusive cross-section there remain the terms PPP, RRP, PPR and RRR, where the first two symbols correspond to the lower Reggeons and the third symbol to the upper Reggeon in Fig. 3.3c (*). In this examination we

(*) See footnote next page

have disregarded the contributions of the poles lying to the left in the j -plane. However as shown by the model calculations /59/, at small $q_\perp^2$ the contribution of the π -pole is quite substantial. For example at $x \lesssim 0.8$ the contribution of $\pi\pi P$ is equal to the contribution of RRP at $p_\perp^2 \lesssim 0.2$ GeV^2.

As follows from an analysis of recent measurements at Batavia of the $p + n \to x + p$ reaction /60/ (which was isolated in a study of the $p + d \to x + p$ process), the inclusive cross-sections of this reaction should be described well by the contribution of the π-pole (term $\pi\pi P$) (see Fig. 3.7). As the role of the π -exchange sharply increases at small $q_\perp^2$ $\left(\rho_{\pi\pi P} \sim \frac{-t}{(t-\mu_\pi^2)^2}(1-x)\right)$, its contribution must be taken into account even when analyzing the data for the $A + p \to x + p$ spectra at not too small $1-|x|$ $((1-|x|) \gtrsim 0.05)$ and fairly small $q_\perp^2$ (less than or of the order of several ~~hundred~~ hundredths GeV^2).

The ISR data at $S \gtrsim 1000$ GeV^2 within the limits of measurement accuracy ($\sim 20\%$) do not depend on energy at a fixed x (see Fig. 3.8). In accordance with (3.7 a), this means that they are sensitive only to the term PPP and RRP. The three-Reggeon description is us able at $|x| \gtrsim 0.8$ /50/. In the interval $0.8 < |x| < 0.9$ the main contribution is RRP , which slowly decreases for $|x| \to 1$. For $|x| \gtrsim 0.95$ it is the contribution of PPP which begins to play the main role, which increases at $|x| \to 1$. A comparison of ISR data

* Let us note that in the theory with the asymptotically constant total cross-section the vertices $g_{PPR}(0)$, $g_{PRP}(0)$, $g_{RPR}(0)$ should also vanish, when p is a true pomeron.

and previous accelerator data indicates the important part played by the non-scaling $\sim 1/\sqrt{s}$ of the term RRR [50]. This confirmation agrees with the Batavia results [55] (see Fig. 3.9, 3.10). Here we should stress the particular importance of the experimental determination of the term RRR, and its dependence on $q_\perp^2$ in the region of small momentum transfers. We shall note first of all that the contribution of this term at small $q_\perp^2$ to the spectrum $\rho_{RRR} \sim \frac{1}{\sqrt{1-|x|}} \frac{1}{\sqrt{s}}$ actually increases at $|x| \longrightarrow 1$, which complicates isolation of the effective contribution of PPP. Furthermore the size of ρ_{RRR} is very substantial, for example, when calculating the contributions of the spectra to the total cross-sections and for checking the various laws of the sums for the inclusive cross-sections.

As far as the PPR term is concerned, there [illegible]ubstantial data relating to such values of S and X where the spectra are not sensitive to the PPR contribut[illegible], which at small $q_\perp^2$ is proportional to $s^{-1/2}(1+x)^{-3/2}$. An indirect representation of this term can be obtained in the following manner [50]. Extrapolation to the "infinite energy" of the missing mass spectra in the $p + p \longrightarrow p + MM$ reaction at $E < 30$ GeV makes it possible to find the "cross-section" of pomeron scattering on a proton σ_{Pp} at $M^2 \leqslant 6$ GeV^2. The same cross-section from the ISR data at $M^2 = 50$ GeV^2 and 100 GeV^2 agrees with the fact that σ_{Pp} = const at $M^2 > 6$ GeV^2 (see Fig. 3.11). As the variation in σ_{Pp} at large M^2 is determined by the term PPR this indicates that the effective vertex of PPR is not great. To isolate directly this term we need measurements of the inclusive spectra at $(1+x) \leqslant 0.05$ (i.e. for small $-t$ at recoil proton momenta of $P_{11} \leqslant 45$ MeV) and 100 GeV$^2 \leqslant S \leqslant 1000$ GeV^2 (i.e. at the initial energies E in the 50-500 GeV range).

Let us now turn to the term PPP . The ISR data at $|t| \gtrsim 0.15$ GeV^2 can be described, by assuming both $G_{ppp}(0) \neq 0$, and $G_{ppp}(t) \sim t e^{At}$ /50/. However, the data of Batavia, obtained in a bubble chamber at $|t| \geq 0.05$ GeV^2 , which are normalized to the ISR data, show clearly that $G_{ppp}(0) \neq 0$. A comparison of the Batavia and ISR data also points to the fact that the slope $G_{ppp}(t)$ at $|t| < 0.1$ (GeV/c)^2 is possibly greater than at $|t| >$ 0.1 (GeV/c)^2 /23/. This change in the slope may have the same nature as in elastic pp -scattering (see section II). It would be very interesting to study this question in greater detail, having progressed into the region of smaller $q_\perp^2$. If subsequent investigations show that $G_{ppp}(0)$ is really non-vanishing, it will mean that either the total cross-section cannot be asymptotically constant, or that pomeron ~~branching~~ cuts is a substantial contribution, imitating the three-pomeron term. In the second case, the question arises as to how to distinguish the effective three-pomeron term from the true one. As the need to review the nature of the pomeron has not been proved yet, we shall start here from the second possibility and discuss in greater detail the contribution of ~~branching~~ cuts.

From the derivation of the expression for the three-pomeron term, it is clear that its contribution to the inclusive cross-section occurs on account of the diffraction dissociation of the incident particle A with the excitation of very large masses M (by the exchange of one pomeron). Consequently the vanishing of the three-pomeron vertex at $\vec{q}_\perp = 0$ denotes that at $\vec{q}_\perp = 0$ the amplitude of diffraction dissociation must vanish, at least, for the case of excitation of fairly large masses. But this in turn means that at $\vec{q}_\perp = 0$ the vertex which links a pomeron with the particle A and with the state with the large mass M vanishes (see Fig. 3.2).

As a result, at $\vec{q}_\perp = 0$ the diffraction excitation of the state with large masses occurs only on account of the exchange of two or more pomerons (Fig. 3.12). Unlike single-pomeron exchange, which at $\vec{q}_\perp = 0$ is asymptotically constant, the contribution of multi-pomeron exchange decreases as a certain power of $\ln s$. This power is smallest for two-pomeron exchange, and it may be expected that it is precisely this contribution which is ~~fundamental~~ dominating already at energies which are not very great. Then the inclusive cross-section at a high energy and M^2 = const, $\vec{q}_\perp = 0$ is determined by the diagram of Fig. 3.13 (instead of diagram 3.3b for the single-pomeron exchange) and we obtain (instead of a constant)

$$M^2 \frac{d^2\sigma}{dq_\perp^2 dM^2} = \text{const} \cdot \frac{M^2}{s} \cdot E\frac{d^3\sigma}{d^3p}\Big|_{\substack{s\to\infty \\ q_\perp^2=0,\ M^2=\text{const}}} \sim \frac{1}{(\ln s)^4} \qquad (3.10)$$

In this way, when taking into account ~~branching~~ cuts the inclusive cross-section at $\vec{q}_\perp = 0$ is non-vanishing, even if $g_{PPP}(0) = 0$. At first sight the two-pomeron exchange may ~~differ~~ be different from the single-pomeron exchange ~~in~~ by the ~~reduction~~ rate with energy. In reality, the situation is not so simple. In effect, the experiments are set up at a small, but finite, $q_\perp^2$, where the single-pomeron contribution is always non-vanishing and always decreases with energy. This decrease is ~~exponential~~ as a power in s ($\sim s^{-2\alpha' p\, q_\perp^2}$), but at a small $q_\perp^2$ and in a finite range of energies it is difficult to distinguish it from the logarithmic. Consequently, in order to clarify what exchange is fundamental at $q_\perp^2 \to 0$, it is necessary to study not only the energy dependence of the inclusive cross-section (at constant $q_\perp^2$ and M^2), but also the variation in this dependence at $q_\perp^2 \to 0$.

If the main exchange remains the single-pomeron exchange (i.e. $g_{PPP}(0) \neq 0$), then

$$M^2 \frac{d^2\sigma}{dq_\perp^2 dM^2} = \text{const} \cdot e^{-(R^2 + 2\alpha' p \ln s) q_\perp^2} . \qquad (3.11a)$$

If, however, $g_{PPP}(0)=0$ and the single-pomeron contribution dies away at $q_\perp^2 \to 0$, then for the purposes of the evaluation the cross-section may be written in the form

$$\left(M^2\frac{d^2\sigma}{dq_\perp^2 dM^2}\right)^{eff}_{3P} = Bg_{PP}^2 e^{-(R^2+2\alpha'_P \ln s)q_\perp^2} - \frac{Cg_{PP}^2 e^{-(R_2^2+\frac{3}{2}\alpha'_P \ln s)q_\perp^2}}{\left(1+\frac{2\alpha'_P}{R_1^2}\ln s\right)^2} + \frac{De^{-(R_3^2+\alpha'_P \ln s)q_\perp^2}}{\left(1+\frac{2\alpha'_P}{R_1^2}\ln s\right)^4}, \qquad (3.IIb)$$

where B, C, D are constant coefficients, R, R_1, R_2, R_3 are certain characteristic radii. Both the coefficients and the radii, generally speaking, are different and vary with M^2. In (3.IIb) the first and third terms describe the contributions of a pomeron and ~~branching~~ cuts, and the second term describes their interference. It is obvious that (3.IIa) has a simple energy dependence, which varies steadily as $q_\perp^2$ decreases. In (3.IIb) both the energy dependence and its variation with $q_\perp^2$ have a more complex form.

Let us examine the structure of the expression (3.IIb) more closely. For any energy and sufficiently small $q_\perp^2$ the main factor is the ~~branching~~ cut contribution. But if we fix this value $q_\perp^2$ and increase the energy, then the main contribution is that of the pole. However, when the energy increases further, again it is the ~~branching~~ cut contribution which is the main contribution. If the coefficient D is sufficiently great, then at a finite energy $M^2\frac{d^2\sigma}{dq_\perp^2 dM^2}$ decreases steadily with an increase in $q_\perp^2$, although in (3.IIb) there are terms which increase at small $q_\perp^2$. However with an increase in S, there appears, in the angular distribution, a maximum. It occurs at $q_\perp^2 = 0$ and with the increase in S at first moves towards large values of $q_\perp^2$ and then again goes towards $q_\perp^2 = 0$.

At a very large energy the position of the maximum almost coincides with the maximum of the pomeron contribution, i.e. it is situated at $q_\perp^2 \lesssim \frac{1}{R^2 + 2d'_P \ln S}$. The possible absence of a maximum at a finite energy is assisted also by the negative sign of the interference term (if it is in fact negative).

The ~~branching~~ cut contribution also leads to a variation in the dependence on X. If, when there is only the contribution of a pomeron $(1+x)\frac{d^2\sigma}{dx\,dq_\perp^2}\Big|_{q_\perp^2=0} \xrightarrow[s\to\infty]{} \text{const.}$, then when ~~branching~~ the cut is taken into account terms appear which contain expressions of the type

$$\left(1 + \frac{2\alpha'_P}{R^2} \ln \frac{1}{1+x}\right)^{-1}.$$

An explanation of the properties of these terms calls for an analysis of the structure of the top block in Fig. 3.13. For example, the diagram of Fig. 3.14a give a contribution which does not depend on energy but decreases according to $\sim \left(\ln \frac{1}{1+x}\right)^4$, whilst the diagram of Fig. 3.14b gives a slower decrease at $X \to -1$, but contains however a ~~reduction~~ decrease with S at $S \to \infty$, $Y = \text{const}$. Apparently, for the break-down of the contributions of + pole and ~~branching~~ cuts it is necessary to have a full analysis of the dependences of the inclusive cross-section on M^2 (or x), t (or $q_\perp^2$) and S. Unfortunately we know very little at present of the structure of ~~branching~~ cuts and cannot give any substantiated knowledge at all about the radii and coefficients in expression (3.IId). As a simple qualitative illustration let us examine more closely the ~~branching~~ cut corresponding to the graph in Fig. 3.12, 3.14a and the interference of this ~~branching~~ cut with the single-pomeron term (Fig. 3.2, 3.14b). The contribution of these diagrams depends only on $q_\perp^2$ and (1 + x)

and leads to a cross-section

$$(1+x)\frac{d^2\sigma}{dx\,dq_\perp^2} = B\Big[q_\perp^2 e^{-(R_4^2+2\alpha'_P \ln\frac{1}{1+x})q_\perp^2} - \frac{2dq_\perp^2 e^{-(R_5^2+\frac{3}{2}\alpha'_P \ln\frac{1}{1+x})q_\perp^2}}{(1+\frac{2\alpha'_P}{R_6^2}\ln\frac{1}{1+x})^2} + \frac{d^2}{(1+\frac{2\alpha'_P}{R_6^2}\ln\frac{1}{1+x})^4}\exp\Big(-(R_7^2+\alpha'_P\ln\frac{1}{1+x})q_\perp^2\Big)\Big]. \qquad (3.12)$$

We select the relationships between the radii in (3.12) starting from an eikonal approximation, which, although not true, nevertheless may, clearly , be used for rough qualitative evaluations

$$R_4^2 = 6\ \text{GeV}^{-2},\ R_5^2 = 5\ \text{GeV}^{-2},\ R_6^2 = R_7^2 = 4\ \text{GeV}^{-2}.*$$

For α'_P let us take the present-day value of /17/ $\alpha'_P = 0.3\ \text{GeV}^{-2}$, and let us take the relative value of the ~~branching~~ cut contribution d equal to I (variant I) for I/2 (variant II). The value d = 1 exceeds several times the value of the ~~branching~~ cut contribution usually obtained in the eikonal model.

In connection with this, let us point out that we are discussing the theory with asymptotic constant total cross-sections

---

* Here we have taken account of the fact that the proton may consist of partons (quarks) and that part of the proton radius ($\sim$ half) corresponds to the small probability of collection of partons after backscattering on to a proton. But the second part of the radius relates to the vertex of parton interaction with a pomeron. If is precisely this part of the radius which is determined by the eikonal approximation.

(equal to each other), when the contribution of the precise (asymptotic) pomeron vanishes for inelastic processes at $q_\perp \to 0$. Consequently, in the evaluation used for d account has been taken also of those ~~branchings~~ cuts which are responsible for the fact that at present-day energies the total cross-sections are markedly different from each other. A real evaluation of the contribution of ~~branching~~ cut is the value

$$d \sim \frac{\sigma_\infty^{tot} - \sigma_{exp}^{tot}}{\sigma_{exp}^{tot}} .$$

Taking as σ_∞^{tot} the cross-section of the pp -interaction ($\sigma_\infty^{tot} = \sigma_{pp}^{tot}$), and as $\sigma_{ex}^{tot} - \sigma_{\pi p}^{tot}$, we obtain

$$d \sim \frac{\sigma_{pp}^{tot} - \sigma_{\pi p}^{tot}}{\sigma_{\pi p}^{tot}} \sim 1 .$$

Figure 3.15 shows graphs which demonstrate the expected dependence for model (3.12) of

$$(1+x)\frac{d^2\sigma}{dx\,dq_\perp^2} \quad \text{on} \quad q_\perp^2$$

for two values of x and two values of the parameter d . As is seen at $d = \frac{1}{2}$ and $(1+x)=0.1$, in the region of $q_\perp^2 < 0.05$ GeV^2 a marked reduction in the slope of the curve (II) is observed, whereas at (1 + x) = 0.01, curve II has a maximum in the region of $q_\perp^2 \approx 0.06$ GeV^2 and the cross-section at zero differs by 25% from the maximum. But here too it is not easy to note a drop, since it occurs in a very narrow region of $q_\perp^2 <$ (0.03-0.04) GeV^2. If, however, the ~~branching~~ cut contribution (and we do not know this precisely) is greater (curve I, d = 1), then it will be extremely difficult to note a variation in the slope at $q_\perp^2 \to 0$ in the interval $0.05 > 1 + x > 0.02$. For this it is necessary to make measurements with an accuracy of

the order of 0.1% in the region of $q_\perp^2 < 0.02$ GeV^2 *. Nevertheless, the dependence of the value

$$F(x) = (1+x)\frac{d^2\sigma}{dx\,dq_\perp^2}\Big/_{q_\perp^2=0}$$

on (1 + x) is fairly strong. As (1 + x) varies from 0.05 to 0.02 F (x) decreases by 40% (irrespective of the value of d , since at $q_\perp^2$ = 0 in formula (3.12) there remains only the ~~branching~~ cuts contribution).

It should be remembered, however, that the evaluations made were obtained in a very primitive concrete model and provide only a qualitative representation of the possible scale of anticipated effects. In this way, even in the model case (3.12) it is not easy to detect a ~~falling away~~ decrease in the pole contribution at $q_\perp^2 \to 0$. The ~~branching~~ cut strongly screens this effect, displacing the maximum of the cross-section towards smaller $q_\perp^2$ and blurring it. In the real case, the situation is even more complicated by the presence of non-pomeron contributions, which cause additional distortion to both the angular and energy dependences.

In order to note the reduction in the single-pomeron contribution at $q_\perp^2 \to 0$, measurements of the inclusive cross-sections are required in the range $q_\perp^2 < 0.05$ GeV^2 with a resolution of

*Of course, at particularly small I+x, which are attainable at very high energies, the maximum for $q_\perp^2$ will nevertheless appear. For example, the curves I (d=1) at $I+x_{(I)} = I.8 \times 10^{-3}$ and $I+x_{(I)} = 0.7 \times 10^{-4}$ coincide with the curve II (d=I/2) at $I+x_{(II)} = 0.I$ and $I+x_{(II)} = 0.01$ respectively.

$\Delta q_\perp^2 < 0.01$ GeV^2 and an accuracy not worse than 1-2%. Consequently it is particularly important to investigate the dependence

$$(1+x)\frac{d^2\sigma}{dx\,dq_\perp^2}$$

on x and on the energy in as wide as possible a range and with the best possible resolution. For a more reliable separation of the non-pomeron contributions which decrease $\sim 1/\sqrt{s}$ (or $\sqrt{1+x}$), it is necessary to make measurements not only at the ends of the interval, but also in as large as possible a number of points inside it for a more accurate determination of the pattern of the energy dependence.

Finally, let us discuss yet one possible feature of inclusive cross-sections, which is required in an experimental check. If the cross-sections is determined by the three-pomeron contribution, then it satisfies the condition of factorization for the incident particle A , i.e. the equality for the inclusive cross-sections of two particles A and B on a proton is fulfilled

$$\frac{1}{\sigma_t^A}\cdot E\frac{d^3\sigma^A}{d^3p} = \frac{1}{\sigma_t^B}\cdot E\frac{d^3\sigma^B}{d^3p}, \qquad (3.13)$$

where σ_t^A and σ_t^B are the total scattering cross-sections of A and B on any (but identical) target. When calculating the contributions of ~~branching~~ cuts and non-pomeron terms, the cross-sections, generally speaking, should not be factorized. However, experimentally factorization is effected in a number of cases with satisfactory accuracy even when there are no grounds for describing the cross-sections by the contribution of one Reggeon. The nature of this phenomenon is not clear and requires detailed study. A check of factorization is particularly important in the region of small $q_\perp^2$, since in this

case in the theory with the asymptotically constant total cross-section the contribution of the true Pomeranchuk pole to the spectra tends to zero ($\sim q_\perp^2$) and at large S, when the secondary poles die away, investigations are in fact made only of the contribution of the pomeron ~~branching~~ cuts.

In order to check factorization we need the inclusive cross-sections of the interaction of the various incident particles with a proton of the target in conditions of $S \gg M^2 \gg S_0 \approx 1\ \mathrm{GeV}^2$. If the pomeron ~~branching~~ cut is factorized, the value of the inclusive cross-sections of the various particles enables a more reliable separation of the three-pomeron contribution (although this is in fact the effective one).

If it proves possible to make measurements ~~up~~ down to $|t| \sim 10^{-4}$ GeV^2, then, generally speaking, it is possible to note electromagnetic corrections owing to excitation of an incident particle by the Coulomb field of the proton in the target. A corresponding contribution to the inclusive cross-section is determined by the diagram of Fig. 3.16, which is similar to diagram 3.3b, but with replacement of the Reggeons by photons. At $S \to \infty$ and $x \to -1$ this contribution is equal to

$$\left(E \frac{d^3\sigma}{dp^3}\right)_c = \frac{\alpha}{\pi^2} \sigma_t^{\gamma A} \cdot \frac{1}{\mu^2} \cdot \frac{q_\perp^2}{(1-x)} \cdot \frac{1}{P_{lab}^2}, \qquad (3.14)$$

where $\sigma_t^{\gamma A}$ is the total cross-section of photo-absorption of the incident particle A. Let us remember that $|t| \geqslant |t|_{min} = m^2(M^2/S)^2$. The corrections owing to interference of the Coulomb amplitude with

the powerful hadronic amplitude in the region indicated are not substantial. If particle A is a proton then at $M^2 \gg m^2$

$$\left(\frac{d\sigma}{dq_1^2}\right)_C \approx 0{,}61\cdot 10^{-4}\,\frac{q_1^2}{|t|}\,\frac{1}{1+x}\,\frac{S_{12}}{|t|}\ \text{mb}/(\text{GeV})^4 \qquad (3.14a)$$

The behaviour of the Coulomb term at $x \to -1$, obviously almost coincides with the behaviour of the three-pomeron term (see (3.9)). As must be the case, as the photon spin is equal to 1, so is the pomeron spin too equal to 1 (at $q_1^2 = t = 0$).

If the incident particle is a proton, the cross-section of photo-absorption is, of course known by means of direct measurement. But a target made up by π- or K -mesons is clearly not accessible in the immediate future. In these conditions, a study of the inclusive cross-sections at very small $|t|$ might be an irreplaceable source of information concerning hadron photo-absorption. If the three-pomeron term does in fact die away at $q_1^2 \to 0$, the Coulomb term may possibly be noticeable already at $|t|$ in the interval 10^{-4} - 10^{-3} GeV^2.

IV. Diffraction excitation of resonances

As was discussed in the previous section, the condition of asymptotic constancy of the total cross-sections requires that the pomeron, at $q_\perp^2 = 0$, cannot transform the particle into a state with a great mass M, i.e. for single-pomeron exchange the upper block in Fig. 3.2 should tend to zero at $\vec{q}_\perp = 0$. It may however be shown that an even stronger assertion is correct, namely: at $\vec{q}_\perp = 0$ the pomeron should not transform the particle into any other state, even with a limited mass /27,64/.

As a result, at $\vec{q}_\perp = 0$, the pomeron may provide a contribution only to elastic scattering of the particles.

In quantum mechanics there is a similar phenomenon /27/. If the coupled quantum-mechanics system (for example a deuteron) is scattered at a zero angle by a potential of a very large radius, then there cannot in this case be any rearrangement of the internal wave function of the deuteron, since only elastic scattering is possible, but not its decay or excitation.

In the relativistic theory, a similar interpretation can be given to the disappearance of the single-pomeron contribution at $\vec{q}_\perp = 0$, if the fast hadrons are considered as coupled states of a system of partons with definite internal wave functions /4/.

Thus, the single-pomeron contribution to diffraction dissociation should ~~decay~~ disappear at $\vec{q}_\perp = 0$ for any excited mass M. Consequently, as in the three-pomeron case, which was discussed above, the cross-section of diffraction dissociation in a state with any given mass at $\vec{q}_\perp = 0$

should decrease with energy, and at a high energy the angular distribution should have a maximum and ~~decay to~~ disappear at a zero angle.

As described in the previous chapter, single-Reggeon contributions to excitation of the states with a large mass M are determined by the value S/M^2. This means that the Reggeon condition is established for small masses at ~~an earlier time~~ smaller S than for the large masses. It is expected that the decrease in the contributions ~~from cuts of branching~~ will begin for small masses at a lower energy. Consequently, the diminution in cross-section ~~to the~~ at zero angle for small excited masses probably occurs earlier than for large ones.

The spectra of diffraction dissociation in the region of small masses M , measured at energies of up to 40 GeV, strongly depend on the mass and have sharply expressed peaks, which correspond to the states with definite values of J^P . It is natural first of all to study the excitation of these states, which occurs with great intensity. We shall, in fact, discuss this later in this section. We shall talk of these ~~conditions~~ states as resonances, although in reality it will be unimportant for us whether these are true resonances or, in fact, kinematic reinforcements which have specific quantum numbers.

Let us examine briefly what sort of states these are.

In the spectrum of diffraction dissociation of the proton, the most intense is the overlapping state of N (1470) with $J^P = 1/2^+$, N (1520) with $J^P = 3/2^-$ and a peak at $M \approx 1700$ MeV, which is formed

by several resonances which lie close to each other. The states with even greater masses are not so sharply distinguishable.

In the dissociation spectra of the π-meson, the peaks A_1 ($M \approx 1100$ MeV, $J^P = 1^+$) and A_2 ($M \approx 1300$ MeV, $J^P = 2^+$) which overlap are clearly visible. Somewhat less visible is the peak A_3 ($M \approx 1600$ MeV, $J^P = 2^-$). Similar states are visible during dissociation of the K -meson. This is a peak in the Q -region ($M \approx 1300$ MeV, $J^P = 1^+$), a resonance K (1420) with $J^P = 2^+$ and an L-region (1700-1800 MeV) with preferential values of $J^P = 2^-$.

For the majority of the resonances, the tendency to zero of the single-pomeron contribution at $\vec{q}_\perp = 0$ is the result of the assumption concerning the asymptotic constancy of total cross-sections. However for some boson resonances, this effect may be the consequence of simpler causes. Thus, in the case of the dissociation $\pi \to A_2$ or K $\to$ K (1420) the pomeron cannot give a contribution at $\vec{q}_\perp = 0$, owing to conservation of parity. In effect, the pomeron has a positive parity and as a result of the factorization of the single-pomeron contribution, the vertex $\pi A_2 \rho$, after it ~~turns~~ has been multiplied with the tensor of polarization A_2, must be pseudo-scalar. But at a zero angle, when all the momenta have identical directions, there are not enough vectors for constructing a pseudo-scalar. For Fermion resonances, this prohibition does not arise, since in constructing the vertex it is possible to use the pseudo-scalar σ_{11} . (Let us remember that as already discussed in the Introduction, the longitudinal and transverse components of the momenta, polarization vectors etc. are included in the Reggeon vertices and amplitudes separately).

Thus, at $\vec{q}_1 = 0$ the contribution to the diffraction excitation of resonances may provide only multi-pomeron exchanges, i.e. ~~branching~~ cuts (see Fig. 3.12). The slowest to decrease with energy is the contribution of two-pomeron ~~branching~~ cut, and consequently it may be expected that it is precisely this contribution which is the main one. As has already been said in the Introduction, two-pomeron contribution to the elastic amplitudes decreases in accordance with $\sim \frac{1}{\ln s}$. In the case of diffraction dissociation, the disappearance of the inelastic pomeron vertices at a zero transverse momentum of the pomeron leads to a more rapid decrease in the contribution of two-pomeron exchange, $\sim \frac{1}{(\ln s)^2}$. This fact has already been used in (3.11 b).

Since the excited resonances have a specific value of spin and parity, the question arises as to the spin structure of the amplitude. In all cases which are of practical interest, the two-pomeron contribution at a zero angle has (taking into account the identicality of the pomerons) the same spin structure, which is attainable kinematically for the single-pomeron contribution. More concretely, this means that at $\vec{q}_1 = 0$ the helicity is conserved in each vertex of the diagram in Figure 3.12 in particular, whereas the spin correlations between the vertices are non-existent. For example, in the reaction $\pi p \to A_1 p$, at $\vec{q}_1 = 0$ the two-pomeron contribution to the amplitude is proportional to $e_{\parallel}$ ($\vec{e}$ is the polarization vector of the resonance A_1 in its rest system), i.e. at a zero angle the two-pomeron exchange may excite A_1 only in the state with zero helicity, as in the case of the incident π-meson. The helicity of the proton in this case, is, of course, conserved. // A variation in the helicity of the resonance in comparison with the helicity of the initial particle may occur at $\vec{q}_1 = 0$ only with a simultaneous variation in the helicity of the proton, i.e. these

Paragraph.

terms in the amplitude describe, in substance, the usual spin correlations. For example for $\pi p \to A_1 p$ they are proportional to $[\vec{e} \times \vec{\sigma}]_n$. The spin correlations occur only during the exchange of three or more pomerons (Fig. 4.1), as also in the case of elastic pp -scattering (see section II). Even the configuration of the three pomerons, which leads to spin correlation, is the same as in pp -scattering. Correspondingly the correlation amplitude at $S \to \infty$ also decreases $\sim (\ln s)^{-5}$, as in pp -scattering (in this case the properties of the inelastic pomeron vertices do not accelerate the decrease in amplitude with energy).

We see that the spin correlations fall more rapidly than the terms which conserve helicity. In practice this means that if the spin resonance is greater than the spin of the initial particle, then at a large energy and at a zero angle the resonance must be excited in the aligned state with the same helicity as in the initial particle. This anticipated result does not contradict the experimental data for the reactions $\pi p \to A_1 p$ /65/ and pp $\to$ N (1700) p /66/ at former accelerator energies.

In this way, the contribution of pomeron ~~branching~~ cuts to the diffraction excitation of resonances at a finite energy, as in the inclusive cross-section, may imitate the single-pomeron contribution at $\vec{q}_\perp = 0$, even if the true single-pomeron contribution in this case tends to zero. Consequently a check of the expected properties of the true single-pomeron contribution should be made for resonances precisely in the same way as in the inclusive case (see discussion

in connection with expressions (3.11b) and (3.12)). When the energy is increased in the angular distribution a dip must occur at $q_\perp^2 = 0$, which will become deeper as the energy increases.

Generally speaking, the dip in the cross-section at $q_\perp^2 = 0$ could occur also on account of the large value of the amplitudes with spin rotation, which die away at $\vec{q}_\perp \to 0$ in a purely kinematic manner. For example, in the reaction $\pi p \to A_1 p$, spin ~~rotation~~ flip of A_1 is possible (production of A_1 with a non-zero helicity) as well as that of a proton. However, the effect of the spin rotation of A_1 does not give a contribution to the element of the spin density matrix ρ_{00} (in the system of the S-channel helicity). Consequently, in ρ_{00} the masking effects may be linked only with the proton spin rotation and they may apparently be evaluated from the data for elastic πp-scattering at the same energies and momentum transfers. The corresponding data /68/ for πp-scattering at energies of up to 25 GeV indicate that the contribution of amplitude with proton spin rotation is not great for pomeron exchanges. In contradistinction to this, in the charge exchange reaction $\pi^- p \to \pi^0 n$ (exchange of a ρ-Reggeon) the spin rotation gives a large contribution and gives rise to a minimum in the cross-section at small t /69/. Let us point out that we may eliminate completely the effects due to the spin rotation of the target, by studying the production of resonances on a ^{4}He nucleus.

In addition, the reactions of resonance production on helium have also other advantages:

I) $\frac{d\sigma}{dt}(\pi + {}^4He \to A_2 + {}^4He) \sim t$ (for small t)

even taking into account ~~branching~~ the cut (on account of the zero spin of ^{4}He), which may increase the accuracy of isolating the A_1 resonance in the 3π-system;

2) owing to the fact that the isotopic spin ^{4}He is equal to zero, in the reactions of the production of G-odd resonances by pions on ^{4}He there are no contributions of $\pi, \rho, \omega, A_2, A_1, B$ trajectories, which simplifies isolating the contribution of the pomeron.

Let us examine more closely what dependence on $q_\perp^2$ and S should be expected for the value

$$\rho_{00} \frac{d\sigma}{dt}(\pi + {}^4He \to A_1 + {}^4He),$$

where there are no masking effects linked with spin rotation. For the sake of illustration, let us take a model which allows for the diffraction excitation of A_1 by one pomeron (Fig. 3.2) and by two-pomeron ~~branching~~ cut (Fig. 3.12). In this case the production amplitude of A_1 (with a zero S-channel helicity) by a single pomeron decreases in accordance with $q_\perp^2$ at $q_\perp \to 0$*. But, accordingly, the cross-section of the single-pomeron exchange

$$\rho_{00} \frac{d\sigma^{(1)}}{dq_\perp^2} = \text{const} \cdot q_\perp^2 e^{-(R^2 + 2\alpha' p \ln S/m_{A_1}^2) q_\perp^2}. \qquad (4.I)$$

The amplitude, however, which corresponds to two-pomeron ~~branching~~ cut will not disappear at $q_\perp = 0$, but on the other hand decreases with energy proportional to

$$\frac{1}{\left(1 + \frac{2\alpha' p}{R_1^2} \ln \frac{S}{m_{A_1}^2}\right)^2}.$$

---

* We have no other vector which has a non-zero transverse component by which it would be possible to multiply $\vec{q}_\perp$, in order to obtain a scalar.

As a result we will obtain

$$\rho_{00}\frac{d\sigma}{dq_1^2} = B\left[q_1^2 e^{\gamma\left(\frac{R^2}{2}+\alpha'_P \ln\frac{s}{m_{A_1}^2}\right)q_1^2} - a'\,\frac{e^{-\left(R_3^2+\alpha'_P\ln\frac{s}{m_{A_1}^2}\right)\frac{q_1^2}{2}}}{\left(1+\frac{2\alpha'_P\ln\frac{s}{m_{A_1}^2}}{R^2}\right)^2}\right]^2 \qquad (4.2)$$

We should notice an interesting feature of expression (4.2) compared with (3.12). Owing to the fact that the contribution of the pole decreases here in accordance with q_1^4 (see 4.1), the interference term (the product of the two terms in square brackets of (4.2)) is more substantial than it was in (3.12) *. Consequently there is now a region where the contributions of the pole and ~~branching~~ cut will compensate each other (the expression in square brackets in (4.2) tends to zero) and the value $\rho_{00}\frac{d\sigma}{dq_1^2}$ will have a dip.

This dip will occur at q_1^2 of the order of several tens of GeV^2 and only at a sufficiently high energy when in a certain region of q_1^2, the ~~branching~~ cut contribution becomes less than the pole contribution which is shown schematically in Fig. 4.2.

At small q_1^2 the ~~branching~~ cut predominates, and then as q_1^2 grows the contribution of the pole becomes substantial. At $q_1^2 = q_{1\perp}^2$ these contributions become equal and a dip is observed. Between $q_{1\perp}^2$ and $q_{3\perp}^2$ a single pomeron exchange dominates, leading to a maximum at

$$q_{2\perp}^2 \simeq \frac{2}{R^2+2\alpha'_P \ln s/m_{A_1}^2}$$

---

* In (3.12) both the contribution of the single-pole and the contribution of the interference terms to the cross-section decreases in accordance with $\sim q_1^4$. This occurs as a result of averaging for polarization of the beam particles which is not present in (4.2).

(see (4.1)). And finally at $q_1^2 = q_{31}^2$ there is again a dip, over which there is again a predominance of the ~~branching~~ cut contribution, which decreases more slowly as q_1^2 increases ($\frac{q_1^2}{2}$ in the exponent of the second term in expression (4.2)).

As the energy increases the position of the first dip (q_{11}^2) and of the maximum (q_{21}^2) will move to the left ($q_{11}, q_{21} \to 0$), and the position of the second dip (q_{31}^2) - to the right (Fig. 4.2 b).

All of this is clearly visible from diagram 4.3, which contains the results of calculations in accordance with formula (4.2). Just as in the previous example (3.12), the relationships between the radii were selected on the basis of an eikonal approximation:

$R^2 = 6/36^{-2}$, $R_1^2 = R_3^2 = 4/36^{-2}$, $\alpha_p' = 0.3/36^{-2}$ whereas the relative size of the ~~branching~~ cut contribution α was assumed to be equal to 1, 1/2, 1/4.

In the case where the ~~branching~~ cut contribution is great (Fig. 4.3 a, α = 1), the characteristic dependence of $\rho_{00} \frac{d\sigma}{dq_1^2}$ on q_1^2, which is coupled with the vanishing of the pole contribution at $q_1^2 \to 0$, does virtually not appear. The interference of ~~branching~~ the cut with the pole leads only to an increase in the slope of the curve as the energy increases. But this increase in the slope can easily be taken as the usual ~~shortening~~ shrinkage of the diffraction cone.

At a smaller ~~branching~~ cut contribution (Fig. 4.3 b, d = $\frac{1}{2}$) the minimum occurs, already starting at S = 100 GeV^2, whereas the ~~shortening~~ shrinkage of the cone as a result of interference corresponds to an increase in R^2

by 5 GeV^{-2} with a change in energy from S = 100 GeV^2 to S = 800 GeV^2. However it should be stressed that in the model of (4.12) only the imaginary part of the production amplitude A_1 is taken into account. The real part of this amplitude does not vanish and at S $\simeq$ 100 GeV^2 it may fill in the dip, either reducing it considerably or even removing it totally. But as the real part decreases more rapidly as the energy increases, at S = 800 GeV^2 the dip will still be present (the dotted line shown in Fig. 4.2 b and c). The development of the minimum with an increase in energy may occur roughly as in elastic pp-scattering at $-t \approx 1.3\ GeV^2$ /15/.

The model examined is, of course, of a particularly qualitative nature and demonstrates only the approximate scale of the effects expected. It also shows the degree of theoretical indeterminacy of our predictions. However one prediction remains valid irrespective of the value of the ~~branching~~ cut contribution, namely: the decrease in the differential cross-section

$$\frac{d\sigma}{dq_1^2/q_1^2=0}$$

as the energy increases in the theory with the asymptotically constant total cross-section.

The behaviour described for the angular distribution is expected for the $\pi p \to A_1 p$, $\pi p \to A_3 p$ reactions, but also for the corresponding K-meson reactions and for reactions of the pp → Np type. These are the reactions in which the single-pomeron contribution at $\vec{q}_1 = 0$ is not prohibited on kinematic grounds.

Recently a Soviet/American group in Batavia obtained preliminary results on the measurement of the diffraction excitation of nucleon resonances

in the energy range 175-400 GeV and at $0.01 < /t/ < 0.05$ $(GeV/c)^2$ /70/. It appeared that, within the limits of fairly large errors, the cross-sections of the diffraction excitation of resonances do not depend on energy and their values are close to the corresponding values obtained at energies of below 30 GeV /71/. The dependence on t for excitation cross-sections N (1470) in the range of energies and momentum transfers studied did not, within the limits of error, change in comparison with the data at lower energies /71/. Let us note, however, that the accuracy of these measurements is still not high enough.

As has been mentioned above, the situation is different in the $\pi p \to A_2 p$ reaction, and in the $Kp \to K(1420)p$ reaction. At $\vec{q}_\perp = 0$, the production of A_2 with zero helicity may be caused only by t -channel exchange with a non-natural parity (the states with $P = (-1)^J$ have a natural parity, and those with $P = (-1)^{J+1}$ have a natural parity). But this contribution to the amplitude is provided only by the non-pomeron terms (the η -Reggeon) and decreases as a power of the energy. But the pomeron terms at $\vec{q}_\perp = 0$ can excite A_2 only with a single helicity and with simultaneous rotation of the proton helicity, i.e. owing to spin correlations. Consequently, for diffraction excitation of A_2 at a zero angle an exchange is required of not less than three pomerons (Fig. 4.1), and the cross-section of this process decreases with energy in accordance with $\sim (\ln S)^{-10}$.

Of course we are not able to compare at a finite energy the contributions of the different ~~branchings~~ cuts. A rapid reduction in any contribution at a high energy by itself does not mean that it is small at finite energies. However, the experiment shows that already at energies of ~ 10 GeV [illegible] resonances with a high spin are excited at

small angles in the aligned state [65,66], i.e. already at such energies the spin-correlation terms are small. Consequently we may naturally expect that at these energies the cross-section of the $\pi p \to A_2 p$ process already falls at $\vec{q}_\perp \to 0$, although in the excitation of other resonances this drop is still not visible. It is, for example, a fact that at an energy of E = 40 GeV the angular distribution of the $\pi p \to A_2 p$ reaction has a sharp maximum at $|t| \sim 0.1$ GeV^2 and falls at $|t| \to 0$, whereas in the $\pi p \to A_1 p$ and $\pi p \to A_3 p$ reactions the cross-sections increase rapidly and steadily as $|t|$ falls to $|t| \sim 0.04$ GeV^2 (see Fig. 4.4) [67]. (We should note that here $|t|$ coincides in practice with $q_\perp^2$). Unfortunately, unlike other resonances, the appearance of a minimum in the angular distribution of the diffraction excitation $\pi \to A_2$ at $q_\perp^2 \to 0$ only indicates the small value of the spin-correlation terms and does not give any non-trivial information concerning the single-pomeron contribution. Another reason for studying the inelastic diffraction processes is the following. Generally speaking it is possible to construct theories in which the total cross-section is asymptotically non-constant, but only slowly falls or increases with S. If in the asymptotic form the total cross-section varies fairly slowly, it is difficult in experiments to distinguish it from the asymptotically constant total cross-section*. Experimentally, the case of the asymptotically constant total cross-section is isolated as a

---

* The increase in the total cross-sections of pp- and K^+p -interactions observed in the experiments in all variants of the theory (irrespective of the assumed asymptotic behaviour of σ_{tot}) is linked with a decrease in the contribution of vacuum ~~branchings~~ cuts. The true asymptotic increase [72] (or drop [73]) of the total cross-section

(*contd.)

may appear only in the region $R^2 \ln s/s_0 \gtrsim 1$. The parameter R is expressed by α_P and the three-pomeron vertex $g_{PPP}(0)$ (which is non-vanishing, if the total cross-section is asymptotically non-constant). From modern experimental data the condition arises of $\ln s/s_0 > 100$. It is precisely in this region that the so-called ~~branching intensification~~ enforced cut becomes substantial (see for example Fig. 4.5).

---

result of the vanishing of the single-pomeron contribution to the inelastic processes at $q^2 = 0$ (see Introduction). As a result, the processes of diffraction production of resonances (particle groups) at a zero angle occur as a result of the exchange of at least two pomerons. The cross-section of these processes in the energy range $\frac{\alpha'_P \ln s}{R_0^2} \gtrsim 1$ should fall in accordance with $\sim \frac{1}{(1+\alpha'_P \ln s/R_0^2)^4}$. In all other cases, in this range, the single-pomeron contributions do not vanish at $q^2 = 0$ and the diffraction dissociation at a zero angle is <u>not qualitatively different</u> from elastic diffraction scattering. In particular, if the reduction in the negative contribution from the non-~~amplified~~ enforced two-pomeron ~~branching~~ cut leads to an increase in the total cross-section, it should lead both to an increase in the cross-section of the forward diffraction dissociation in roughly the same energy region and roughly to the same increase as a square of the total cross-section (since $\frac{d\sigma}{dt}\Big|_{t=0} \approx (\mathrm{Im}A)^2 \sim \sigma_{tot}^2$).

In this way, we may expect that if the total cross-section is asymptotically constant, the cross-section of the $\pi + p \to A_1 + p$ forward process will decrease in the energy range $S > 400$ GeV^2. As a result of the higher power of the logarithm ($\sim \frac{1}{(\ln s)^4}$) this effect in the inelastic processes may possibly occur even at lower energies. In the cases involving an asymptotically non-constant total cross-section in this same energy range an increase of the following type may be expected*)

$$\frac{d\sigma}{dq_\perp^2}\Big/_{q_\perp=0} \sim \left(a - \frac{b}{1+\frac{\alpha' \ln S/M^2}{R_0^2}}\right)^2 .$$

Measurements of the slopes of the cross-sections of the inelastic diffraction processes at small q^2 and of the energy dependence of these slopes is of particular interest. Thus, the measurement in the range of small q^2 of the slope of the $\pi p \to A_1 p$ cross-section assists the explanation of the nature of the A_1 resonance (in particular, the question as to whether it is in fact a resonance or a kinematic reinforcement). In addition, information concerning the values of the slopes of the cross-sections of inelastic diffraction processes is necessary for carrying out calculations of the contributions of these processes to the total cross-sections of the pp^-, $\pi^\pm p^-$, $K^\pm p$ -interaction and verification of compliance with the various sum rules for cross-sections.

---

* In the eikonal approximation in the theory with the asymptotically non-constant total cross-section, the cross-section of the forward process $\pi + p \to A_1 + p_2$ increases by 5 - 12% as S increases from 100 to 800 GeV^2.

The study of the diffraction excitation of resonances at high energies and small $|t|$ is a fairly complicated problem. It imposes severe requirements on the resolution of the equipment. For example in order to see the shape of the peak in the mass spectrum, it is necessary to have a ~~stream~~ forward mass resolution of $\Delta M^2 < 0.1$ GeV^2. At $S \sim 1000$ GeV^2, this means that for the recoil proton $\Delta(p_{lab} = T) \lesssim 10^{-4}$ (see (3.2) and (3.4)). In order to obtain such a high angle resolution it is necessary to fix with a high degree of accuracy the emission angle of the recoil proton in relation to the incident beam: $\Delta\varphi \sim 2$ mrad at $\varphi \approx 90°$ and $T \sim 1$ MeV. In addition, in order to separate the overlapping resonances and remove the possible influence of the background on the angular distribution at $q_\perp^2 \to 0$, it is necessary to isolate the state with specific quantum numbers. This can be done by means of phase analysis of the final fast particles ~~in the stream~~. A phase analysis is necessary also in order to determine the helical state of the resonance. In this way it is necessary to detect not only the slow recoil proton but also some fast particles. The situation is to some extent simplified by the fact that for all of the resonances of interest to us there are [illegible] modes of decay into three charged particles, so that there is no need to restore the kinematics of the neutral particles.

Above we have discussed the diffraction production of Reggeons (by the exchange of a pomeron and pomeron ~~branching~~ cuts). However it is also interesting to examine the production of resonances caused by other exchanges, and examine more closely those basic qualitative consequences resulting from the theory of complex momenta, which are obtained for this type of process. This question was examined in

detail in the communications by Kajdalov /74/ . Let us enumerate some of the consequences formulated therein of the theory of complex momenta and the relations of 1.1, which should be experimentally checked at small t.

I) In the $\pi, K)N \to \begin{cases} f(\omega, \varphi, K^*)N \\ f(A_2, f', K^{*a})N \end{cases}$ reactions

$$\rho_{00}\frac{d\sigma}{dt} \sim t \qquad \text{at} \quad t \to 0 (t \ll \mu^2),$$

where ρ_{00} is an element of the spin density matrix of the vector (tensor (2^+)) particle.

2) In the reactions involving the production of two pseudo-scalar mesons the $\pi(K)N \to \pi\pi(K\pi, \rho\pi, K\bar{K})N$ differential cross-section should be vanishing when $t = (p_N - p_{N'})^2 \to 0$ and the angle Θ in the centre of mass system of two mesons between the momentum of one of them and the direction of the momentum of the initial meson tends to zero (or π)

$$\frac{d^2\sigma(s, \cos\theta, t)}{dt\, d\cos\theta} \to 0 \qquad \text{at} \quad \begin{matrix} t \to 0 \\ \theta \to 0 (\pi). \end{matrix}$$

Let us point out that the corrections to these predictions (without taking into account electromagnetic effects) decrease exponentially in accordance with $\sim 1/s^{\gamma}(\gamma \geq 1)$ as the energy increases.

As was discussed in the previous section in connection with inclusive cross-sections, if it were possible to carry out measurements of resonance production up to $|t| \sim 10^{-4}$ GeV^2 , then it would be possible to isolate the contribution of the Coulomb excitation of resonances (Fig. 4.6) and determine from it the photo-absorption cross-section by π- and K-mesons in the resonance region.

V. Doubly inclusive spectra and double-Reggeon processes

In this section we shall study the doubly inclusive reactions

$$A + P \rightarrow A + P + \ldots , \qquad (5.1)$$

in which a small recoil proton and a weakly deflected initial particle are observed, and in addition other particles are formed. We shall be interested in the case where this process is described by the double-Reggeon contribution (Fig. 5.1).

But before discussing it in greater detail we shall again have to concern ourselves with kinematic relationships.

Let us assume that two particles with momenta of P_1 , P_2 , and masses m_1 , m_2 collide and are transformed into three particles (or three groups of particles) with momenta of P_3, P_4, P_5 and masses of m_3, m_4 , m_5 (Fig. 5.2). We shall examine the kinematics of this reaction in the laboratory system ($\vec{p}_1 = 0$), assuming that q_1^2 and q_2^2 are limited.

In accordance with the equalities (3.1) we obtain

$$\begin{aligned} s &= (p_1 + p_2)^2 \approx m_1^2 + m_2^2 + 2 m_1 E_2 , \\ m_3^2 &= (p_2 + q_1)^2 = m_1^2 + q_1^2 + 2 m_1 q_{10} , \\ m_4^2 &= (p_2 - q_2)^2 = m_2^2 + q_2^2 - 2 E_2 q_{20} + 2 |\vec{p}_2| \cdot q_{2n} . \end{aligned} \qquad (5.2)$$

In addition, we insert the values of S_3 and S_4, which can be considered as the square of the invariant mass of the system of final particles, which remains after ~~separation~~ exclusion of particle 3 or 4, respectively. Then

$$s_4 = (p_3 + p_5)^2 = (q_2 + p_1)^2 = q_2^2 + m_1^2 + 2m_1 q_{20},$$
$$s_3 = (p_4 + p_5)^2 = (-q_1 + p_2)^2 = q_1^2 - 2E_2 q_{10} + 2|\vec{p}_2|\vec{q}_{11} + m_2^2. \qquad (5.3)$$

We shall now find the components of the momentum transfers. In this we shall consider that the initial energy is very great and all the masses are limited so that $\frac{m_i^2}{s} \ll 1, \frac{q_i^2}{s} \ll 1$. The values of S_3 and S_4 will be regarded as great and the relations of $\delta_3 = \frac{s_3}{s}$ and $\delta_4 = \frac{s_4}{s}$ shall be accurately calculated. Then from (5.2) and (5.3) we shall obtain expressions for the time and longitudinal components q_1 and q_2 :

$$q_{211} - q_{210} = \delta_3 \cdot m_1,$$
$$q_{20} = \frac{s_4 - m_1^2 - t_2}{2m_1}, \quad \frac{q_{20}}{E_2} = \delta_4, \qquad (5.4)$$
$$q_{20} - q_{211} = \frac{m_1}{s}(m_2^2 - m_4^2 + t_2 - m_2^2 \delta_4),$$

whereas the transverse components are determined from the equalities

$$t = q_1^2 = -\frac{\vec{q}_{11}^2 + \delta_3(m_3^2 - m_1^2 + m_1^2\delta_3)}{1 - \delta_3},$$
$$t_2 = q_2^2 = -\frac{\vec{q}_{21}^2 + \delta_4(m_4^2 - m_2^2 + m_2^2\delta_4)}{1 - \delta_4}. \qquad (5.5)$$

The momentum transfers must satisfy the condition

$$m_5^2 = (q_2 - q_{11})^2, \qquad (5.6)$$

from which we obtain

$$m_5^2 + \vec{p}_{51}^2 = \delta_3\delta_4 s + \delta_3(t_1 - t_2 - m_3^2) +$$
$$+ \delta_4(t_2 - t_1 - m_4^2) - \delta_4^2 m_2^2 - \delta_3^2 m_1^2. \qquad (5.7)$$

At a high energy, the main term in the right-hand part of the equality (5.7) is the first one. Since $\vec{P}_{5\perp}^{\,2} = (\vec{q}_{2\perp} - \vec{q}_{1\perp})^2$, as the energy increases $\vec{P}_{5\perp}^{\,2}$ remains restricted if q_1^2 and q_2^2 are fixed. Consequently $\delta_3 \delta_4 \sim \frac{m_5^2}{s}$, i.e. as the energy increases at least one of the δ_i should fall if m_5^2 is restricted. If S_3 and S_4 are identical in magnitude, then $\delta_3 \sim \delta_4 \sim \frac{m_5}{\sqrt{s}}$ and the equality (5.7) can be further simplified :

$$m_5^2 + \vec{P}_{5\perp}^{\,2} = \delta_3 \delta_4 s = \frac{S_3 S_4}{s} . \qquad (5.7a)$$

It is this relation that we shall use in future.

If we insert as in the usual inclusive processes (in the c.m.s.)

$$x_3 = \frac{2p_{3c.m.}}{\sqrt{s}} , \quad x_4 = \frac{2p_{4c.m.}}{\sqrt{s}} , \qquad (5.8)$$

we obtain

$$1 - |x_3| = \delta_3 ; \quad 1 - |x_4| = \delta_4 . \qquad (5.9)$$

(cf. (3.5) at $m_4^2 \to S_3$). The sign of x_i is determined on the basis of which of the momenta is considered to have a positive direction. Although the determination (5.8) for x_i contains the momenta in the c.m.s., we see from (5.9) and (5.4.) that at a high energy x_i can easily be expressed by the momenta in the laboratory system. Here, $|x_3|$ is determined by the energy and emergence angle of the recoil particle 3

$$1 - |x_3| = \delta_3 = \frac{|\vec{P}_3| \cdot \cos\varphi - T_3 + m_1 - m_3}{m_1} , \qquad (5.10)$$

but $|x_4|$ depends only on the fraction of energy lost by the fast incident particle

$$1 - |x_4| = \delta_4 = \frac{E_2 - E_4}{E_2} . \qquad (5.11)$$

In these equalities $|\vec{p}_3|$ and T_3 are the momentum and kinetic energy of particle 3, φ is its angle of emission in relation to the momentum of initial particle 2, and E_2 and E_4 are the total energies of particles 2 and 4.

Let us now return to the ~~double~~ Reggeon process (Fig. 5.1). As far as the theory is concerned, the first to point to the existence of such processes were Ter-Martirosyan and Kibble /75/. They have also recently been discussed in papers /76/.

The amplitude corresponding to the diagram of Fig. 5.1 contains the Reggeon multipliers

$$(1-|x_p|)^{-\alpha(q_{1\perp}^2)}(1-|x_A|)^{-\beta(-q_{2\perp}^2)}$$

and the "amplitude" of the conversion of two Reggeons into the particles of the ~~stream~~ produced system. In order to obtain the cross-section of the doubly-inclusive reaction (5.1), as in the case of the normal inclusive reaction, we shall summate and integrate over the variables linked with the particles of the ~~stream~~ jet (Fig. 5.3a and b; cf. Fig. 3.3a and b). The inclusive cross-section will be expressed by the "cross-section" $\sigma_{\alpha\beta}$ of the interaction of two Reggeons (more precisely the cross-section of the conversion of Reggeons into the usual particles).

$$\frac{d\sigma}{d\bar{q}_{1\perp}\,dx_p\,d\bar{q}_{2\perp}\,dx_A} = \frac{1}{(16\pi^3)^2}\, g_\alpha^2(q_{1\perp}^2)\, g_\beta^2(q_{2\perp}^2)\, |\xi_\alpha(q_{1\perp}^2)|^2 |\xi_\beta(q_{2\perp}^2)|^2 \times \quad (5.12)$$

$$\times s^{-\cdots}(1-|x_p|)^{-2\alpha(-q_{1\perp}^2)}(1-|x_A|)^{-2\beta(-q_{2\perp}^2)} \times$$

$$\times \cdots(M^2, \bar{q}_{1\perp}, \bar{q}_{2\perp}).$$

If $\cdots, q_{1\perp}^2 \ll M^2$,

then we can use relation (cf. formula (5.7a))

$$M^2 = s(1-|x_p|)(1-|x_A|). \qquad (5.13)$$

At large M^2 the Reggeon cross-section $\sigma_{\alpha\beta}$ may also be described by the sum of the Reggeon contributions, and the doubly-inclusive cross-section is fully defined by the three-Reggeon vertices. It may be expected that at small M^2 the cross-section $\sigma_{\alpha\beta}$, like the cross-sections of interaction of the usual particles, is basically described by the contributions of the resonances permissible in accordance with the quantum numbers.

Let us examine, for example, the expected behaviour of the interaction cross-section of two pomerons. It is clear that the system of normal particles which is produced should also have vacuum quantum numbers. This is already possible for two π-mesons in the S-state, so that the cross-section is non-vanishing at $M^2 > 4\mu^2$. However, the cross-section will obviously remain small until the resonance region is reached. The resonances (or intensifications) in the two-pomeron system should have a zero value for the baryon number, strangeness and isospin, a positive charge parity (and G-parity) and the natural values of spin and parity. In this way the following states appear permissible: $\varepsilon(J^P=0^+, M^2 \approx 0{,}5\,(\text{GeV})^2)$, $S^*(J^P=0^+, M^2 \sim 1\,(\text{GeV})^2)$, $f(J^P=2^+, M^2 = 1{,}6\,(\text{GeV})^2)$ and $f'(J^P=2^+, M^2 = 2{,}3\,(\text{GeV})^2)$. No suitable resonances with a high mass have yet been discovered. Thus, the pomeron-pomeron cross-section will obviously be relatively large at M from ~ 0.3 GeV^2 to 2.5 GeV^2. It is probable that the cross-section will be largest in the region of the f-resonance. At $M^2 \gtrsim 2.5$ GeV^2 it begins to diminish, approaching a constant value which is determined by the three-pomeron vertex which is included in the usual inclusive cross-sections.

The possible trend of the pomeron-pomeron cross-section σ_{pp} as a function of M^2 is shown in drawing 5.4. Of course, the relative height of the various peaks, shown in the diagram, is based only on conjectures, and not on any precise knowledge. Apart from the resonances, the cross-section may display an S -wave ~~intensification~~ enhancement in the two- π -meson system at small M^2 (dotted line in Fig. 5.4). This ~~intensification~~ enhancement may be caused by the so-called Deck effect, which is clearly observed in the inelastic diffraction processes.

It is possible to describe in a similar way the expected behaviour of other Reggeon-Reggeon cross-sections. But however likely such descriptions may appear, they are only hypotheses. Consequently any experimental information concerning the interaction of Reggeons would be very interesting.

Let us consider at what energies we should search for double-Reggeon processes. In order to be able to apply the Reggeon description the following conditions are necessary

$$(1-|x_p|) \ll 1, (1-|x_A|) \ll 1. \qquad (5.14)$$

In addition to enable the usual particles to be produced, the following conditions should be achieved

$$s(1-|x_p|)(1-|x_A|) \geq m_0^2. \qquad (5.15)$$

Here m_0^2 is the production threshold of the normal particle system with the appropriate quantum numbers. However, as has already been said, the cross-section probably becomes pronounced only in the resonance region. Consequently, in (5.15) it is necessary to replace m_0^2 by the square of the resonance mass. This value coincides in magnitude with

$S_0 \approx$ I GeV^2. In this way, we obtain

$$\frac{S}{S_0} \geq \frac{1}{(1-|x_p|)(1-|x_A|)}, \quad \frac{1}{1-|x_p|} >> 1, \quad \frac{1}{1-|x_A|} >> 1. \qquad (5.16)$$

These conditions are reminiscent of the conditions of (3.8) required for applicability of the three-Reggeon formula in the single-particle inclusive process. As in that case too, the necessary energy is substantially greater than the energy required for observing the Reggeon process in two-particle reactions. For example, if we take $(1-|x_p|) \sim (1-|x_A|) \sim 0.1$ (this corresponds to $E \sim 5$ GeV for a two-particle reaction on a proton), then in accordance with (5.16), $S \gtrsim 100$ GeV^2, i.e. $E \gtrsim 50$ GeV. However, already at $E \leqslant 25$ GeV some attempts have been made to detect the double-Reggeon, and in particular the double-pomeron contribution.

In the reaction $\pi^- p \to \pi^-(\pi^+\pi^-)p$ at 25 GeV /77/, it is clear that a double-Reggeon contribution has been discovered, in which a pomeron is linked with a proton, and the π-meson with a Reggeon with $\alpha(0) = \frac{1}{2}$.

In the $\pi^+ p \to \pi^+(\pi\pi)^0 p$ reaction at 8 and 16 GeV/c /78/ it has generally not been possible to isolate the double-Reggeon contribution owing to strong overlapping with the contributions of other mechanisms.

In the $pp \to p(\pi\pi)^0 p$ reaction at 12 and 24 GeV/c /79/ an S-wave peak have been discovered in the $(\pi\pi)^0$ spectrum at $M_{\pi\pi} < 0.6$ GeV, which might be caused by double-pomeron contribution. However, having investigated the correlation of π-mesons with protons, the authors of this paper have come to the conclusion that

the peak is formed by the decay products of nucleon excited states. Only at 24 GeV/c is there ~~any~~ some indication of the possibility of a small double-pomeron contribution. On the basis of the energy behaviour of the experimental data, the authors of paper /79/ hope that the resonance contributions will cease to screen the double-pomeron contribution at $p > 50$ GeV/c.

This particular group studied the $pp \rightarrow pxp$ reactions at the same energies, where $X = \rho^0, \omega, \eta, f$ /80/. The authors consider that their data may satisfactorily be described by the following double-Reggeon contributions: ω and π -Reggeons for production of the ρ^0-meson, ρ - and π -Reggeons for the ω -meson, A_2 and π -Reggeons for the η -meson. The production of the f -meson can clearly be better described by a superimposition of the contributions of $P + P'$ and $P + P$, although within the limits of accuracy it may be described also by each of these contributions individually. It should, however, be noted that owing to the insufficient energy, the comparison of the experimental data was carried out with model expressions, which took into account in a random manner the corrections to the Reggeon terms. Consequently the conclusion of the authors of paper /80/ cannot be considered as completely ~~precise~~ verified. Their measurements should be continued into the region of higher energies. In addition, the resonances were isolated only in accordance with the mass spectrum of the $\pi^+\pi^-$ or $\pi^+\pi^-\pi^0$ system, whilst the background was removed by comparing with neighbouring regions. If a phase analysis is made of the meson system, it would help to reduce the background which is particularly high under the f -meson peak, and lower the requirements on accuracy when determining the mass. The $pp \rightarrow pp\pi^+\pi^-$ reaction was studied

also in Batavia on a hydrogen bubble chamber of the NAL at 205 GeV/c /81/. In this case it was also not possible to isolate unambiguously the double-pomeron exchange owing to the large value of the contributions from the diffraction dissociation of nucleons in the event observed with four tracks. As an upper evaluation of the double-pomeron contribution to the total cross-section in the kinematic configuration, when all of the effective masses of the πp -systems exceeded 2 GeV, a value of 44 ± 15 μb was obtained.

With an additional limitation on the mass of the $\pi\pi$ -system, $M_{\pi\pi} < 0.6$ GeV, the upper evaluation was of the order of 9 mb. The estimates quoted are, apparently, very much over estimated.

Let us now consider a proposed experimental layout at a large energy with detection of a slow recoil proton and a fast weakly scattered particle A. We shall, for example, consider that the transverse momenta $\vec{q}_{1\perp}$ and $\vec{q}_{2\perp}$ of the recoil proton and scattered particle A are fixed, and also the value

$$\delta_p = 1 - |x_p| \approx \frac{p_\mu - T_p}{m_p}.$$

Each time we shall select the value $\delta_A = 1 - |x_A| \approx 1 - \frac{E'}{E}$ (E and E' = energy of particle A before and after scattering), in order to keep the mass M^2 constant (see Fig. 5.1). Then we shall obtain for the cross-section

$$M^2 \delta_p \cdot \frac{d\sigma}{d\vec{q}_{1\perp} d\vec{q}_{2\perp} dM^2 d\delta_p} \approx \delta_p^{-2(\alpha-\beta)} \cdot \left(\frac{s}{M^2}\right)^{2(\beta-1)} \tilde{G}_{\alpha\beta}(\vec{q}_{1\perp}, \vec{q}_{2\perp}, M^2) \quad (5.17)$$

Here we have written out only the ~~multipliers~~ factors which depend on δ_p, s and M^2.

Before studying the dependence of the cross-section on δ_p, let us briefly examine the possible values and measurement accuracy of δ_p. Here we shall base ourselves on the LNPI set up /1, 38/. If the kinetic energy of the recoil proton $T_p \lesssim$ 5 MeV, and its exit angle φ varies from $\sim$ 90° to 60°, then $\delta_p \lesssim$ 0.05. The errors, which are equal to ΔT_p = 40 keV and $\Delta \varphi$ = 2° $\approx$ 35 mrad,

might provide ~ 10 intervals of δ_p , in which case the extreme values of δ_p would differ by about 10 times. This would give grounds for hoping for a precise ~~breakdown~~ separation of the various double-Reggeon contributions. In reality, the ~~position~~ situation is more complex, since it is necessary to take into account also the permissible values of $\delta_A = 1 - |x_A|$. In order to remain in the region of applicability of the Reggeon formulas, it is clearly necessary to take $\delta_A \lesssim 0.2$. As $\delta_A \cdot \delta_p = \frac{M^2}{S}$ we obtain $0.05 \gtrsim \delta_p \gtrsim \frac{5M^2}{S}$. When $M^2 = 0.6$ GeV^2, i.e. for ρ and ω resonances and with $S = 200$ GeV^2 δ_p may vary only by three times: $0.05 \gtrsim \delta_p \gtrsim 0.015$. For the f - resonance ($M^2 = 1.6$ GeV^2) the permissible interval is narrower still. But in any case it widens out with energy.

Let us also discuss the necessary accuracy when measuring the energy of particle A after scattering. The relative measurement accuracy of M^2 is composed of relative accuracies δ_A and δ_p . For the I.N.P.I. set-up the relative accuracy of δ_p is ~ 0.1 (at $\varphi \sim 70°$ and $\varphi \sim 2°$) and is determined basically by the error in measuring the angle. To ensure that the relative error of δ_A does also not exceed 0.1, it is sufficient to measure, in the conditions discussed, the finite energy of particle A with an accuracy not worse than 0.5%. This provides a value of $\frac{\Delta M^2}{M^2} \sim 0.2$ i.e. $\frac{\Delta M}{M} \sim 0.1$ ($\Delta M \sim 100$ MeV at $M \sim 1$ GeV), which would, of course, be quite satisfactory.

Let us now consider the behaviour of the right-hand side of (5.17) in various cases. If we study the production of resonances ρ , ω , and f , then in the conditions we are discussing it is probably sufficient to take into account the pomeron and Reggeons ρ' , ω , ρ and A_2 for which $\alpha(0) \approx \frac{1}{2}$. (For the evaluation we shall consider the transverse momenta to be small

and use the zero trajectories).

For the production of ρ and ω, one Reggeon must be of the non-vacuum type. In this case the right-hand side of (5.17) either decreases $\sim \delta_p$ at $\delta_p \longrightarrow 0$, if $\alpha(0) = \frac{1}{2}$, $\beta(0) = 1$, or increases $\sim \frac{1}{\delta_p}$, if $\alpha(0) = 1$, $\beta(0) = \frac{1}{2}$. In this way for small δ_p a configuration is determined in which the α Reggeon is a pomeron, and the β Reggeon is a non-vacuum Reggeon (ρ or ω). Here the cross-section decreases with the energy $\sim \frac{1}{S}$. Other double-Reggeon contributions (for example, ρ and π or ω and π) decrease with energy more rapidly, $\sim \frac{1}{S^2}$, but may have the same behaviour at S = const, $\delta_p \to 0$. ρ and ρ' contribute to the production of f.

If both Reggeons are identical, the right-hand side of (5.17) is constant at $\delta_p \longrightarrow 0$, S = const. Here the cross-section either does not depend on energy, if both Reggeons are pomerons, or decreases according to $\sim \frac{1}{S}$ in the case of two P'. If the Reggeons are different, then for small δ_p the case is again determined where α is a pomeron, and β is P', so that the cross-section decreases in accordance with $\sim \frac{1}{S}$.

When one of the Reggeons is a pomeron, then, as in the usual inclusive case, the case of small transverse momenta is of interest. Here also the vanishing of the single-pomeron term can be predicted, as in diffraction dissociation, but ~~branching~~ the cut may again screen this effect so that it is necessary to study the change in the angular distribution with energy. For the second Reggeon it is not essential to have very small transverse momenta. But they should not be selected too large, for example < 0.1 GeV^2.

When both Reggeons are pomerons, the vertex which links them with the usual particles (see Fig. 5.1) should vanish with a decrease in the transverse momentum of any of the pomerons. The reason is as follows. The contribution of the double-pomeron process (Fig. 5.1) to the total cross-section decreases logarithmically with energy. However, if we sum the contributions of all the so-called multi-pomeron processes (Fig. 5.5), the total cross-section proves to increase with energy ~~in an exponential manner~~ as a power in S /28/, and the ~~exponential~~ power-law is proportional to the value of the pomeron vertex at zero transverse momenta of the pomerons. The exponential increase of the cross-section contradicts not only the assumption concerning the asymptotic constancy of the total cross-section, but also such general representations of modern theory, such as unitarity of the S-matrix and the analyticity of the amplitudes. There is only one case where there is no contradiction, namely when the vertex which links two pomerons with the particle is equal to zero at zero transverse momenta of both pomerons. (This question has already been discussed theoretically by Ter-Martirosyan in one of the previous schools /3/). The vertex might vanish in accordance with $\sim(\vec{q}_{1\perp}\ \vec{q}_{2\perp})$ or another law. Because of this it would be interesting to measure the dependence of the cross-section not only on $\vec{q}^{\,2}_{1\perp}$ and $\vec{q}^{\,2}_{2\perp}$, but also on the angle between $\vec{q}_{1\perp}$ and $\vec{q}_{2\perp}$, i.e. on the relative azimuthal angle of the recoil proton and the weakly deflected fast particle A.

We shall now attempt to evaluate the expected values of the cross-section of the double-pomeron process. The simplest solution is to do this at large M^2, when the pomeron-pomeron cross-section is constant, and does not depend on M^2. Then the double-inclusive cross-section is described by the diagram of Figure 5.6, where all Reggeons

are pomerons. This diagram is referred to as the double-three-Reggeon diagram (cf. Fig. 3.3c), and it is sometimes referred to as the "Beetle". The contribution of this diagram to the double-inclusive cross-section can be subdivided ~~decays~~ into the product of two factors ~~multipliers~~, corresponding to the upper and lower halves of the diagram in Figure 5.6 (see expression (5.12) and (5.13) at $\sigma_{\alpha\beta}$ = const.).

Let us examine for comparison, the three-pomeron diagram of the type shown in Figure 3.3c. This also breaks down into factors ~~multipliers~~, one of which (from the lower half of the diagram) has the same structure as the factors ~~multipliers~~ in the diagram of Figure 5.6, whilst the other is simply a constant of the pomeron link with particle A , which in turn is one of the factors ~~multipliers~~ in the expression for the total interaction cross-section of particle A with any target. By accurately following all of these factors ~~multipliers~~, we arrive at a factorization formula which links the twice-inclusive cross-section with the single-inclusive and total cross-section. For example, in the case where particle A is a proton, we obtain

$$\frac{d\sigma^{pp}}{d\vec{q}_{1\perp}\,dx_1\,d\vec{q}_{2\perp}\,dx_2} = \frac{d\sigma^{pp}}{d\vec{q}_{1\perp}\,dx_1}\cdot\frac{d\sigma^{pp}}{d\vec{q}_{2\perp}\,dx_2}\cdot\frac{1}{\sigma_T^{pp}}, \qquad (5.18)$$

where $x_p = x_1$, $x_A = x_2$. If the incident particle A is not a proton, then in the right-hand part of (5.18) there occurs an additional factor ~~multiplier~~

$$\left(\sigma_{tot}^{pA}/\sigma_{tot}^{pp}\right)^2,$$

where σ_{tot}^{pA} is the total interaction cross-section of particle A with the proton. For the total cross-section of pp -scattering, we shall take the value of $\sigma_{T}^{pp} \approx$ 40 mb. As for the three-pomeron contribution to the singly - inclusive cross-section, we shall now concern ourselves only with the contribution of the effective pomeron, and shall not separate the contribution of the true pomeron from its accompanying ~~branching~~ our. Consequently in (5.18) we insert a phenomenological three-pomeron term which contain a vertex which is non-vanishing.

The processing of the inclusive proton spectra of the ISR, described in paper /50/, shows that it is possible to have slightly different parameters for the effective three-pomeron contribution depending on the assumption concerning the size of the term PPR and on the slope of the pomeron trajectory. By using one of the parametrizations described in /50/, and using (5.18), we obtain, for the double-inclusive proton-proton cross-section

$$\frac{d\sigma^{pp}}{dq_{1\perp}^2 dx_1\, dq_{2\perp} dx_2} \approx \frac{g_1 \omega S^{\prime}/(E_0^2)^4}{(1-/x_1/)(1-/x_2/)} \cdot e^{-3,5(q_{1\perp}^2 + q_{2\perp}^2)} \times \quad (5.19)$$

$$\times (1-/x_1/)^{2\alpha' p q_1^2} (1-/x_2/)^{2\alpha' o\, q_{2\perp}^2},$$

where $q_{i\perp}^2$ is measured in GeV^2. In order to understand what this expression denotes, we shall find a total doubly -inclusive cross-section in conditions of the experimental geometry. By again basing ourselves on the set up at LNPI /1, 38/, we may, at S = 800 GeV^2, pose $0 < q_{1\perp}^2 <$ 0.03 GeV^2, $0.03 < 1 - /x_1/ < 0.05$. For x_2 and $q_{2\perp}^2$ we shall take a wider range $0 < q_{2\perp}^2 <$ 0.1 GeV^2, $0.03 < 1 - /x_2/ < 0.1$. If we now integrate over the angles and intervals indicated $q_{i\perp}^2$ and x_i, we obtain for the total cross-section of the

doubly-inclusive proton-proton reaction the value $\sim$ 0.15 mb. If for $q_{2\perp}^2$ and x_2 the same region was selected as for $q_{2\perp}^2$ and x_1 then we would obtain $\sim$ 0.02 mb. When obtaining these estimates we can take into account sufficient accuracy only the first ~~multiplier~~ factor in (5.19), i.e. we may assume that $q_{i\perp}^2 = 0$. Then integration over $q_{i\perp}^2$ is simply reduced to a multiplication by $q_{i\perp}^2$ max. In this connection it should be pointed out that measurements of the inclusive (cross) sections were made in the region 0.15 GeV^2 < $q_\perp^2$ < 1 GeV^2. If at $q_\perp^2$ < 0.1 GeV^2 the dependence of the three-pomeron contribution on $q_\perp^2$ becomes steeper (and this is possibly indicated by the measurements at Batavia /23/), then the cross-section at $q_\perp^2 = 0$ is greater than would follow from the parametrization obtained in /50/. In this case it is necessary to increase also the evaluations quoted here for the doubly-inclusive cross-section.

The small value obtained for the cross-section is partly due to the small value of the asymptotic pomeron cross-section in comparison with the cross-sections of normal particles (for example $\sigma_{pp} \approx$ 1 mb, $\sigma_{pp} \approx$ 40 mb), but it ~~largely~~ esencially reflects the small value of the accessible phase volume.

Thus we have obtained an evaluation for the anticipated value of the double-pomeron contribution in the region of large M^2, where the pomeron-pomeron cross-section is constant. However at S $\leqslant$ 800 GeV^2, this region is practically unattainable. In reality, it follows from

an analysis of the inclusive spectra /50/, that the pomeron exchange can be isolated only at $(1-|x|) \lesssim 5 \cdot 10^{-2}$, but for the constancy of the interaction cross-section of two pomerons it is necessary that the value of M^2 is greater than at least 4 - 5 GeV^2. Consequently, strictly speaking, the region in which formulas (5.18 and 5.19) can be applied begins at $S \gtrsim 2000$ GeV^2.

At energies of $S \lesssim 800$ GeV^2 we may hope to measure the pomeron-pomeron cross-section only at small M^2 in the region of resonances. As has already been explained, in this region σ_{pp} clearly exceeds the asymptotic value (see Figure 5.4). Accordingly, the double-pomeron contribution to the doubly inclusive cross-section in this region is also greater than for large M^2. Thus, although at $S \lesssim = 800$ GeV^2 the region to which the above cross-section evaluations refer is unattainable, the evaluations nevertheless retain a meaning as the lower boundary of the anticipated cross-section.

The fact that at finite M^2 the double-pomeron contribution is greater than at large M^2, is clear if, for example, we take into account the correction to the pomeron-pomeron cross-section which arises from exchange of a Reggeon P' (Figure 5.7). It is in fact similar to the contribution examined in 5.6, but is expressed by the vertex PPR, g_{PPR} (in this case R may correspond only to the Reggeon P') and contains a decrease according to M^2. The overall contribution of the diagrams of Figures 5.6 and 7 to the doubly inclusive proton-proton cross-section at $g_{1\perp}^2 = g_{2\perp}^2 = 0$ is (see (5.19))

$$\left.\frac{d\sigma^{pp}}{dq_{12}^2 dx_1 dq_{21}^2 dx_2}\right|_{\substack{q_{12}=0\\ q_{21}=0}} = \frac{g_1 \cdot 136^4}{(1-x_1)(1-x_2)}\left[1+\frac{g_{PPR}^2}{g_{PPP}^2}\left(\frac{S_0}{M^2}\right)^{+1/2}\right] \qquad (5.20)$$

It is obvious that with the decrease in M^2, the right-hand part of (5.20) increases. However it is difficult to use this relation for numerical evaluation since we do not know the value of g_{PPR} We only know that

$$\frac{g_{PPR}}{g_{PPP}} \leq 1{,}5\ /50/^{*}.$$

In addition, at small M^2 the expansion over the contributions of Reggeons cannot be used. Owing to this, it is not clear to what extent we may decrease M^2 in order to remain in the region of applicability of expression (5.20).

In order to obtain a more accurate representation of the resonance region, we shall use another approach. In accordance with the idea of duality (cf. for example the review of /19/), the contribution of the resonances is described, on an average, by the sum of Reggeon exchanges (but not pomeron exchanges). If we apply this idea to the "reaction" $pp \longrightarrow \pi\pi$, then we arrive at an examination of a single-pion Reggeized exchange (Figure 5.8). Accordingly for the amplitude of the two-pomeron contribution to the reaction $pp \longrightarrow p(\pi\pi)p$ we obtain the diagram of Figure 5.9, and for the contribution to the cross-section of the doubly -inclusive process, the diagram of Figure 5.10.

Let us evaluate this contribution at $q_{1\perp}^2 = q_{2\perp}^2 = 0$. We shall first examine the structure of the amplitude corresponding to the diagram of Figure 5.9. At values of M^2 which are not too large, the values of $|t_\pi|$ are also not too great. In these conditions we may use as the vertex linking the π -meson with the π -Reggeon and pomeron the usual pion-pomeron vertex. Then, for example, the lower pomeron in Figure 5.9 contributes to the amplitude the ~~multiplier~~ factor $iS' g_{\pi P} a_P$. But the product $g_{\pi P} a_P$ is equal to the contribution of the pomeron to the total cross-section $\sigma_T^{\pi p}$. This contribution can be identified with $\sigma_T^{\pi p}$ at $E \sim 30$ GeV, where the total cross-section varies weakly and is approximately 24 mb (let us recall that we are using here not a true pomeron which strictly will work only at very large energies, but an effective pomeron which occurs at $E \gtrsim 10$ GeV). Furthermore, we shall use as the π -Reggeon propagator the usual pion propagator $\frac{1}{t_\pi - \mu^2}$, where μ is the mass of the pion. In order to take into account ~~measure-~~ the effect on ~~ment of~~ the vertices and the propagator, which is introduced by ~~the descent~~ being away from the mass ~~surface~~ shell (i.e. the virtual exchange π -meson), we shall introduce the form factor $F(t_\pi)$. Let us point out that we have not introduced a specific dependence on M^2. This means that we do not, in reality, Reggeize the π -meson. In this connection let us point out that Reggeization is substantial only at $M^2 > S_0$. At $M^2 \lesssim S_0$ it practically does not change the result.

---

* In order to obtain this evaluation it is necessary to use the fact that $a_p \approx a_{p'}$.

Thus we can write the amplitude for the diagram of Figure 5.9 in the following form :

$$A = (iS')\sigma_T^{\pi p} \cdot \frac{F(t_\pi)}{t_\pi - \mu^2}(iS'')\sigma_T^{\pi p} \quad . \tag{5.21}$$

For the contribution to the cross-section (Fig. 5.10) we obtain

$$p_{30}p_{40}\frac{d\sigma}{d^3p_3\,d^3p_4} = \frac{3}{2S}\cdot\frac{1}{[2(2\pi)^3]^4}\int\frac{d^3k_1}{k_{10}}\cdot\frac{d^3k_2}{k_{20}}\cdot(2\pi)^4\delta^{(4)}(k_2+k_2'+p_3+p_4-p_1-p_2). \tag{5.22}$$
$$\times (S'S'')^2\,(\sigma_T^{\pi p})^4\cdot\frac{F^2(t_\pi)}{(t_\pi-\mu^2)^2} \quad .$$

Here $\frac{1}{2S}$ describes the invariant flow of initial particles at high energy. The ~~multiplier~~ factor 3 is linked with the three possible charge states of the π -meson (π^+, π^-, π^0) in the diagrams of Figures 5.9 and 5.10. The remaining ~~multipliers~~ factors in (5.22) which do not directly follow from (5.21), are the normal ~~multipliers~~ factors linked with normalization or phase space.

In the region of small values of $q_{i\perp}^2$ and $(1-|x_i|)$ which is of interest to us the following relation is correct :

$$p_{30}p_{40}\frac{d\sigma}{d^3p_3\,d^3p_4} \approx \frac{d\sigma}{d\vec{q}_{1\perp}\,dx_1\,d\vec{q}_{2\perp}\,dx_2}$$

Integration in (5.22) can now be carried out conveniently in the centre-of-mass system of a pair of final pions. Then, neglecting the mass of the pion μ , we obtain

$$\frac{d\sigma}{d\vec{q}_{1\perp}\,dx_1\,d\vec{q}_{2\perp}\,dx_2} = \frac{3}{2S}\cdot\frac{1}{(8\pi^2)^4}(\sigma_T^{\pi p})^4\int\frac{2\pi\kappa\,d\cos\theta}{M}\times \tag{5.23}$$
$$\times (S'S'')^2\,\frac{F^2(t_\pi)}{t_\pi^2},$$

where $K = |\vec{K}_1| = |\vec{K}_2| \approx \frac{M}{2}$. θ is the angle between $\vec{K}_1$ and $\vec{q}_1$ (in fact at a large energy this is the angle between $\vec{K}$ and $\vec{p}_1$). The kinematics of the conversion of two particles into four leads, at large S, S', S'' and fixed q_i^2 , t_π to the relations

$$S'S'' \approx \frac{S}{M^2} \cdot t_\pi^2 ; t_\pi \approx -\frac{M^2}{2}(1-\cos\theta); \frac{K}{M} d\cos\theta = \frac{dt_\pi}{M^2} . \qquad (5.24)$$

(Their derivation is similar to examination of the kinematic relationships for conversion of two particles into three, which was examined at the beginning of this section). Integration over the angle should be limited to the region $0 < \cos\theta < 1$.* Let us explain this in greater detail for the case of two π^0-mesons. In reality, we are interested in the total amplitude of the process $p+p \to \pi^0\pi^0$. Obviously in view of identicality it is sufficient to examine the range of angles $0 < \cos\theta < 1$. It is precisely at such angles (angles which are not too large) that it is reasonable to describe the total amplitude by the contribution of the single-pion exchange. For charged pions, the range $-1 < \cos\theta < 0$ corresponds to another

*

We should point out here that the relation (5.21) which we in fact used, and the formulas (5.22), (5.23) based on it, are valid only for fairly large values of S', S'' (S', $S'' > S_M$, where S_M $\sim$ 5 - 10 GeV^2). Consequently the calculations carried out by us are, strictly speaking, applicable only in the region $|t_\pi| \geq |t_\pi|_{min}$ $= S_M^2/S$, i.e. are not valid for very small t_π . However in future when carrying out the evaluations we shall not take this factor into account.

charged configuration of final particles. As we have already effected a summation over the charged configuration (the ~~multiplier~~ factor three (5.22) and in (5.23)), it is sufficient to take into account only the first range of angles. Let us point out that we take into account the diagrams of the type shown in Figure 5.10, but not the diagram with the cross as shown in 5.11. This is due to the fact that the mechanism of single-pion exchange is substantial only at relatively low angles of particle emergence whilst in the diagram of Figure 5.11 both in the initial and final states the process occurs at large angles.

If we insert the expression $F^2(t_\pi) = e^{bt_\pi}$ for the form factor, the cross-section takes the form* :

$$\frac{d\sigma}{dq_{1\perp}^2\, dx_1\, dq_{2\perp}^2\, dx_2} = \frac{1}{(1-|x_1|)(1-|x_2|)}\left(\frac{\sigma_T}{8\pi}\right)^4 \cdot \frac{3}{4\pi b^2}\, J\left(\frac{bM^2}{2}\right), \qquad (5.25)$$

where $J(z) = \frac{1}{z^2}\int_0^z e^{-y} y^2\, dy$. At small M^2 $J\left(\frac{bM^2}{2}\right) \approx \frac{bM^2}{6}$, at large M^2 $J\left(\frac{bM^2}{2}\right) \approx \frac{8}{b^2 M^4}$. This corresponds to the fact that the cross-section of the $P+P \to 2\pi$ reaction increases at small M^2, and at large M^2 it decreases in accordance with $\sim \frac{1}{M^4}$. At $M^2 \approx \frac{3}{b}$, it has a very ~~slightly sloping~~ broad maximum ($J_{max} = 0.17$). If we were to take account of Reggeization, the cross-section would drop slightly quicker as M increased. However the position and value of

---

* A similar evaluation was obtained also by A.B. Kajdalov and K.A. Ter-Martirosyan /82/.

the maximum is only weakly affected by Reggeization, since the maximum is located at relatively small M^2.

For a numerical evaluation of the contribution of single-pion exchange, we shall take the value of $b = 5.5\ \text{GeV}^{-2}$, which ensures a reasonable description of all the experimental data collected for the reactions $NN \to \pi NN$, $pn \to np$, $\pi N \to 2\pi N$ in the model of single-pion exchange /83/. Inserting also $\sigma_T^{\pi p} = 24$ mb, we may rewrite (5.24) in the form :

$$(1-/x_1/)(1-/x_2/)\frac{d\sigma}{dq_{1\perp}^2 dq_{2\perp}^2 dx_1 dx_2}\Big/_{q_{i\perp}^2=0} = 0{,}6\ \text{mb/GeV}^4 \cdot \pi\left(\frac{5}{2}M^2\right), \qquad (5.26)$$

where M^2 is measured in GeV^2. The right-hand part of (5.26) attains, at $M^2 \approx 0.53\ \text{GeV}^2$, a maximum value of $\approx 0.1\ \text{mb/(GeV)}^4$, after which it drops as M^2 increases. Thus, the greatest value of the right-hand side of (5.26) corresponds to the evaluation of (5.19), obtained at large M^2. Let us remember that in (5.26) account has been taken not only of the charged π -mesons but the neutral π -meson. If we confine ourselves only to the charged pions, it is necessary to multiply the right-hand side of (5.26) by 2/3.

At first sight, the result of (5.26) may appear contradictory with (5.19). In reality, this is not so. In (5.26) account has been taken of only the cross-section of the "reaction" $PP \to 2\pi$, which

attains a maximum and then drops as M^2 increases. But at the same time the transition cross-section of $PP \to 4\pi$ increases. ~~After-~~ At even higher M^2 ~~wards~~ this cross-section also begins to decrease but the cross-section of $PP \to 6\pi$ etc. increases, so that the total cross-section of pomeron-pomeron scattering is constant. (It is precisely in this way that the constancy of total cross-sections occurs in accordance with the multi-peripheral models). Thus, the cross-section of pomeron-pomeron interaction at large M^2 is determined by the sum of the contribution of π-meson states (see Figure 5.12).

By reasoning further in this way, we arrive at the conclusion that also the effective pomeron itself is equivalent to the summation of the π-meson ladder diagrams of the type shown in Figure 5.12. We should also point out that as has already been shown by Boreskov, Kajdalov and Ponomarev (see for example /84/), the model of the single-pion exchange reproduces well the fundamental features of the experimental data for proton spectra at $0.15 \leqslant q_\perp^2 \leqslant 0.5$ GeV^2 and gives, for a three-pomeron vertex $g_{PPP}(q_\perp^2)$, a value close to that found when processing the experimental data /50/.

The evaluation of (5.26) points to the fact that the pomeron-pomeron cross-section may, possibly become constant (or more precisely almost constant) already at $M^2 \approx 0.5$ GeV^2 and that the threshold reinforcement in it may not occur, or at least be relatively small.

As has already been said, it may be expected that the model of single-pomeron exchange describes the average trend of the cross-section in the resonance region of the values of M^2. But immediately

in the resonance peak the cross-section will increase. Let us briefly discuss the development of concrete resonances. The states ε and S^*, if they in fact are resonances, will have large widths. Consequently they will, probably, develop weakly in the pomeron-pomeron cross-section.

The peak of the f-meson may be much more distinct. Its value is determined by the vertex which links the f-meson with two pomerons. We cannot evaluate this vertex. It is, however, possible to use the following ~~maneuver~~ arguments. By using dual models it is possible to find a "precise" vertex for linking f with two ρ'-Reggeons (the authors are grateful to V. A. Kudryavtsev, who carried out these calculations). In the dual model this value is expressed by the linking vertex $\rho\pi\pi$, which obviously is linked with the life-time of the ρ-meson. On the other hand, we may consider the "reaction" $P' + P' \longrightarrow 2\pi$ in the model of the single-pion exchange. It so happens that the "precise" cross-section, integrated over the peak of the f-meson exceeds by several times the prediction of the single-pion exchange. Probably this statement is valid also for pomerons.

Finally let us examine the f'-meson. It can be compared with a f-meson, if we use the quark model (see for example the Frankfurt lecture [41]). From the point of view of the quark model the total cross-section of interaction of a non-strange quark (or anti-quark) with a proton is approximately $\frac{1}{2}\sigma_T^{\pi p} \approx 12$ mb, and the interaction cross-section of a strange quark with a proton $\sigma_T^{Kp} - \frac{1}{2}\sigma_T^{\pi p} \approx$ 17 mb - 12 mb = 5 mb. In this way the effective pomeron is linked with a strange quark which is almost twice

as weak as the non-strange quark. But f' is almost completely composed of strange quarks, whilst f is composed of non-strange quarks. If we describe the production of resonances of the diagram as shown in 5.9 (by replacing the π -meson pair by a quark-anti-quark pair) then it is clear that the f' -meson must be produced approximately four times weaker than f .

In conclusion let us stress that here we have confined ourselves basically only to the discussion of contributions from double-pomeron exchange. In effect, as has been shown by the calculations we have made, and also by the experimental data which exist, the background contributions from non-pomeron exchanges and from diffraction dissociation of initial particles are quite significant, particularly in the energy range $S \lesssim 400\ \text{GeV}^2$, where the problem of separating the various contributions is fairly complex. Let us point, however, that in the region of the f -meson resonance the backgrounds from diffraction dissociation may prove to be less substantial.

Let us also make an evaluation of the lower boundary for the value of the cross-section of the doubly -inclusive process (5.1) in the region $|x_A|, |x_p| \longrightarrow 1,\ q_{1\perp}^2,\ q_{2\perp}^2 \longrightarrow 0$. We are now speaking of the contribution of the purely electromagnetic process of Figure 5.13, where a central group of hadrons is produced in a collision of two gamma quanta. The corresponding contribution to a cross-section of the process (5.1) for ~~a random~~ any charged particle A is of the form

$$\frac{d\sigma^{\gamma\gamma}}{dq_{1\perp}^2\, dq_{2\perp}^2\, dx_A\, dx_p} = \left(\frac{\alpha}{\pi}\right)^2 \frac{1}{(1-|x_A|)(1-|x_p|)} \frac{q_{1\perp}^2}{t_1^2} \frac{q_{2\perp}^2}{t_2^2} \sigma_{\gamma\gamma} \approx \tag{5.27}$$

$$\approx \frac{1{,}6 \cdot 10^{-9}}{(1-|x_A|)(1-|x_p|)} \left(\frac{q_{1\perp}^2}{t_1^2}\right)\left(\frac{q_{2\perp}^2}{t_2^2}\right) \frac{\mu b}{\text{GeV}^4} ,$$

where $\sigma_{\gamma\gamma}$ is the total cross-section of hadron generation in a $\gamma\gamma$ -collision (by factorization

$$\sigma_{\gamma\gamma} \approx \frac{\sigma_{\gamma p}^{2}}{\sigma_{pp}} \approx 0{,}3\ \mu\mathrm{b}\ ).$$

The cross section $\dfrac{d\sigma}{dq_{1\perp}^2\, dq_{2\perp}^2\, dx_A\, dx_p}$ is compared with the evaluation of (5.19) only at $q_{1\perp}^2$, $q_{2\perp}^2 \sim 10^{-4}$ GeV^2.

VI. SCATTERING ON A DEUTERON

Tests with a deuteron target are of interest for the following reasons.

I. In many cases the use of a deuteron is the only possible way of studying interactions with a neutron. This is the case, for example, for Kn^- , $\bar{p}n$ -scattering, as distinct from pn -scattering, where it is possible to use a neutron beam.

2. The proton and neutron in the deuteron are weakly linked, so that the nuclear corrections are small (of the order of 10%). Consequently, when studying the scattering of fast particles it is possible to ignore the interaction of a neutron and proton in a deuteron (impulse approximation). The corrections related to the processes in which the incident particle interacts with both nucleons (double re-scattering) may be computed /85-90/ by the inclusive scattering cross-sections on one nucleon. Consequently the measurement of such corrections both for total and for differential cross-sections enables a check to be made of the correctness of our present concepts of the deuteron as a weakly linked system of nucleons. In this respect the most convenient incident particle is the π -meson, since as a result of charge symmetry $\sigma(\pi^+ p) = \sigma(\pi^- n)$. Consequently by comparing the data for the $\pi^+ d^-, \pi^- d-$ and the $\pi^- \bar{p}^-, \pi^+ p^-$ interaction we can determine unambiguously the contribution of double re-scattering in πd -processes.

3. The deuteron is not only the simplest compound system, whose properties are interesting to investigate and which can be used

for obtaining neutron data, but it is also the simplest target with ~~an~~ the isotopic spin equal to zero. Consequently it is interesting to examine the inclusive reactions on a deuteron (i.e. reactions of the type $a+d \to d$ + all the remainder, where a is the incident particle), especially in the three-Reggeon region (see chapters II and III above), as in this case the value of the cross-section will be determined by the contributions of a slightly different combination of Reggeons (i.e. Reggeons with $T=0$, p' and ω) in comparison with the inclusive cross-section on protons. In addition, the measurement of the difference in the differential cross-sections of $\pi^+ d$ and $\pi^- d$ scattering enables a much more accurate determination of the electromagnetic corrections (~~beta~~ Bethe phase, /97/ and below).

Let us now turn to a more detailed evaluation of the necessary experimental accuracy and a discussion of the character of the data which can be obtained in deuteron target experiments.

I. The deuteron as a neutron target at small t

We shall first examine the scattering of any fast particle (for example, a proton) on a deuteron in the region of Coulomb interference, which is the most interesting for the LNPI set-up. In this region of momentum transfers

$$A_{pd} = (A^c_{pp}(t) + A_{pp}(s,t) + A_{pn}(s,t))\, S(t) + \Delta(s,t), \qquad (6.1)$$

where A^c_{pp}, A_{pp} are the amplitudes of the Coulomb and strong interactions of two nucleons (see Fig. 6.1 a-c), $\Delta(s,t)$ is the contribution of double re-scattering (Fig. 6.1d), $S(t)$ is the electro-

magnetic form factor of a deuteron derived from data on ed -scattering (more precisely $S(t) = \frac{G_d(t)}{G_p(t)}$, where G_d, G_p is the electromagnetic form factor of the deuteron and electrical form factor of the proton). Below, we shall use in the evaluations

$$S(t) = e^{-a|t|}, \tag{6.2}$$

where $a = 10$ $(GeV/c)^{-2}$. However it is important to point out here that in the region of small $|t|$ $S(t)$ behaves more rapidly, and a better approximation is /92/

(6.3)

$$S(t) = b\, e^{-a_1|t|} + (1-b)\, e^{-a_2|t|},$$

where

$$b = 0{,}40 \pm 0{,}01,$$
$$a_1 = (29{,}7 \pm 0{,}25)\ (GeV/c)^{-2},$$
$$a_2 = (5{,}68 \pm 0{,}06)\ (GeV/c)^{-2}.$$

The interference term in the pd -scattering is of the form :

$$\frac{d\sigma}{dt} \sim A^S_{pp}(t)\{Re(A_{pp}(s,t) + A_{pn}(s,t))S(t) + \\ + Re\,\Delta(s,t)\}\, S(t) + \beta. \tag{6.4}$$

where β is expressed by the total cross-section and Bethe phase (see below). From the data on pd -scattering we can attempt to determine $ReApn$ (or $\rho_{pn} = \frac{ReApn}{ImApn}$, see Fig. 2.1). This can be done either in the case when $Re\Delta(s,t)$ is small in comparison with $ReApp - ReApn$, or when it is possible to distinguish the first term in (6.4) from the second as a function of t

$\Delta(s,t)$ depends on t exactly as any strongly interacting amplitude (i.e. $\Delta(s,t) \sim e^{-b|t|}$, where $b \sim$ 4-6 $(\text{GeV/C})^{-2}$, whilst S(t) falls more sharply in accordance with small t (see (6.2) and (6.3)).

EVALUATION OF $\mathrm{Re}\,\Delta(s,t)$

A contribution to $\Delta(s,t)$ is given by various processes (see Fig. 6.1d) and the basic condition (linked with the fact that the deuteron should not collapse) is that q^2 (at t = 0) should be smaller than $1/R_d^2$ (R_d is the radius of the deuteron*). Since

$$q^2_{min} = \left(\frac{M^2-m^2}{s}\right)^2 m^2, \qquad (6.5)$$

where m is the mass of the nucleon, and M is the mass of the system of particles produced in the intermediate state (Fig. 6.1) $M^2 = (k_1 + \text{---} + k_n)^2$, then

$$\frac{M^2-m^2}{s} \leq \frac{1}{R_d m}. \qquad (6.6)$$

---

* By R_d we understand the radius which characterizes the reduction in the electromagnetic form factor of the deuteron ($S(t) = e^{-R_d^2|t|}$, i.e. $R_d^2 \approx 10\left(\frac{\text{GeV}}{c}\right)^{-2}$ or (6.2)) Thus, a specific $R_d \sim \frac{1}{\mu}$ (μ is the mass of a π-meson), which is considerably less than $R \simeq 1/2\sqrt{m\varepsilon}$ (ε is the binding energy of the deuteron). This comparison already shows that the deuteron cannot be represented as a very brittle system. Below we shall make considerable use of the fact that the radius of the deuteron ($R_d \sim 1/\mu$) is nevertheless considerably greater than the radius of the strong interactions of hadrons, which is of the order of $1/m_\rho$ (m_ρ is the mass of the ρ-meson).

For elastic and quasi-elastic processes (i.e. for processes in which a finite number (not depending on S) of particles with a small mass (for example with $M^2 < M_0^2$, where $M_0^2 = 4 - 5\ \mathrm{GeV}^2$) the condition of (6.6) is always fulfilled and the main contribution to double re-scattering is given by the graphs with the exchange of two vacuum Reggeons (at a large total energy S). (see Fig. 6.2a). The real part of these graphs is small, since the exchange of a vacuum Reggeon gives a purely imaginary contribution ($\alpha' p$ is small) and the overall smallness of the contribution of figure 6.2c to the ~~material~~ real part is

$$Re\,\Delta' \sim \alpha' p / R_{ad}^2\ Im\,\Delta \approx \tfrac{1}{3}\cdot 0{,}1\ Im\,\Delta \sim 0{,}04\ \text{mb}$$

($Im\,\Delta \sim$ 4 mb is from the experiment). Let us recall that the ~~material~~ real part of the exchange of the vacuum pole is proportional to $\alpha' p t \cdot S^{\alpha p(t)}$. We shall note here that /86/*

$$Im\,\Delta(s, t=0) = 2 \int S(4q^2) \frac{d^2\sigma}{dq^2 dM^2}\, dq^2 dM^2 . \qquad (6.7)$$

It can be seen from (6.6) that a contribution may be given to the re-scattering by the processes in which many particles are produced (their number increases as S grows), but M^2/S should be lower or of the order of $\frac{1}{R_{ad} m}$. As $m^2\ S/M^2 \approx S_{CN} >> m^2$, the range of the large masses is described by the three-Reggeon limit. At an energy of p_{lab} = 100 - 400 GeV/c M^2 is not very great and as

---

From here onward $\frac{d\sigma}{dq^2 dM^2}$ is $\frac{d\sigma(pp \to px)}{dq^2\, d\,M^2} \approx \frac{d\sigma(pp \to nx)}{d\,q^2\, d\,M^2}$ (V. V. Anisovich, L. G. Dakhno, Preprint IHEP STF-74-II). When deriving this formula it was assumed that the isotopic spin of the upper Reggeon was zero. This is clearly true for a very high energy.

the ~~material~~ real part of the scattering amplitude increases as the energy decreases, generally speaking $Re\,\Delta''$ may be fairly large. The greatest contribution** is given in this case by the vertex RRR, which is great in comparison with present-day processing values for inclusive proton cross-sections /50/ and which precisely reflects the growth in $Re\,A_{NN}$ in the small energy region. It turns out that, having taken G_{RRR} from /50/, and S(t) in the form of (6.2) we obtain

$$Re\,\Delta_{RRR} \leq (s/s_0)^{-1/2} \cdot 3\,\mu b\,, \quad s_0 = 1\ GeV^2$$

($S = 200\ GeV^2$ $\Delta_{RRR} \leq 0.1$ mb). This value is fully comparable with the difference $Re\,App - Re\,A_{pn}$ which we expect on the basis of the theory of complex moments, since $Re\,A_{pp} - Re\,A_{pn}$ is determined by the ρ-Reggeon, the contribution of which falls as the energy increases in accordance with $1/\sqrt{s}$ and in addition is suppressed in the nucleon system (see /36/). The remaining contributions to $Re\,\Delta$ are considerably smaller :

$$Re\,\Delta_{PPR} < 0{,}1\,m\sigma_H,\ Re\,\Delta_{KRP} \simeq 0{,}1\,m\sigma_H,$$
$$Re\,\Delta_{PPP} \leq 2 \cdot 10^{-2}\,m\sigma_H$$

** Below, we shall use for the evaluations the analysis of the inclusive proton cross-sections on the basis of the Regge pole model, disregarding ~~branching~~ cuts contribution. With the present-day experimental accuracy the contribution of ~~branching~~ cuts and poles should not be broker down.

(if $G_{ppp} \sim t$ at $t = 0$)*. Thus, we cannot consider that $R_e\,\Delta$ is small, and the experiment to determine $R_e A_{pp} - R_e A_{pn}$, disregarding $R_e \Delta$, can be performed, relying solely on the fact that for some causes which we do not know $R_e A_{pn} - R_e A_{pp} \geq$ 0.3 - 0.4 mb. We can attempt to determine $R_e A_{pn} - A_e A_{pp} \equiv \delta$, using a different dependence on t for the first and second terms in expression (6.1). As the Coulomb interference is great at small t ($|t|$ is $\leq$ 0.01 GeV^2), then for A_{pn}, A_{pp}, $\Delta(s,t)$, which depend on the momentum transfer approximately in accordance with $e^{-b|t|}$ (where $|t|$ is in (GeV/c^2), we may use the linear expansion over $|t|$. $b|t|$ depends sharply on t and for $|t| \leq$ 0.01 (GeV/c)^2 it is necessary at least to take into account the quadratic term for t (see (6.3)). In this way

$$\frac{d\sigma}{dt} = A^c_{pp}(t)(a + bt + ct^2)\,St\,, \qquad (6.8)$$

where $a = R_e A_{pp}(s,0) + R_e A_{pn}(s,0) + R_e \Delta(s,0)$,

b is determined by the dependence of the strong amplitudes on small t, whereas

$$c = (R_e A_{pp}(s,0) + R_e A_{pn}(s,0)) \frac{1}{2} \frac{d^2 s(t)}{dt^2}\Big/_{t=0},$$

in particular for (6.3)

$$c = (R_e A_{pp} + R_e A_{pn})\, 190. \frac{GeV^4}{c}$$

In determining C, we can determine $R_e A_{pp} + R_e A_{pn}$, not knowing the corrections from double re-scattering. In comparing A and C, we

* If $G_{ppp} \neq 0$ at $t = 0$, $R_e \Delta_{ppR} \leq$ 0.15 mb.

can determine $R_e \Delta (s,0)$, which also is of interest (see below). In measuring the cross-section with an accuracy of up to 1%, the term will be determined with an accuracy of not less than 20% at $|t|$ 0.01 GeV^2, and consequently it is possible to determine δ only in the case where

$$\delta \sim R_e A_{pp}$$

Thus the value anticipated in this way for $\delta (\delta \sim 0.1 R_e A_{pp})$ can be determined only when the measurement accuracy of the cross-section is 0.1%.

2. MEASUREMENT OF DOUBLE RE-SCATTERING

When measuring the scattering on a deuteron at small momentum transfers, it is possible to measure the correction from double re-scattering not only in the imaginary but also the ~~material~~ real part of the scattering amplitude (see formulas (6.1), (6.4), (6.8)). Here it is best to use (as has already been pointed out above), the π -meson beam or make the assumption that $A_{pn} = A_{pp}$ at large energies. Various processes have essentially different contributions to $Im\Delta$ and $Re\,\Delta$. This can be seen even from the fact that a significant contribution to $Im\,\Delta$ is given by the processes of the quasi-elastic type (6.2a), which have a contribution to $R_e\,\Delta$ which is so small that it can be ignored. The formulas which determine $Im\,\Delta$ and $R_e\Delta$ have been written out below (see also /86,88,90/).

$$\begin{aligned} Im\,\Delta = {} & 2\int_0^{-\infty} dt\, S(4t)\, \frac{d\sigma_{NN}}{dt} + \\ & + 2\int_0^{M_0^2} dM^2 \int_0^{-\infty} dt\, \frac{d\sigma}{dt\,dM^2}\, S(4t) \\ & + 2\int_{M^2_{min}}^{\infty} dM^2 \int_0^{-\infty} dt\, S(4t) \cdot \\ & \cdot \left\{ \left[\frac{1}{\sin\frac{\pi}{2}(\alpha_i - 2\beta_j^+)}\, \frac{d\sigma(\alpha_i, \beta_j^+)}{dt\,dM^2} - \frac{1}{\sin\frac{\pi}{2}(\alpha_i - 2\beta_j^-)}\, \frac{d\sigma(\alpha_i, \beta_j^-)}{dt\,dM^2} \right] \right. \\ & \left. + \frac{2}{\pi} c_i \frac{M^2}{S} \left[\frac{d\sigma}{dt\,dM^2}(\alpha_i = 2\beta_j^+) - \frac{d\sigma}{dt\,dM^2}(\alpha_i = 2\beta_j^-) \right] \right\} \end{aligned} \qquad (6.9)$$

$$\mathrm{Re}\,\Delta = 2\int_{M_0^2}^{\infty} dM^2 \int_0^{-\infty} dt\, S(4t)\cdot \mathrm{ctg}\,\frac{\pi\alpha_i}{2}\cdot$$
$$\cdot\left\{\left[\frac{1}{\sin\frac{\pi}{2}(\alpha_i - 2\beta_j^+)}\cdot\frac{d\sigma(\alpha_i,\beta_j^+)}{dt\,dM^2} - \frac{1}{\sin\frac{\pi}{2}(\alpha_i - 2\beta_j^-)}\cdot\right.\right.$$
$$\left.\left.\cdot\frac{d^2\sigma(\alpha_i,\beta_j^-)}{dt\,dM^2}\right] + 2\ln\frac{M^2}{S}\left[\frac{d^2\sigma}{dt\,dM^2}(\alpha_i = 2\beta_j^+) = \frac{d^2\sigma}{dt\,dM^2}(\alpha_i = 2\beta_j^-)\right]\right\}. \qquad (6.10)$$

For the designations see Fig. 6.2c. In (6.9) and (6.10) it was considered, for the sake of simplicity, that the Reggeon α has a positive signature. For the poles with a negative signature, the formulas vary insignificantly. In addition, we have written out in (6.10) only the contribution from the large masses, since the contribution to $\mathrm{Re}\,\Delta$ of the elastic and quasi-elastic processes is small (see above). The inclusive cross-section over the same poles can be written in the following form

$$\frac{d\sigma}{dt\,dM^2} = \sum_{i,j}\left[\frac{d\sigma(\alpha_i,\beta_j^+)}{dt\,dM^2} + \frac{d\sigma(\alpha_i,\beta_j^-)}{dt\,dM^2}\right].$$

We see that $\mathrm{Re}\,\Delta$ gives us essentially new information concerning three-Reggeon vertices. The main advantage of determining Δ at present is that the three-Reggeon PPP vertex determines the dependence of $\mathrm{Im}\,\Delta$ on energy. In order to determine $G_{PPP}(0)$ it is necessary to measure $\mathrm{Im}\,\Delta$ at various energies and isolate logarithmically the increasing term

$$\mathrm{Im}\,\Delta = d + c\ln S/M_0^2 \quad (R\,d\,m), \qquad (6.11)$$

where

$$c = \frac{1}{2}\pi G_{PPP}(0)/R_d^2. \qquad (6.12)$$

If $G_{PPP}(t) = \gamma t$ when $t \to 0$, then

$$c = \gamma\frac{\pi}{8}/R_d^2, \qquad (6.13)$$

i.e. is considerably smaller than in the previous case. What should be the measurement accuracy of the total cross-section, for example, of pd -scattering, in order to determine Δ ? For this we will insert in (6.12) and (6.13) $G_{ppp}(0)$ and γ from the experimental inclusive spectrum of protons in accordance with the processing method /50/. Then

$$\Delta_{ppp} < 0{,}1 \text{ mb} \cdot \ln S/M_0^2 (m_R d). \quad \text{for} \quad (6.12)$$

This means that when S varies from 20 to 200 GeV^2 Δ_{ppp} varies only by 0.23 mb. For (6.13) we have

$$\Delta_{ppp} < 1{,}5 \cdot 10^{-2} \text{ mb} \cdot \ln S/M_0^2 (m_R d).$$

Consequently in order to notice this variation it is necessary to measure the cross-section of pd -scattering at least with an accuracy of 0.1%. If the cross-section is measured with an accuracy of up to 1%, then, quite obviously, we can measure only G_{RRR}, which generally speaking is extremely important, since after its measurement it is possible to isolate accurately the contribution of PPP in the inclusive spectrum of the protons. Here it is convenient to use $R_e \Delta$, since, in fact, it is basically determined precisely by the contribution of G_{RRR}

$$R_e \Delta_{RRR} = \frac{\pi}{R_d^2} G_{RRR} (S/S_0)^{-1/2} (1-x)^{1/2}_{max} \quad (6.14)$$

(for this, use was made of the expression (6.2) for S (t)). From /50/

$$R_e \Delta_{RRR} \leq 3.0 \, \mu\delta / \sqrt{\frac{S}{S_0}} \quad (S_0 = 1 \text{ GeV}^2)$$

3. The deuteron as a target with an isotopic spin equal to zero

When measuring inclusive cross-sections on a deuteron in the range $|x| \to 1$, it is possible to obtain information concerning the contribution of the different Regge poles, if we describe this inclusive cross-section by the frequently used formulas (see above under chapter 3). It is most interesting to determine the contribution of the PPR and RRR terms, since in this case a contribution is given only by the non-vacuum Reggeons with I = 0 (ω and f), as distinct from the inclusive process on the proton, where (ρ and A_2) Reggeons are also substantial. In addition, when comparing the cross-sections of the processes

$$a + d \to d + \text{---} \qquad (6.15)$$

$$a + p \to p + \text{---}, \qquad (6.16)$$

it is possible to check the factorization relation

$$\frac{1}{(\sigma_{ad})^2} \cdot \frac{d^2\sigma\,(6.15)}{dx\,dq_1^2} = \frac{1}{(\sigma_{ap})^2} \cdot \frac{d^2\sigma\,(6.16)}{dx\,dq_1^2} . \qquad (6.17)$$

The relation (6.17) is valid only for $x \to 1$ in the range where the contribution is given only by the graph ppp. Consequently this, provided that (6.17) is properly fulfilled, will enable us to make a judgment concerning the size of the contributions of types RRR and PPR, the isolation of which is essential in order to determine G_{ppp}, and the study of this as a function of t is indeed one of the fundamental tasks of the projected experiment.

Let us now show that having measured the difference

$$\Delta\sigma = \frac{d\sigma(\pi^- d)}{dt} - \frac{d\sigma(\pi^+ d)}{dt},$$

it is possible to determine the relation of the real part to the imaginary part for a scattering amplitude of πd $(\rho_{\pi d})$ with an accuracy of $\alpha/\sqrt{s/s_0}$ /91/.

In reality, at high energies

$$\frac{d\sigma(\pi^\pm d)}{dt} = |A^{(+)}|^2 \pm 2 Re\, A^{(-)} A^{*(+)} + |A^{(-)}|^2 \qquad (6.18)$$

where $A^{(+)}$ and $A^{(-)}$ are the contribution of Reggeon or gamma-quanta exchange with a positive or negative signature. It can be seen from (6.18) that

$$\Delta\sigma = 4 Re\, A^{(-)} A^{*(+)}. \qquad (6.19)$$

As the isotopic spin of the deuteron is equal to zero, a contribution to $A^{(-)}$ is given only by the exchange of one photon (as we know, the photon has a negative signature and contains a state with I = 0) or graphs of the type shown in Fig. 6.3b. As a γ exchange gives terms of the order of α/t in the cross-section, and the graphs of Figure 6.3b give terms only of the order of $\alpha \ln \frac{1}{|t| R^2}$, which in reality are not great, we shall take into account only the exchange of Figure 6.3a in $A^{(-)}$. A contribution to $A^{(+)}$ may, generally speaking, be given by the exchanges expressed in Figure 6.4. It should be pointed out that the graphs of Figures 6.4a - 6.4f determine the contribution to the ~~material~~ real part of the scattering amplitude of strong πd -interaction and only the graph of Figure 6.4g gives the electromagnetic corrections to it. But this graph has an order of

$\alpha/\sqrt{s}/s_0$, so that the contribution of ω and ρ Reggeons falls with an increase in S . Finally, (6.19) can be re-written in the following form /91/

$$-4\mathrm{Re}\,A_c^{\pi d}\left(A_s^{\pi d}+O(\alpha/\sqrt{s})\right), \qquad (6.20)$$

where $A_c^{\pi d}$ is the contribution to the amplitude of photon exchange (Fig. 6.3b), equal to $\sim \frac{\alpha}{t} e^{i\varphi_{cc}}$, where φ_{cc} is the Coulomb phase equal to $\alpha \ln t/\lambda$. $A_s^{\pi d}$ is the amplitude of strong interaction. Thus, (6.20) enables a determination of $\mathrm{Re}(A_s^{\pi d} e^{-i\varphi_{cc}})$ with an accuracy of $\alpha\sqrt{s}$. Returning to the contribution to the cross-sections of the $\pi^+ d$ -scattering of the interference terms of the α/t type (Coulomb interference), we have

$$\frac{d\sigma(\pi^+ d)}{dt} = 2\left|A_c^{\pi d}\right|\left(\mathrm{Re}\left(A_s^{\pi d(+)} e^{-i\varphi_{cc}}\right) + \mathrm{Re}\left(A_{sc}^{\pi d(-)} e^{-i\varphi_{cc}}\right)\right) \qquad (6.21)$$

where $\mathrm{Re}(A_s^{(+)} e^{-i\varphi_{cc}})$ is determined from a measurement of $\Delta\alpha$, and the contribution to $\left(\mathrm{Re}\left(A_{sc}^{\pi d(-)} e^{-i\varphi_{cc}}\right)\right)$ is given by the graphs of the type shown in 6.3b, bearing in mind that at high energies the main contribution fits the diagram of Figure 6.5 ab. The diagrams of Figure 6.5a determine the so-called Bethe ~~beta~~ phase /93/, for which there is the generally accepted expression /94/.

$$\varphi_B = \alpha\left(\ln|t|\left(R_p^2+R_e^2\right)^{-1} - \gamma\right) = \alpha \ln \frac{1.2}{|t|R^2} \qquad (6.22)$$

(the latter equality forming part of the potential approach), whilst the diagrams of Figure 6.5b give the corrections.

In this way, by measuring the differential cross-section of $\pi^+ d$ and $\pi^- d$ -scattering in the region of Coulomb interference, it is possible to find with an accuracy of $\alpha/\sqrt{s/s_0}$ the corrections to the ~~beta~~ Bethe phase and determine how well the generally accepted formula agrees with experiment.

The questions touched upon in this lecture are now being subjected to intense experimental research. The authors hope that in the next volume of material for the present school they will be able to report some new experimental data.

The authors are grateful to V. N. Gribov, whose work was the theoretical basis of these lectures. The numerous discussions with him have also played a substantial part in preparing the lectures. The authors are also grateful to A. A. Vorob'ev and A. B. Kajdalov for some stimulating discussions.

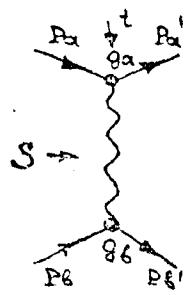

$$\sim g_a g_b \, S^{\alpha(t)}$$

$$S = (P_a + P_b)^2$$
$$t = (P_a - P_a')^2$$

a)

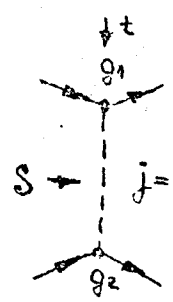

$$\sim \frac{g_1 g_2}{t - \mu^2} \sim S^0$$

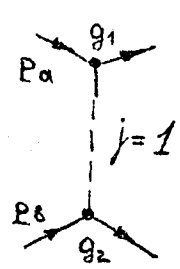

$$\sim \frac{g_1 g_2 (P_a P_b)}{t - \mu^2} \sim \frac{g_1 g_2}{t - \mu^2} S^1$$

b)

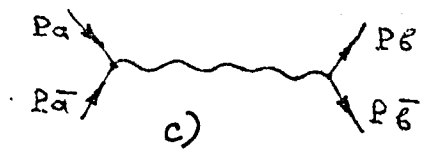

Fig. 1.1.

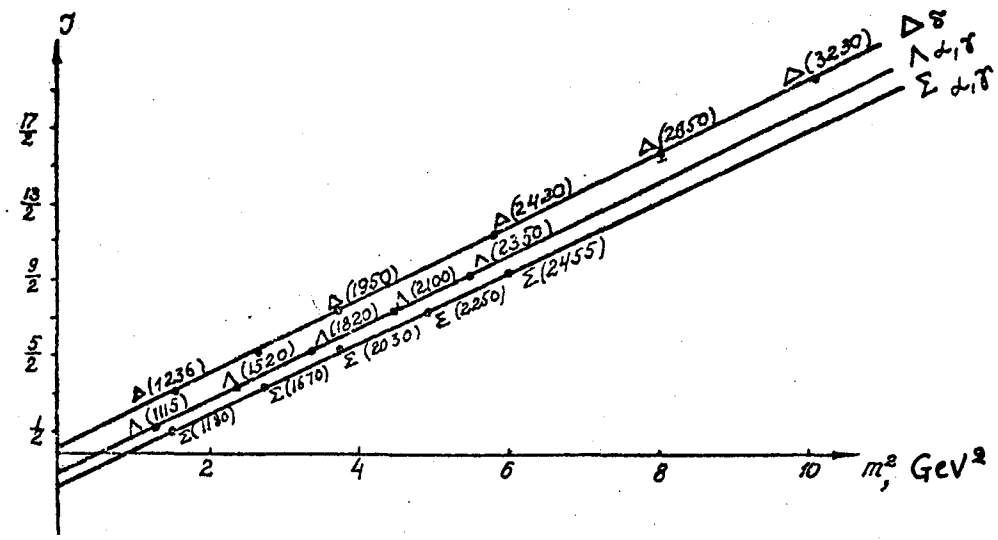

Fig. 1.2. Relation between spin and square of the mass for Δ, Λ, Σ states.

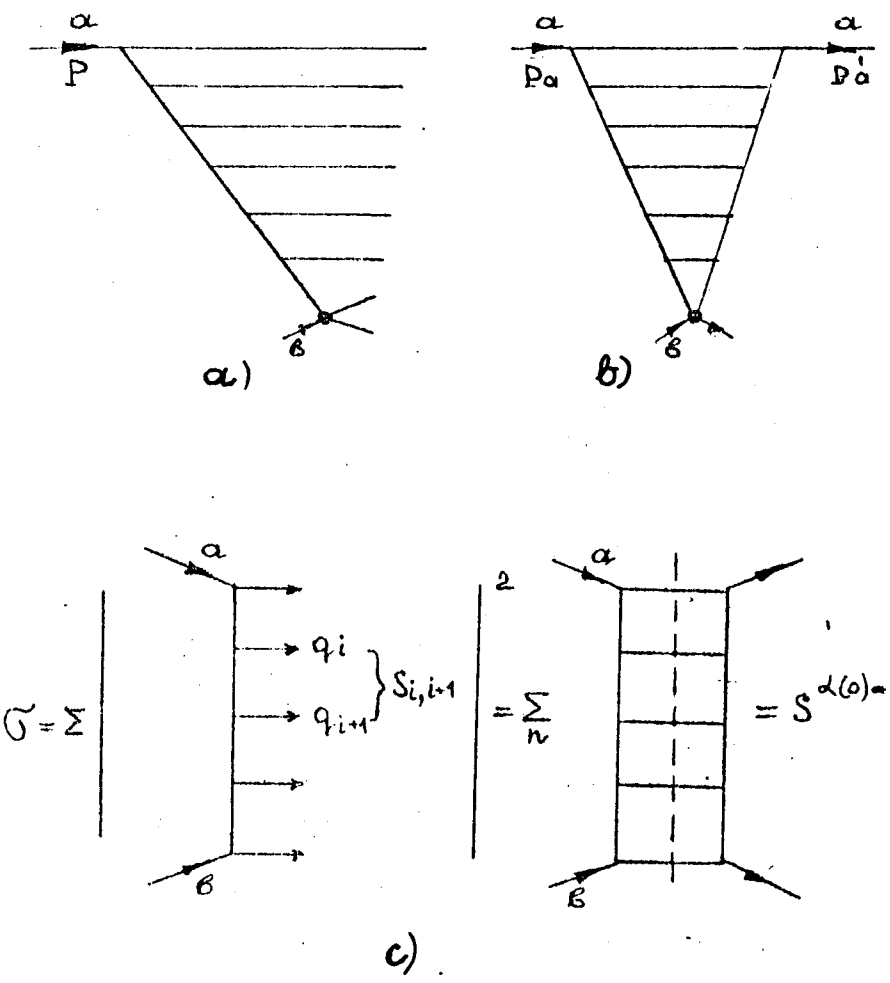

Fig. 1.3.

Table I

Reggeons	Quantum number *							Trajectories **		Resonances
	σ	I	S	B	G	P	P_2	$\alpha(0)$	α' (GeV/c)^2	
P^{***}	+	0	0	0	+	+	+	I	0,278±0,024	No
$f(P)$	+	0	0	0	+	+	+	0,5 ± 0,2	0,3 ± 2,2	f (I270)
A_2	+	I	0	0	−	+	+	0,4 ± 0,I	0,6 ± 0,2	A_2 (I3I0)
ω	−	0	0	0	−	−	+	0,4 ± 0,I	0,7 ± 0,3	ω (784)
ρ	−	I	0	0	+	−	+	0,57± 0,02	0,95± 0,I	ρ (765), g (I660)
π	+	I	0	0	−	−	−	0,I5± 0,I2	0,62±0,23	π (I40)
K^*	−	I/2	±I	0		−	+	0,33±0,02	0,84±0,03	K^*(890)
K^{**}	+	I/2	±I	0		+	+			K^{**}(I420)
$\Delta\delta$	−	3/2	0	I		+	−	0,I9±0,05	0,87±0,20	**See Fig. 1.2.**
N_α	+	I/2	0	I		+	+	-0,38±0,04	0,88±0,09	N (980), N(I688), N(2650)
N_γ	−	I/2	0	I		−	+	-0,94	0,92	N(I520), N(2I90)
Σ_α	+	I	-I	I		+	+	-0,84	I,0	**See Fig. 1.2.**
Σ_δ	−	I	-I	I		−	+			
Λ_α	+	0	-I	I		+	+	-0,7	0,97	**See Fig. 1.2.**
Λ_γ	−	0	-I	I		−	+			

* σ is the Reggeon signature, I is isotopic spin, S is strangeness, B is the baryon number, G is the parity equal to $C(-1)^I$, where C is the charged parity, P is the Reggeon parity, $P_2 = \sigma P$.

** The Reggeon trajectories are reproduced from the data on particle scattering, with the exception of the values underlined. The latter, when drawn through the resonances shown in the table, provided a straight line (the trajectory parameters were taken from [47]).

*** P is the vacuum Reggeon or Pomeranchuk pole (pomeron). It has been introduced to ensure the constancy of total cross-sections at $S \longrightarrow \infty$.

Table 2

Reaction	Reggeons providing a contribution	General characteristics of $\frac{d\sigma}{dt} = A e^{-b\|t\|}$ behaviour
$pp \to pp$	$P+f-\omega+A_2-\rho$	b = 9-13, cone shrinkage with $\alpha' P = 2 = 0.28$*, minimum at t = -1 3 $(GeV/c)^2$.
$\bar{p}p \to \bar{p}p$	$P+f+\omega+A_2+\rho$	b = 13-10, cone widening, minimum at t ~ = -0.6 $(GeV/c)^2$.
$K^+p \to K^+p$	$P+f-\omega+A_2-\rho$	b = 3-6, cone shrinkage , no minimum at t = -0.6 $(GeV/c)^2$.
$K^-p \to K^-p$	$P+f+\omega+A_2+\rho$	b = 7, the cone does not shrink, the minimum is at t ~ -0.6 $(GeV/c)^2$.
$\pi^+p \to \pi^+p$	$P+f-\rho$	b = 6-7, cone narrowing, minimum at t ~ -0.6 $(GeV/c)^2$.
$\pi^-p \to \pi^-p$	$P+f+\rho$	b = 7.5, the cone does not shrink, minimum at t ~ -0.6 $(GeV/c)^2$.
$\pi^-p \to \pi^0 n$	ρ	b = 9, minimum forward and at t ~ -0.6 $(GeV/c)^2$.
$\pi^+p \to \varrho n$	A_2	b = 5.5 no minimum.
$K^+p \to \pi^0\Delta^{++}$	ρ	b = 10, minimum forward and at t ~ -0.6 $(GeV/c)^2$.
$\pi^+p \to \eta\Delta^{++}$	A_2	Minimum forward.
$K^+p \to K^{*0}\Delta^{++}$	$\pi+A_2+\rho$	Peak forward ("b" in the peak ~ 40 (GeV/c^{-2}).
$pn \to \Delta^{++}\Delta^-$	$\pi+A_2+\rho$	Peak forward.
$\bar{p}p \to \bar{\Delta}^{++}\Delta^{++}$	$\pi+A_2+\rho$	b = 12.
$\pi^-p \to \rho^-p$	$\omega+\pi$	b = 8, minimum at t ~ -0.6 $(GeV/c)^2$.
$\pi N \to \omega N$	ρ	b = 3, minimum forward.
$\gamma N \to \pi^+N$	$\rho+\pi$	Peak forward.
$\pi p \to A_2 p$	$P+\rho+f$	Minimum forward b = 8.
$pn \to np$	$\rho+A_2+\pi$	Peak forward, at -t = 0-0.02 $(GeV/c)^2$, "b" in it 57.4, at large t, b = 4.3.
$\pi^+p \to p\pi^+$	$\Delta\delta+N_\alpha+N_\gamma$	b = 10-12, minimum at u = -0.19 $(GeV/c)^2$.
$\pi^-p \to p\pi^-$	$\Delta\delta$	b = 10-12, no minimum at $u \approx$ -0.19 $(GeV/c)^2$.

* For further details on cone shrinkage see Figures 1.4, 1.5 and 1.6 and also in the text.

Table 3a

Reggeon exchange	n	$2 - 2\alpha(0)$
P	0.3	0
Reggeon with S = 0	1.3-2.3	1 for ρ, A_2 1-1.4 for ω 2.0 for π
Reggeon with S = 1	2.0-2.8	1.4
Fermion	3 - 6	2 - 3

Values of n , taken from processing the dependence of the cross-sections of various reactions on S according to the formula $\sigma = A p_{lab}^{-n}$ [7, 35].

a) n are reproduced, averaged over the total collectionof reactions with the exchange indicated.

Table 3b

Reaction	Reggeon	Energy region P_{lab} in GeV/c	n
$\pi^- p \to \pi^0 n$	ρ	5 - 50	I,I2 ± 0,03
$\pi^+ p \to \pi^0 \Delta^{++}$	ρ	2 - I3	I,6 ± 0,I
$\bar{p} p \to \eta n$	A_2	6 - 50	I,35 ± 0,04
$\pi^+ p \to \eta \Delta^{++}$	A_2	2 - I9	I,57 ± 0,I5
$K^+ p \to K^{*0} \Delta^{++}$	π	4,6 - I6	I,68 ± 0,08
$p p \to \Delta^{++} \Delta^-$	π	3 - 30	I,45 ± 0,22
$\bar{p} p \to \bar{\Delta}^{++} \Delta^{++}$	π	3 - 6	I,09 ± 0,I0
$\pi^- p \to \rho^- p$	ω, π	4 - 40	I,87 ± 0,09

Table 3b gives a representation of the scatter of n over the reactions with the exchange of strange meson Reggeons ($2 - 2\alpha(0)$, see Table 3a).

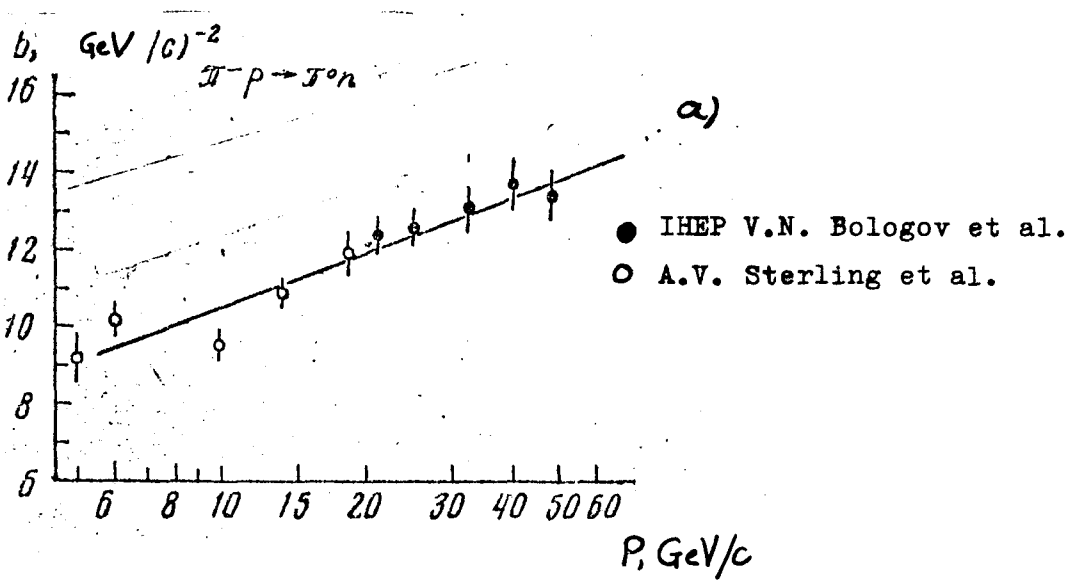

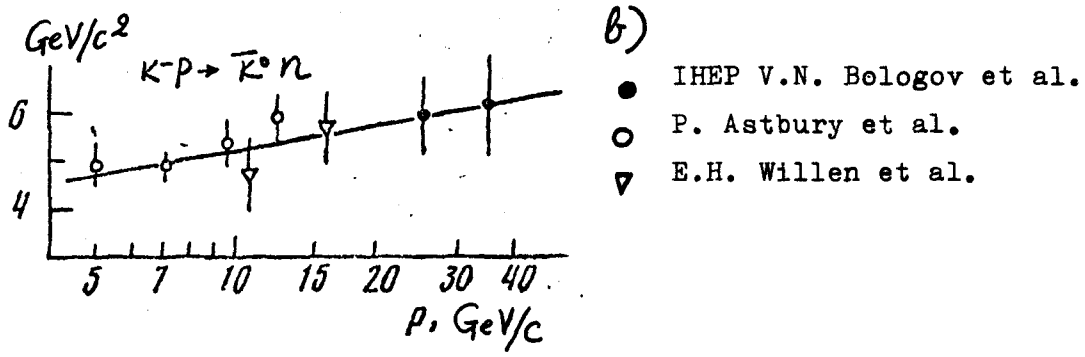

Fig. 1.4. Momentum dependence of slope parameters with the exchange of non-vacuum quantum numbers in the t channel.

a) Reaction of charge exchange $\pi^- p \longrightarrow \pi^0 n$ $(0.15 \leq -t \leq 0.5\ (\mathrm{GeV/c})^2)$. The straight line corresponds to the formula $b = (4.2 \pm 0.9) + (2.1 \pm 0.3) \ln S$ (S - in GeV^2).

b) Charge exchange reaction $K^- p \to \bar{K}^0 n$ $(-t \gtrsim 0.2\ (\mathrm{GeV/c})^2)$. The straight line corresponds to the formula $b = (4.7 \pm 0.5) + (0.8 \pm 0.4) \ln S/S_0$ ($S_0 = 10\ \mathrm{GeV}^2$).

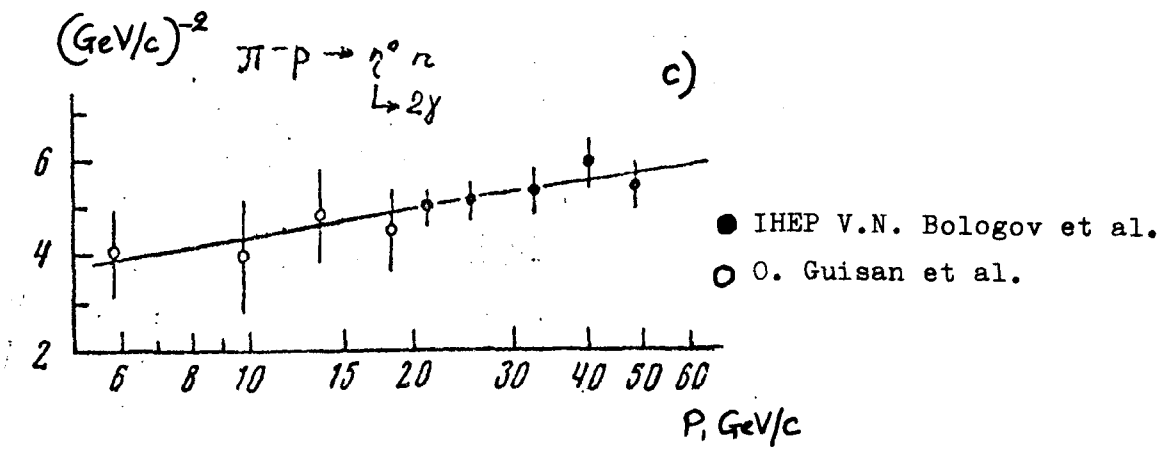

c) Reaction $\pi^- p \to n_0 n_2 \gamma$ ($0.2 \leq -t \leq 1.0$ $(\mathrm{GeV}/c)^2$).
The straight line corresponds to the formula
$b = (3.7 \pm 0.6) + (0.9 \pm 0.4) \ln s/s_0$ ($s_0 = 10\ \mathrm{GeV}^2$).

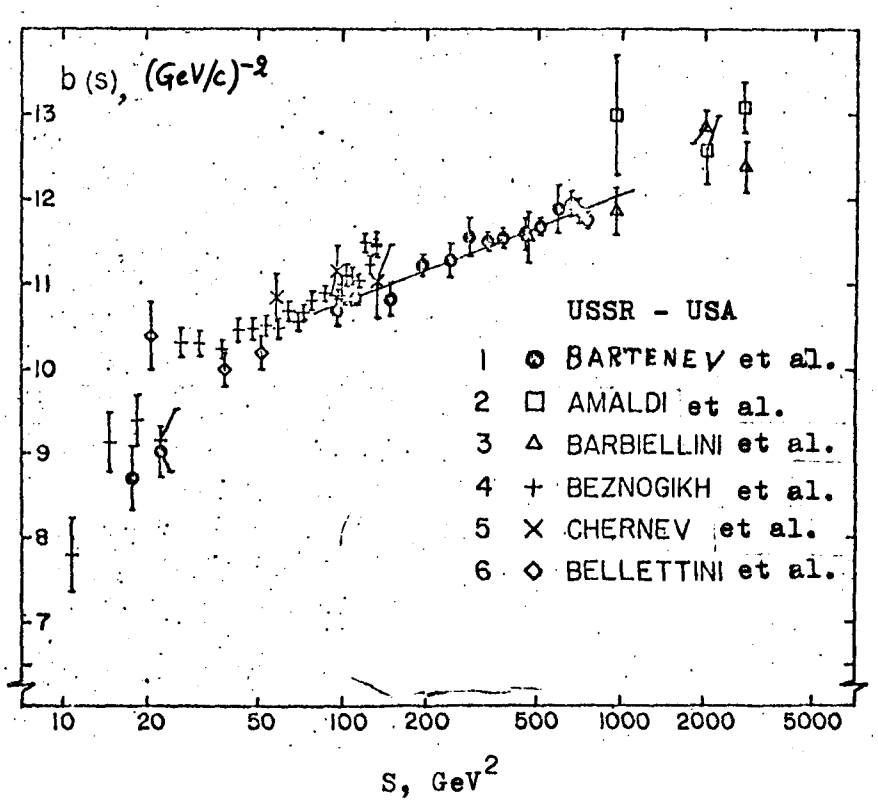

Fig. 1.5. Parameter of the slope in pp-scattering of b at $|t| \leq 0.12$ (GeV/c)^2 as a function of S. The straight line corresponds to $b(s) = b_0 + 2\alpha' \ln s/s_0$ ($b_0 = 8.23 \pm 0.27$, $\alpha' = 0.278 \pm 0.024$ (GeV/c)$^{-2}$).

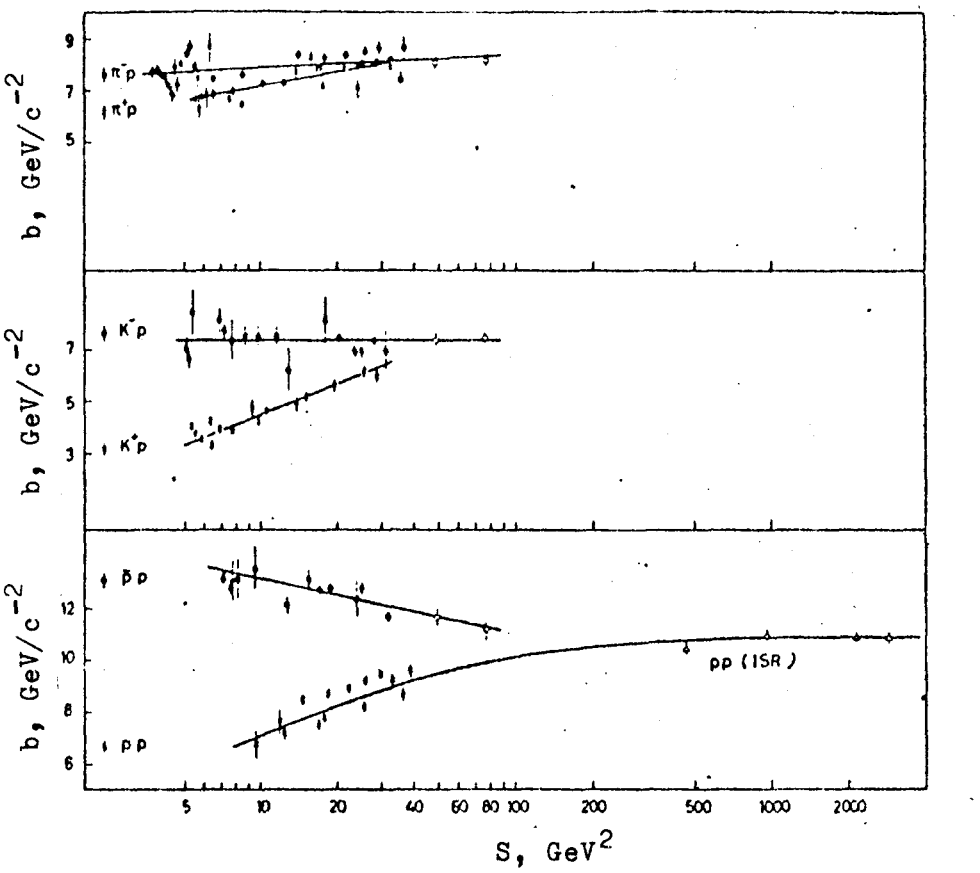

Fig. 1.6. Compilation of slope parameters in various elastic reactions at $-\bar{t} = 0.2$ (GeV/c)^2.

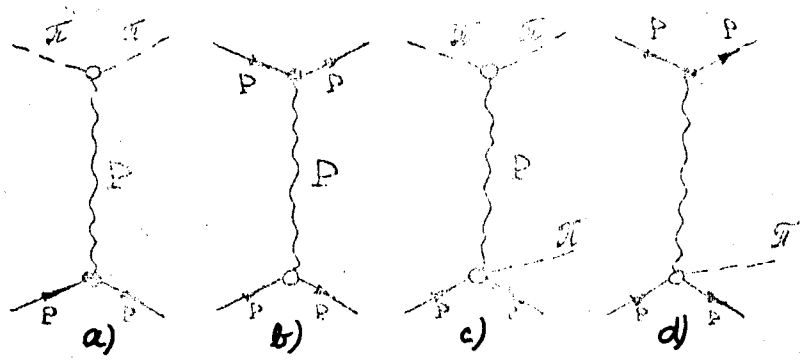

Fig. 1.7.

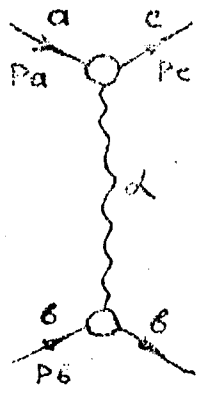

Fig. 1.8.

Table 4

$$R_1 = \frac{\sigma(\pi^- p \to \pi^- \rho)}{\sigma(pp \to p\rho)} = 0,43$$

$$R_2 = \frac{\sigma(\pi p \to \pi(p\pi^0))}{\sigma(pp \to p(p\pi))} = 0,46 \pm 0,15$$

$$R_3 = \frac{\sigma(\pi p \to \pi(p\pi^+\pi^-))}{\sigma(pp \to p(p\pi^+\pi^-))} = 0,35 \pm 0,18$$

$$R_4 = \frac{\sigma(\pi p \to \pi(p\pi\pi\pi))}{\sigma(pp \to p(p\pi\pi\pi))} = 0,15 \pm 0,15$$

Table 5

	Momentum, GeV/c		
	6-10	10-14	14-18
$R_1 = \frac{\sigma(\gamma p \to \rho^0 p)}{\sigma(\gamma p \to \rho^0(p\pi^+\pi^-))}$	0,053 ± 0,014	0,035 ± 0,014	0,055 ± 0,024
$R_2 = \frac{\sigma(pp \to pp)}{\sigma(pp \to p(p\pi^+\pi^-))}$	0,064 ± 0,007	0,061 ± 0,008	0,060 ± 0,009
$R_3^+ = \frac{\sigma(\pi^+ p \to \pi^+ p)}{\sigma(\pi^+ p \to \pi^+(p\pi^+\pi^-))}$		0,061 ± 0,006	0,063 ± 0,003
$R_3^- = \frac{\sigma(\pi^- p \to \pi^- p)}{\sigma(\pi^- p \to \pi^-(p\pi^+\pi^-))}$		0,052 ± 0,005	0,059 ± 0,003

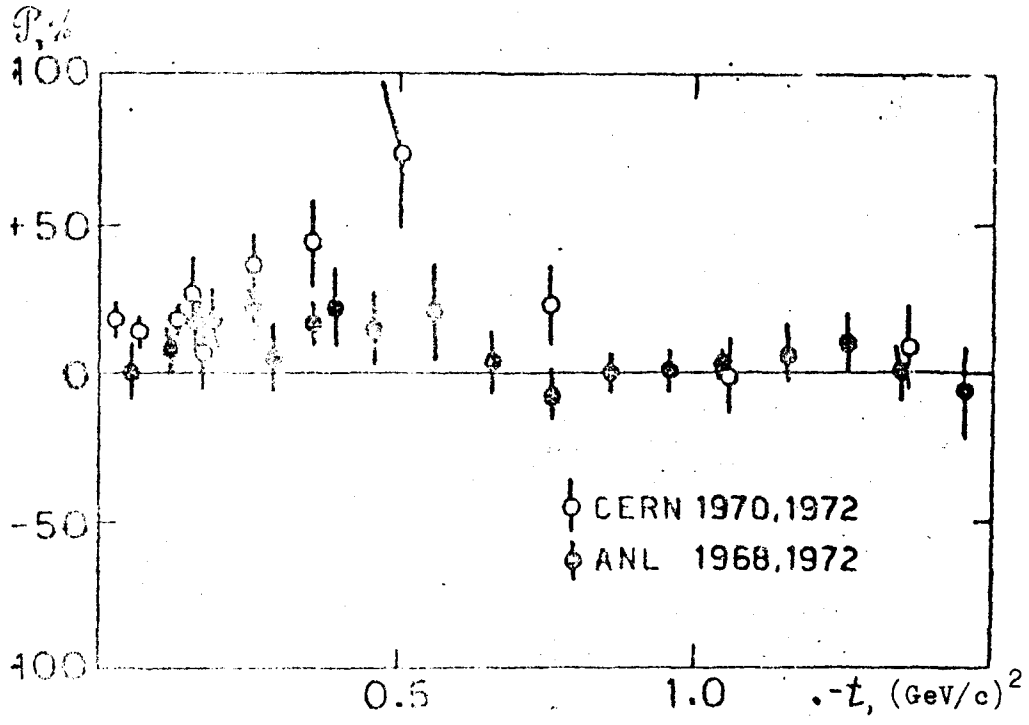

Fig. 1.9a. Polarization in the $\pi^- p \to \pi^0 n$ reaction at 5 GeV/c.

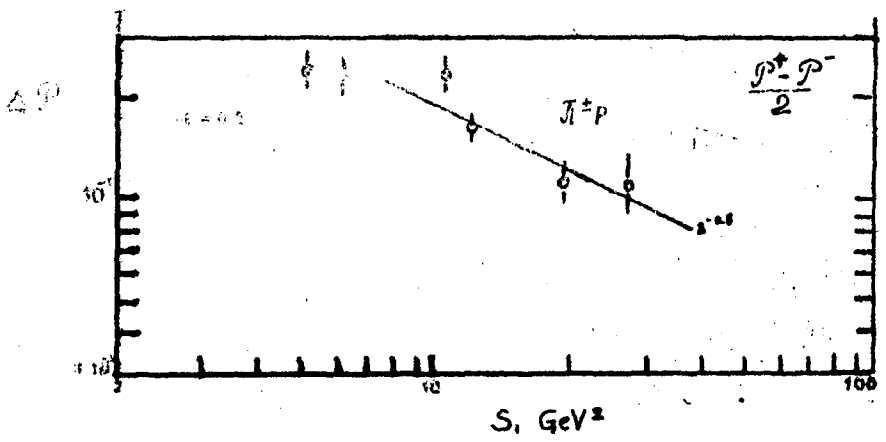

Fig. 1.9b. Energy dependence of the half-difference of the polarizations $\Delta P = \frac{P(\pi^+ p) - P(\pi^- p)}{2}$ in $\pi^\pm p$ - scattering at $-t = 0.2$ GeV^2. The data were taken from the report of L. Van Rossum (International Seminar on Binary Reactions of Hadrons at High Energies, Dubna, 1971). The main contribution to the value ΔP is given by the Pomeranchuck pole interference with the ρ trajectory.

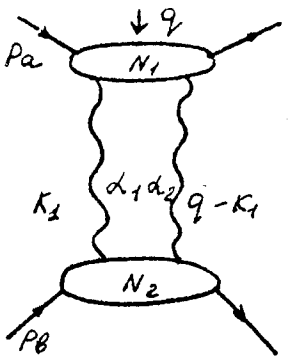

Fig. 1.10.

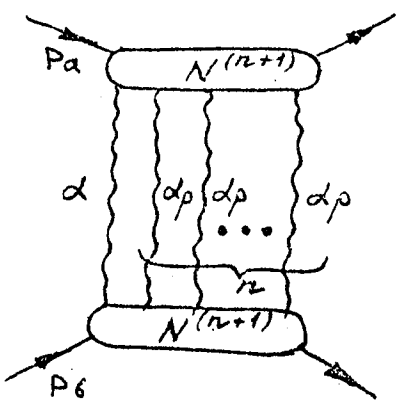

Fig. 1.11.

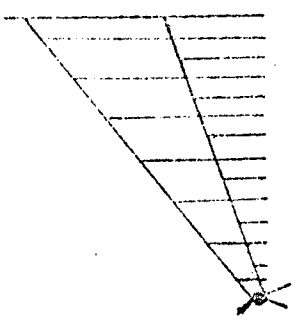

Fig. 1.12.

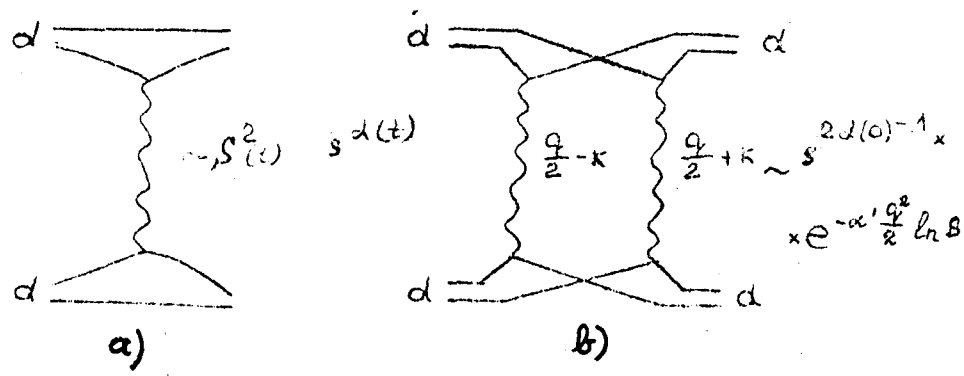

Fig. 1.13.

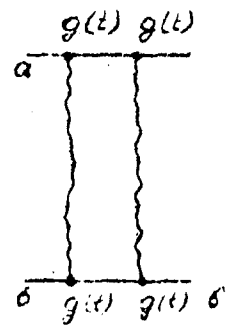

Fig. 1.14.

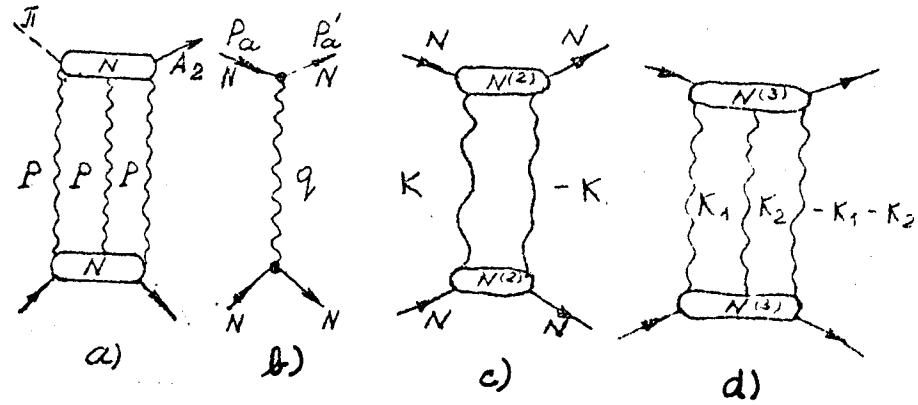

Fig. 1.15.

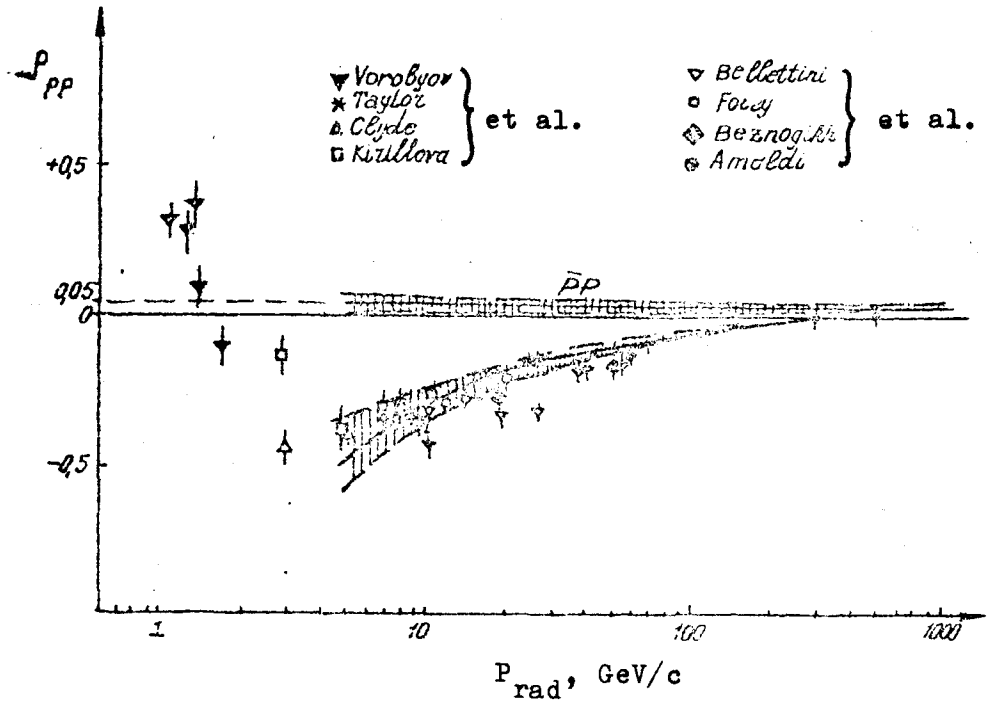

Fig. 1.16a. Relationship between the real and imaginary parts of the amplitude of forward pp -scattering, ρpp.

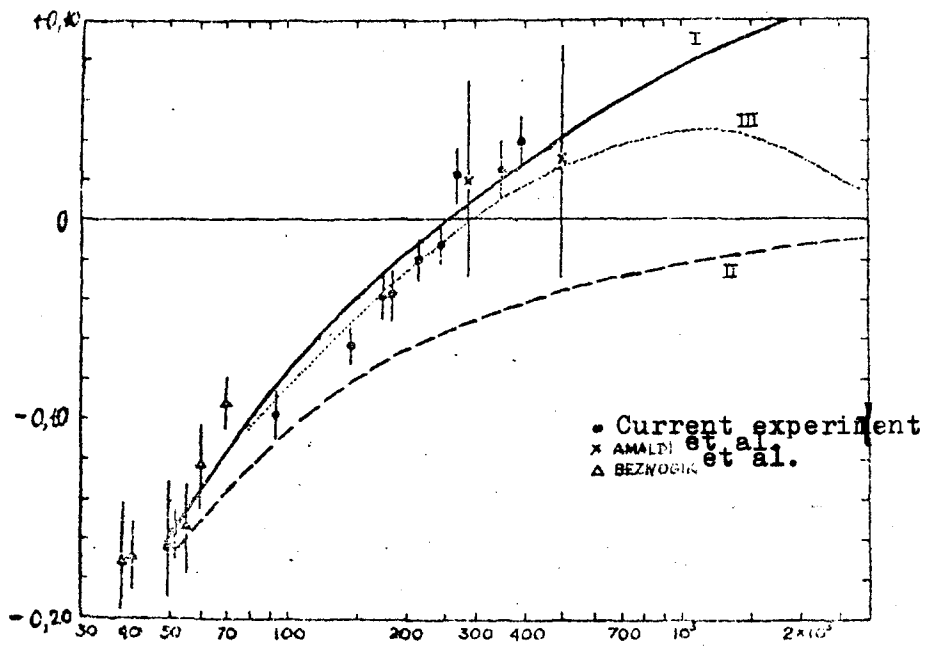

Fig. 1.16b. Relationship between the real and imaginary parts of the amplitude of forward pp -scattering ρpp, measured by the Soviet/American group. The curves are calculations of ρpp from the dispersion relationships on the following assumptions:

I. $\sigma_T(pp)$ and $\sigma_T(\bar{p}p)$ increase according to $0.49\ \ln^2(s/122)$;
II. $\sigma_T(pp)$ is constant at $E > 120$ GeV and equal to 38 mb;
III. $\sigma_T(pp)$ become constant and equal to 44.2 mb at $E > 2000$ GeV.

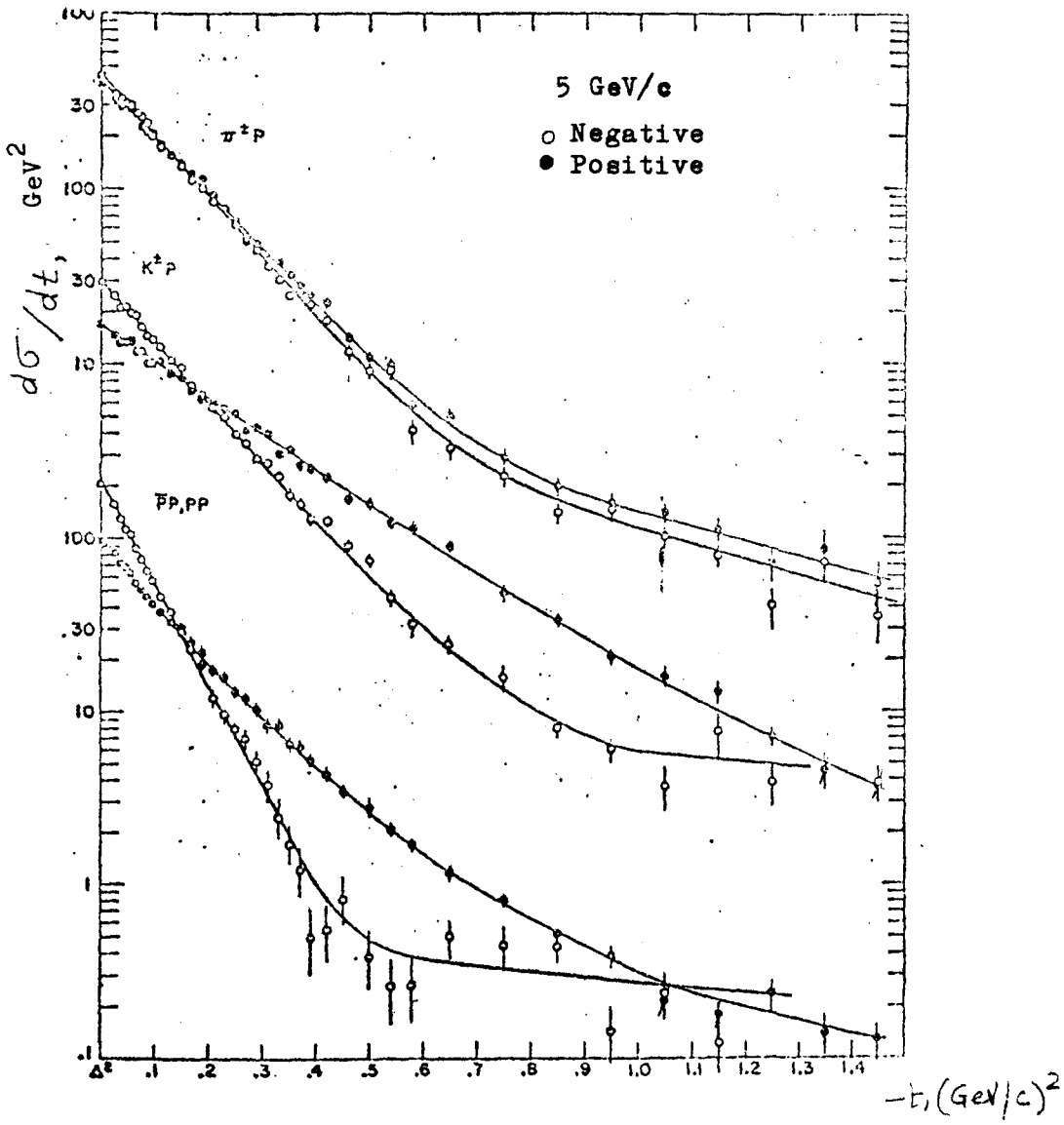

Fig. 1.17. Crossover of differential cross-sections of the elastic scattering of particles and anti-particles on a proton at 5 GeV/c.

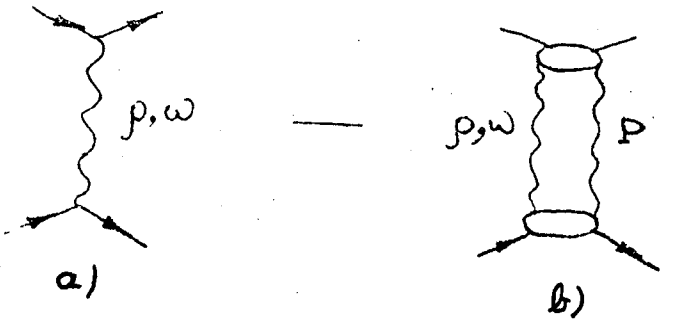

Fig. 1.18.

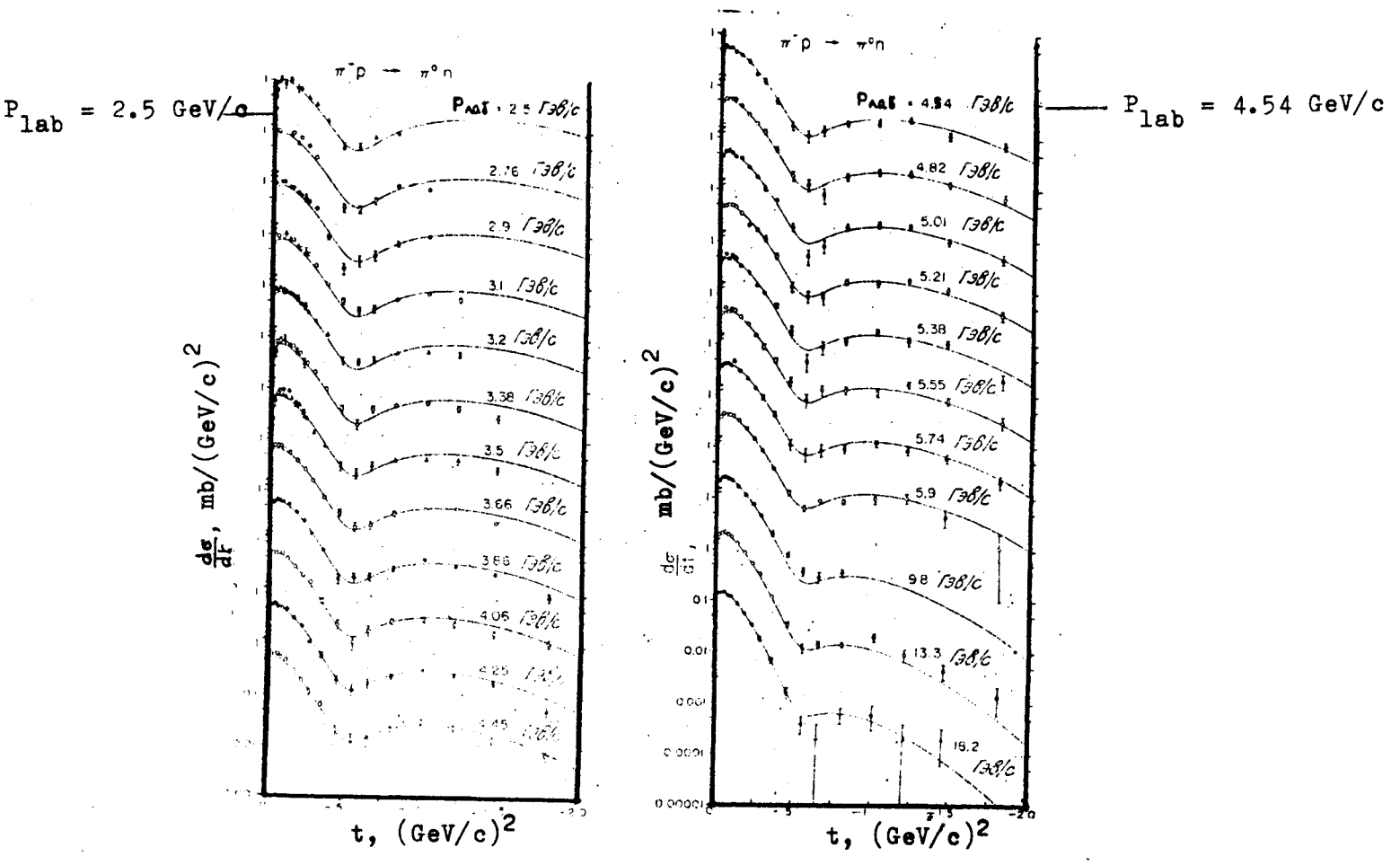

Fig. 1.19a. Angular distribution of the cross-section of the charge exchange $\pi^- p \to \pi^0 n$.

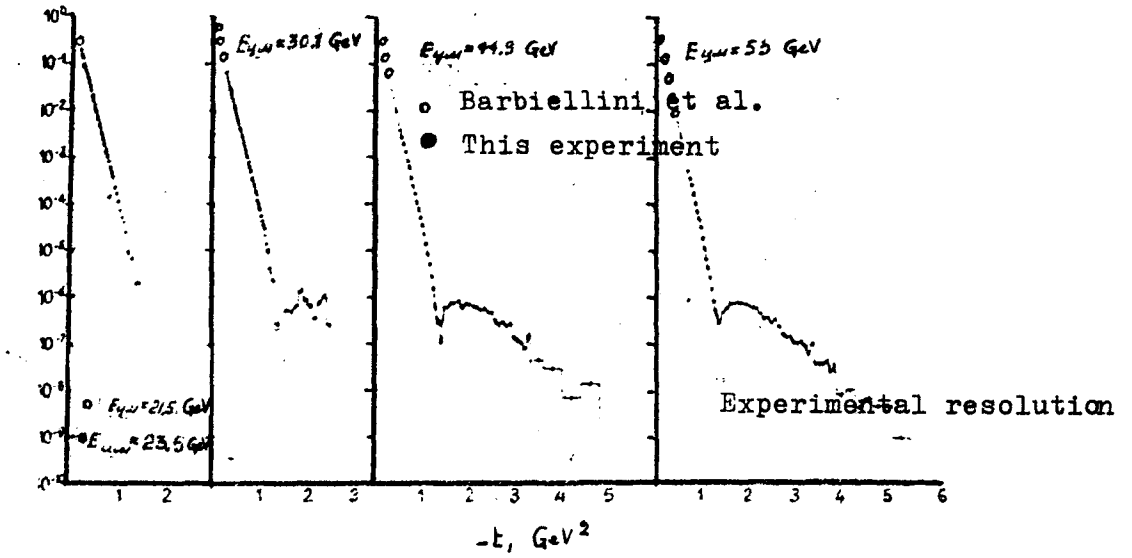

Fig. 1.19b. Dependence of the differential cross-section of pp-scattering on t at 4 ISR energies.

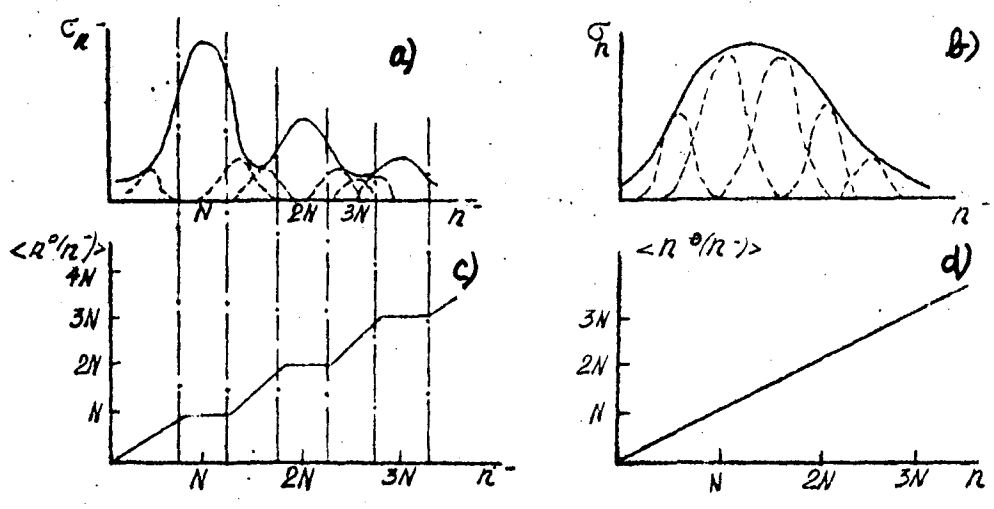

Fig. 1.20.

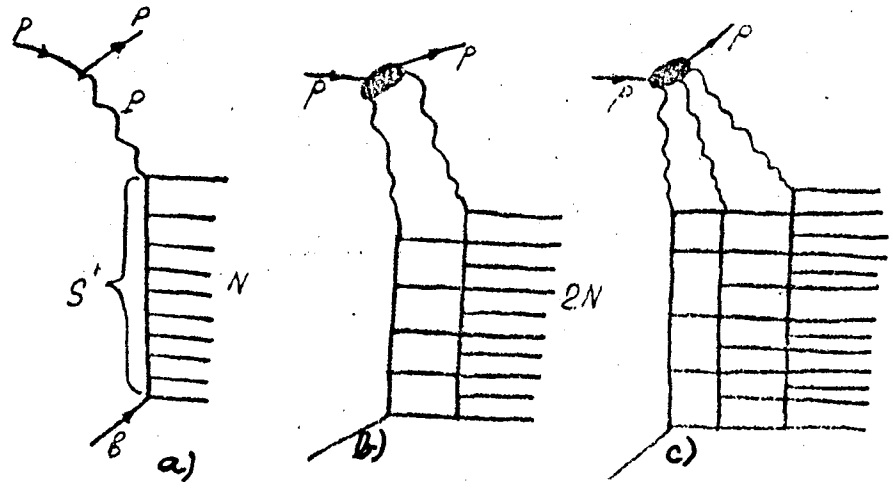

Fig. 1.21.

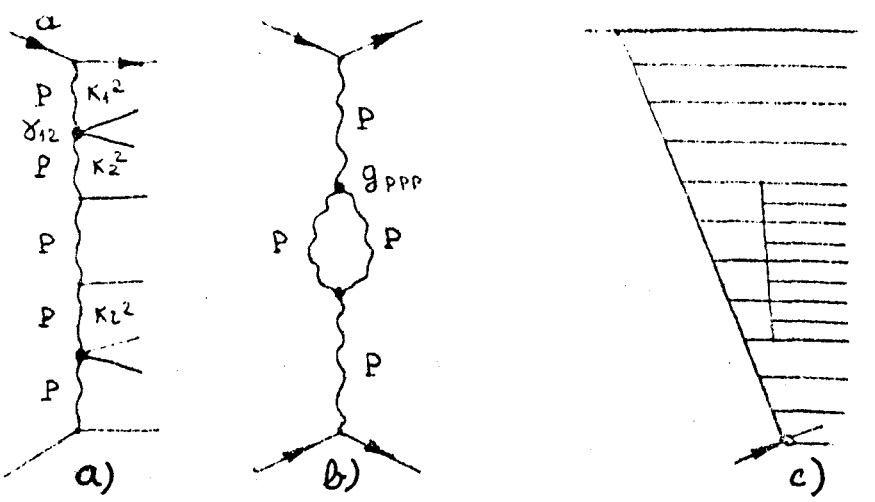

Fig. 1.22.

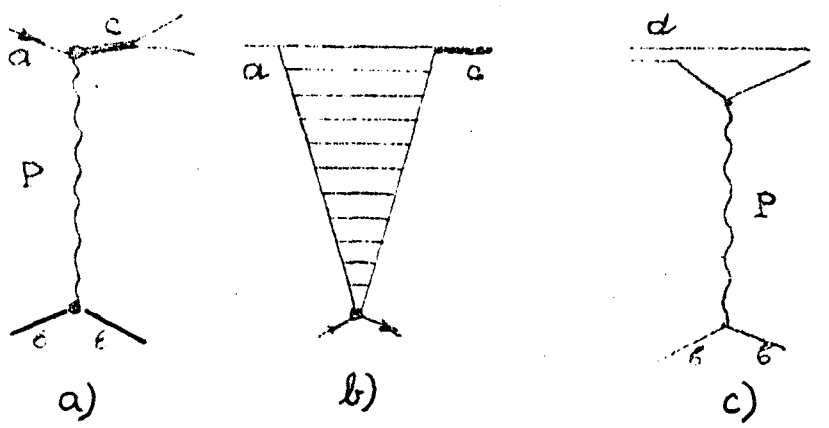

Fig. 1.23.

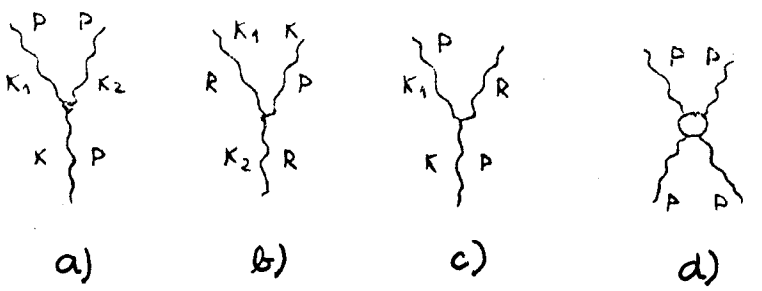

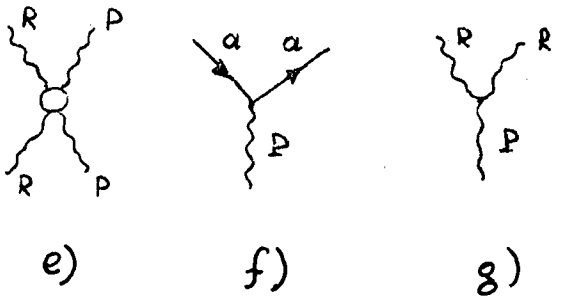

Fig. 1.24.

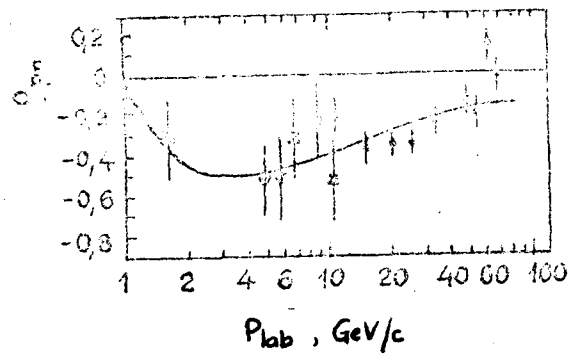

Fig. 2.1. Relationship between the real and imaginary parts of the amplitude of pn-forward scattering at E < 70 GeV.

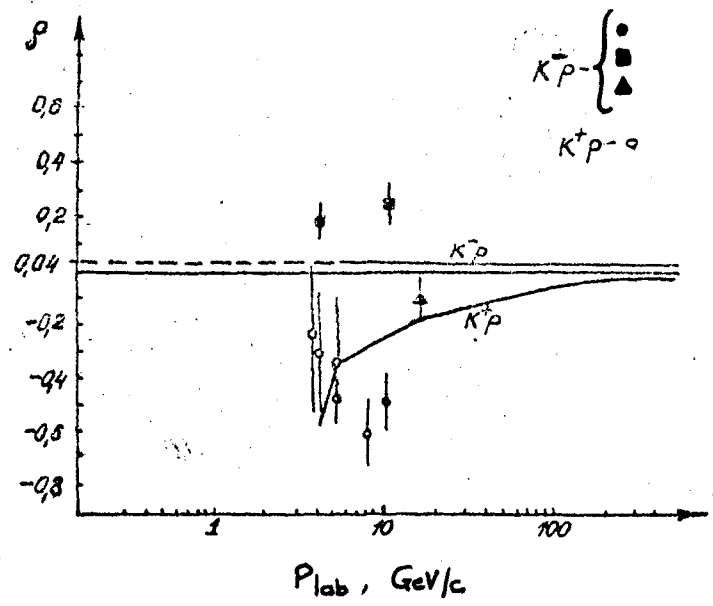

Fig. 2.2. Relationship between the real and imaginary parts of the amplitudes of k^-p and k^+p -forward scattering.

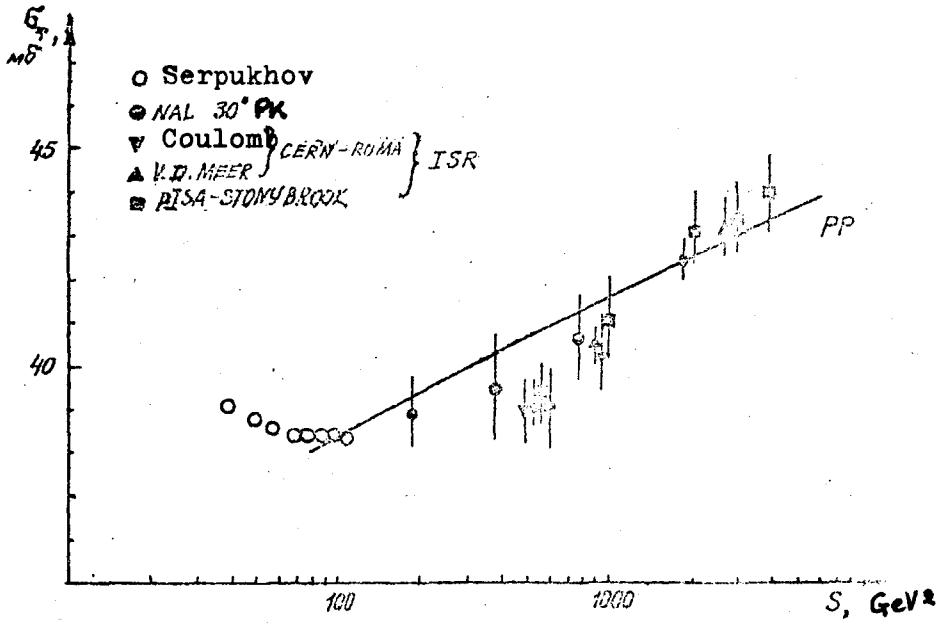

Fig. 2.3a. Total cross-section of pp-interaction at high energies.

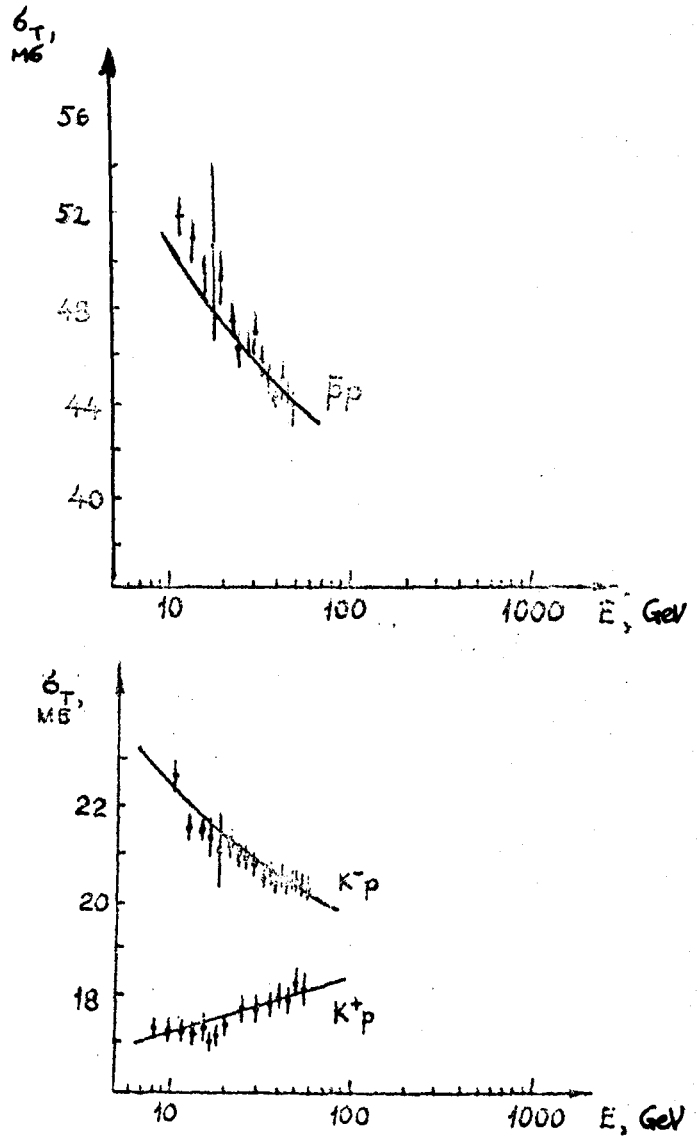

Fig. 2.3b. Behaviour of the total cross-sections of $\bar{p}p$, $k^{\pm}p$ at $E \leqslant 60$ GeV.

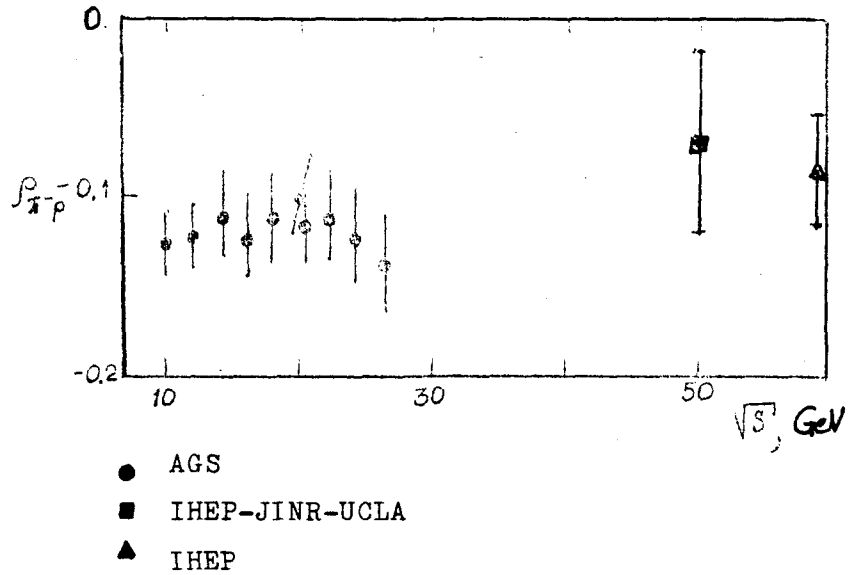

Fig. 2.4a. Relationship between the real and imaginary parts of the amplitude of π^-p-forward scattering.

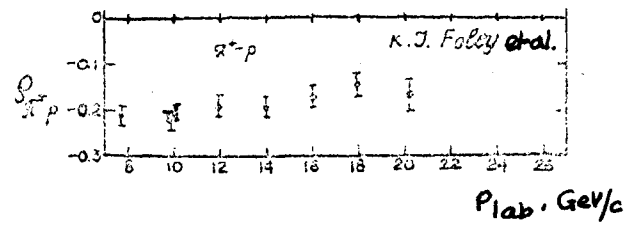

Fig. 2.4b. Relationship between the real and imaginary parts of the amplitude of π^+p-forward scattering.

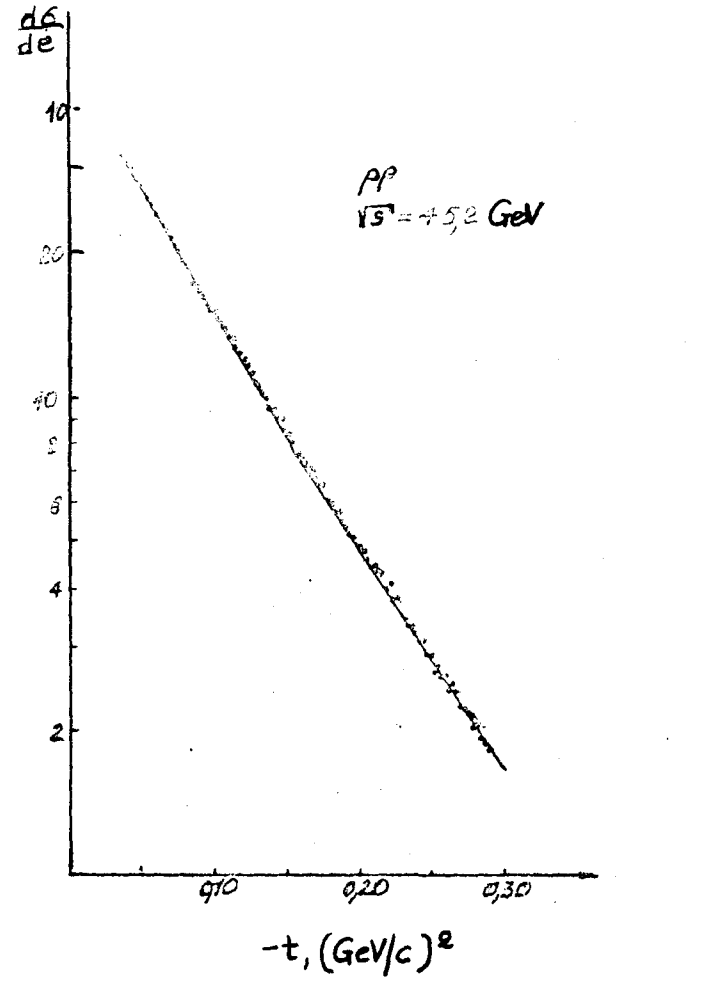

Fig. 2.5. $\frac{d\sigma_{pp}}{dt}$, analyzed in accordance with the formula $\frac{d\sigma_{pp}}{dt} = G_p^4(t)\, s^{-2\alpha' |t| \ln s/s_0}$, where $G_p(t)$ is the electrical form factor of the proton.

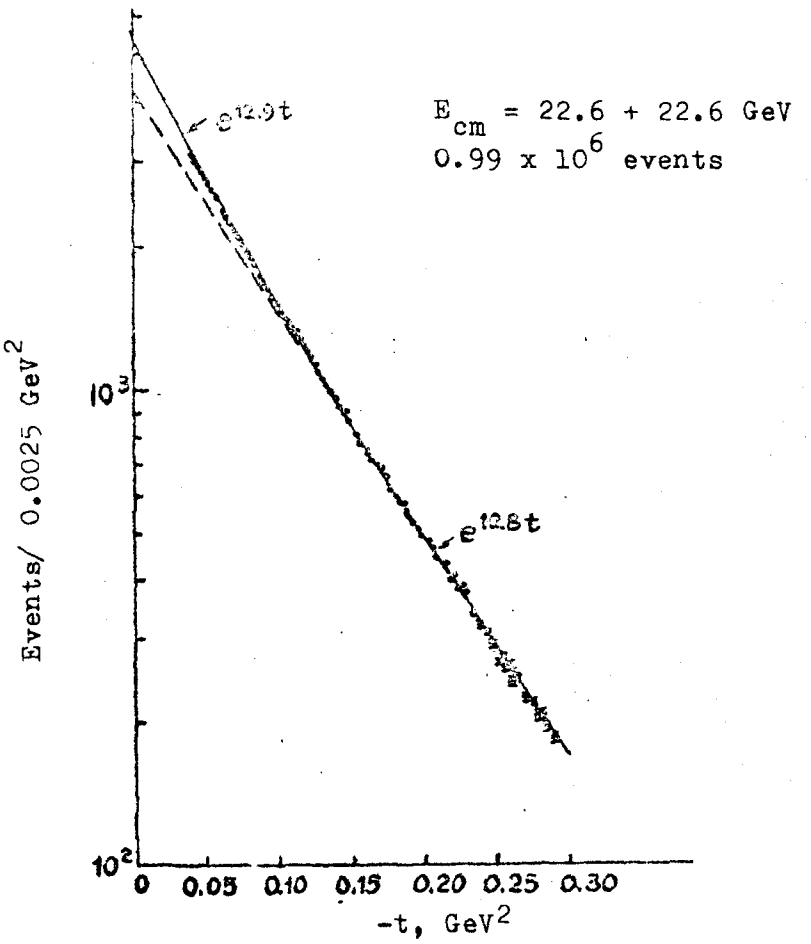

Fig. 2.6. Experimental data for $\frac{d\sigma_{pp}}{dt}$, taken from [39].

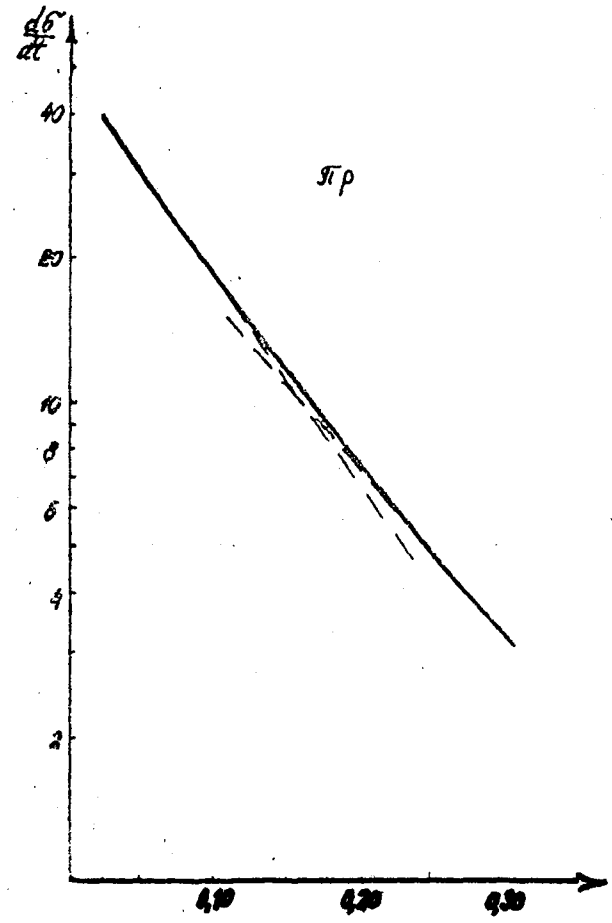

Fig. 2.7. $\frac{d\sigma_{\pi p}}{dt}$ constructed in accordance with the formula $G_{\pi}^{2}(t)\,G_{p}^{2}(t)\,l^{-2\alpha'|t|\ln s/s_0}$.

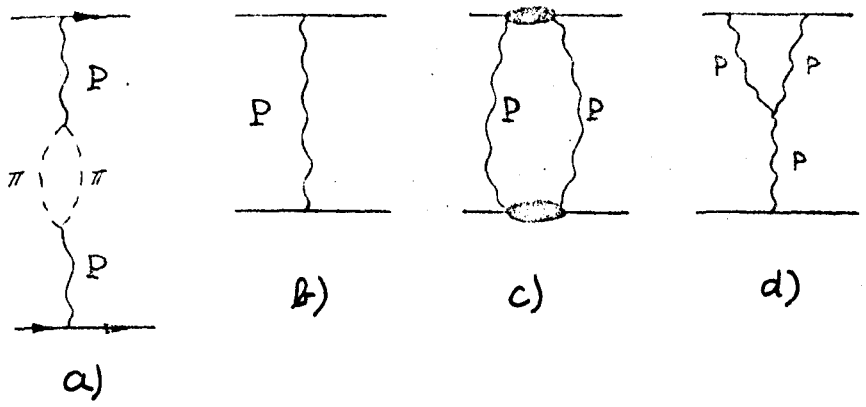

Fig. 2.8.

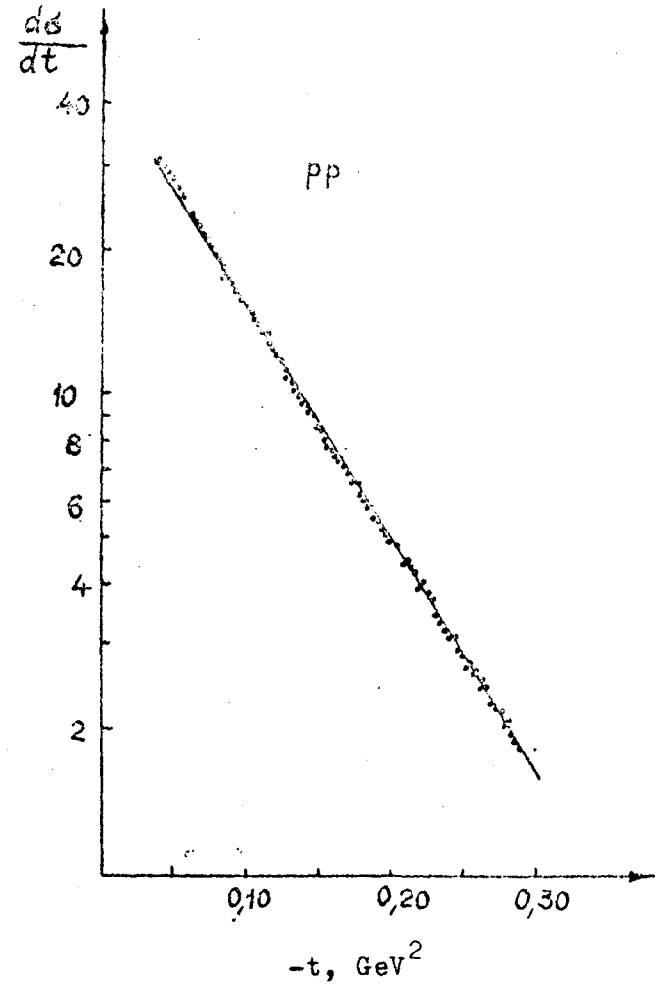

Fig. 2.9a. Dependence of $\frac{d\sigma}{dt}$ on t, calculated in accordance with formula (2.5) at $\sigma_{\pi\pi}$ = 16 mb ± 5%.

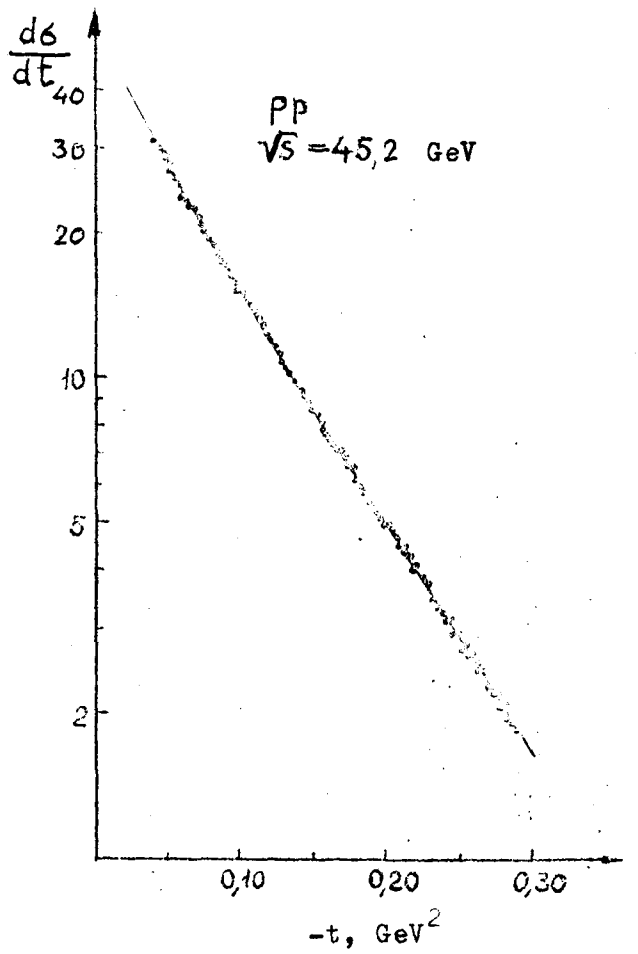

Fig. 2.9b. Dependence of $\frac{d\sigma_{pp}}{dt}$ on -t calculated in accordance with formula (2.5) at $\sigma_{\pi\pi}$ = 32 mb ± 5%.

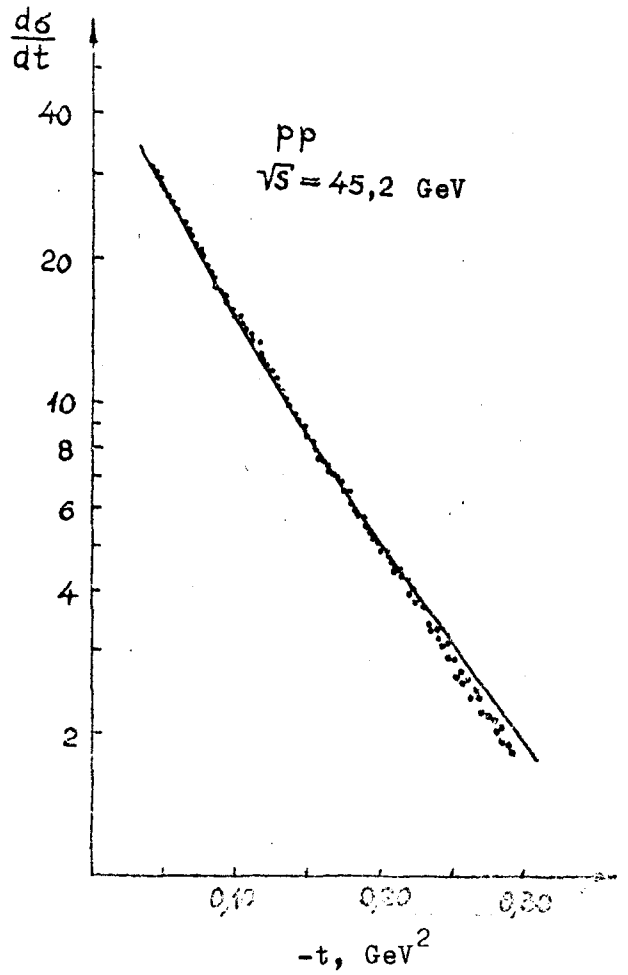

Fig. 2.10. $\frac{d\sigma_{pp}}{dt}$, calculated in accordance with formula (2.9).

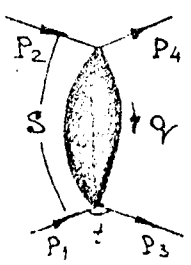

Fig. 3.1.

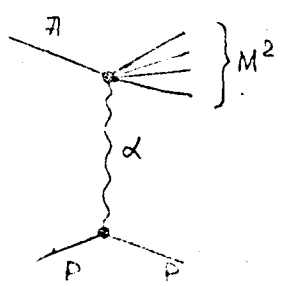

Fig. 3.2.

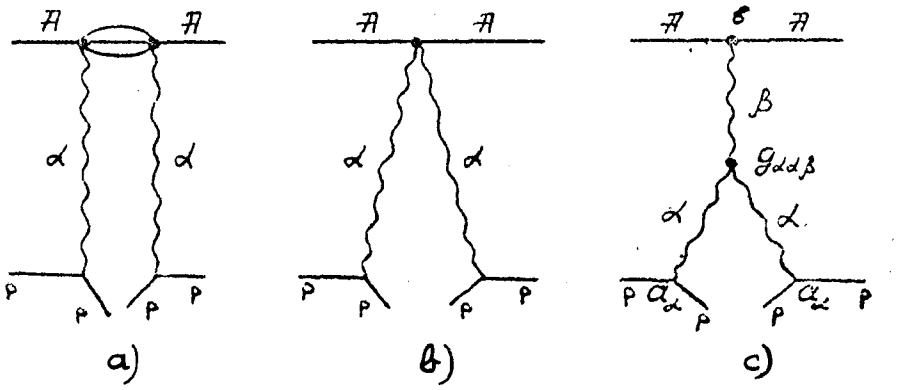

Fig. 3.3.

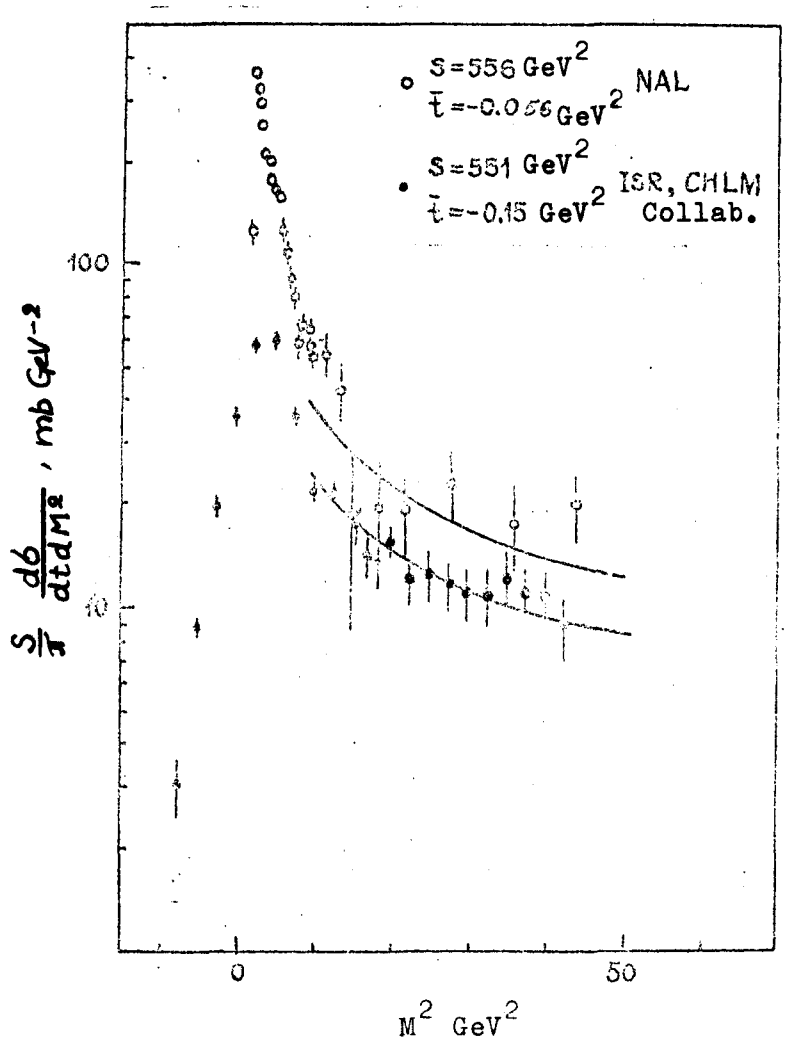

Fig. 3.4a. Invariant cross-sections of the $pp \rightarrow pX$ process as a function of M^2 at $S = 556$ GeV^2 and $\bar{t} = -0.056$ GeV^2 /54/ and at $S = 551$ GeV^2 and $\bar{t} = -0.15$ GeV^2 /56/. The curves indicate the results of analysis in accordance with /50, 62/.

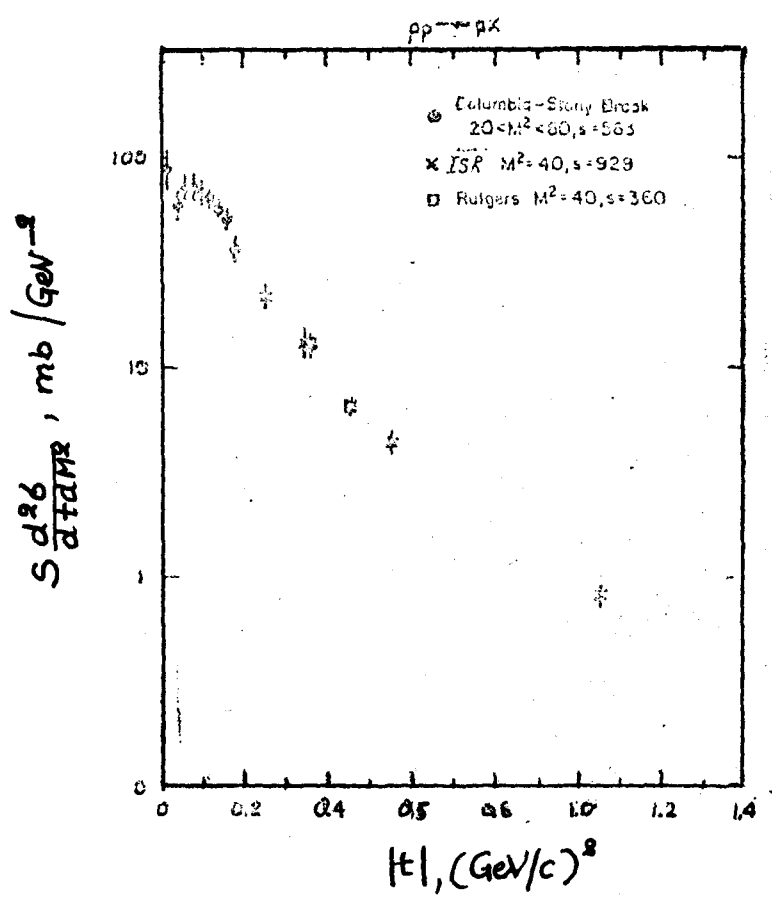

Fig. 3.4b. Results of some new experiments shown in drawing 3.4 b-c taken from the review by D.W.G.S. Leith (SLAC-PUB-1330 (T/E) October 1973). these data point to a possible flattening out or even a drop in the inclusive cross-section as a function of $p_\perp^2$ when there is a reduction in $p_\perp^2$ if the excited masses M are small. These results are to some extent preliminary. They do not agree with the results of other experiments (see for example Fig. 3.6, Fig. 3.5) since the situation requires more accurate experimental details.

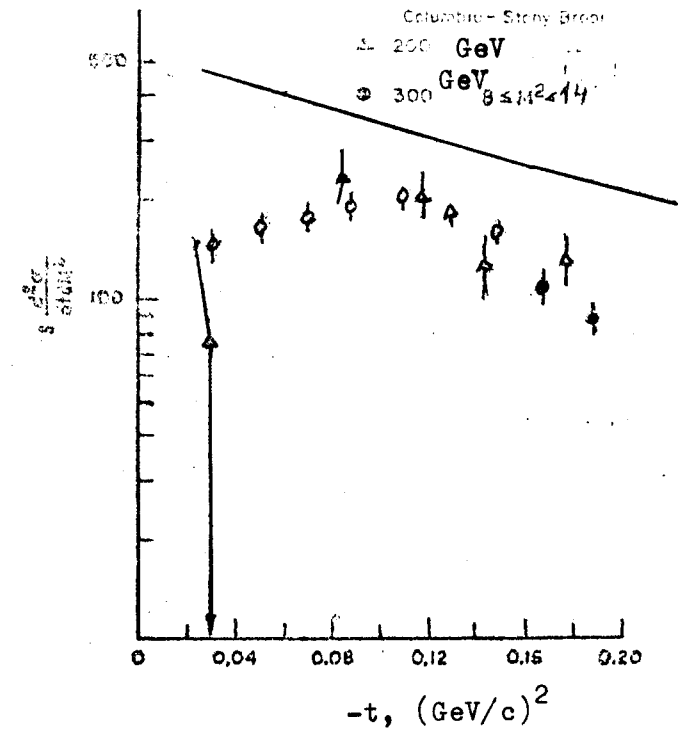

Fig. 3.4c.

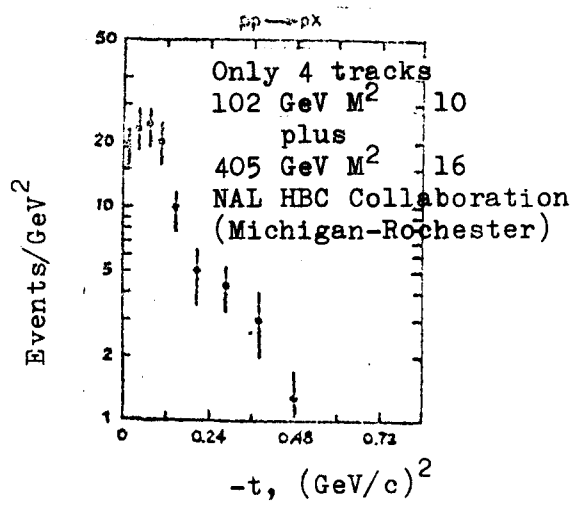

Fig. 3.4d.

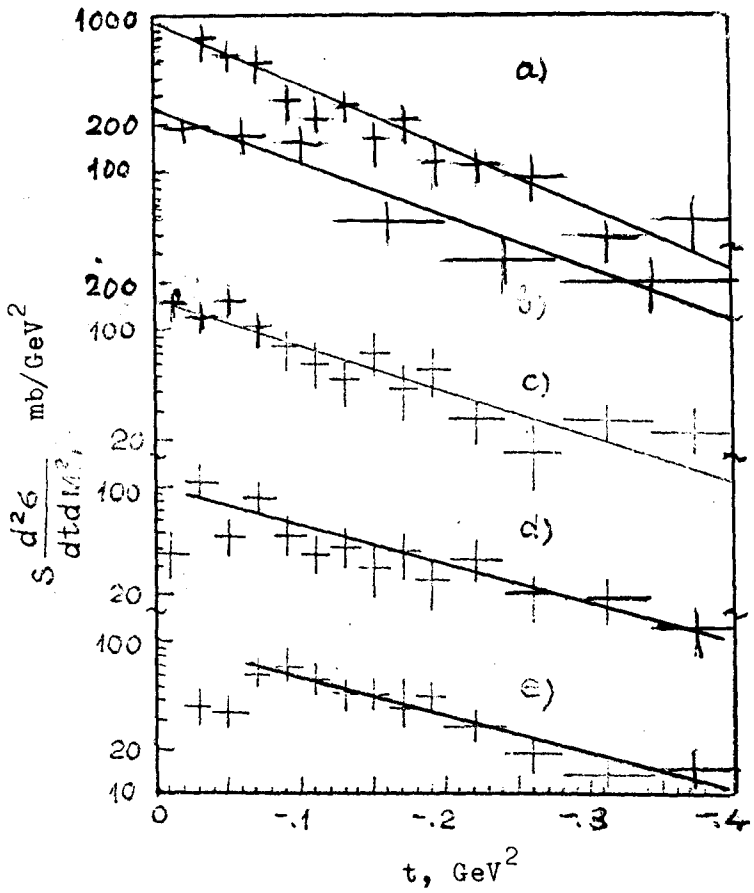

Fig. 3.5. Invariant cross-section of the pp-pX process as a function of t for different cross-sections of M^2 at 205 GeV/c [58]. The straight lines correspond to the analysis in the form of A_{exp} (in t).

a) $M^2 < 5$ GeV^2, $b = 9.1 \pm 0.7$ GeV^{-2}.
b) $5 \leqslant M^2 < 10$ GeV^2, $b = 8.0 \pm 1.1$ GeV^{-2}.
c) $10 \leqslant M^2 < 25$ GeV^2, $b = 6.1 \pm 0.7$ GeV^{-2}.
d) $25 \leqslant M^2 < 50$ GeV^2, $b = 5.8 \pm 0.7$ GeV^{-2}.
e) $50 \leqslant M^2 < 100$ GeV^2, $b = 5.8 \pm 0.6$ GeV^{-2}.

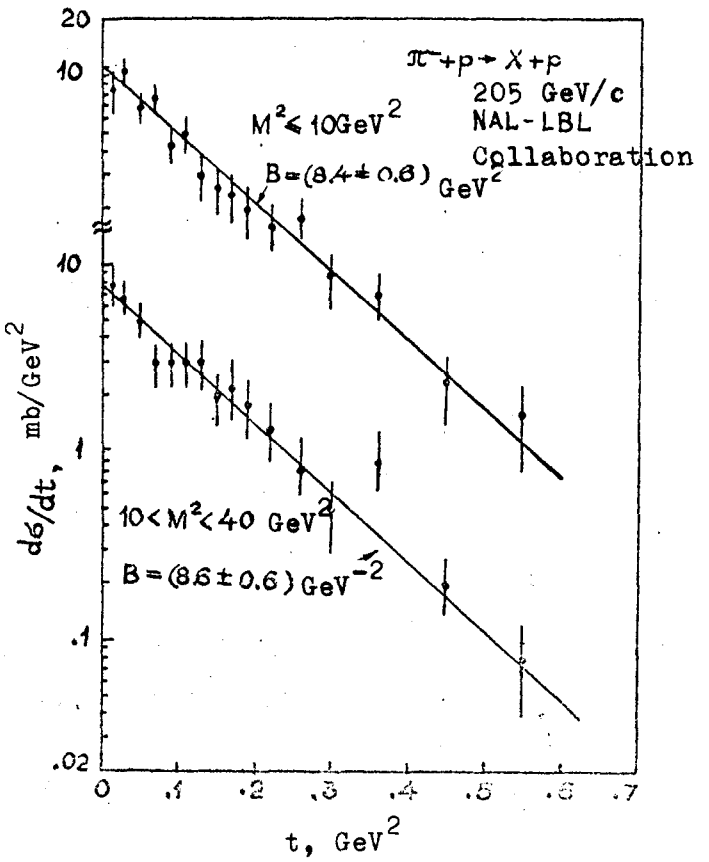

Fig. 3.6. Inclusive cross-section $d\sigma/dt$ of the $\pi^- p \to Xp$ reaction at 205 GeV/c [57] as a function of t for two intervals over M2: $M^2 \leq 10\ GeV^2$ and $10 < M^2 < 40\ GeV^2$.

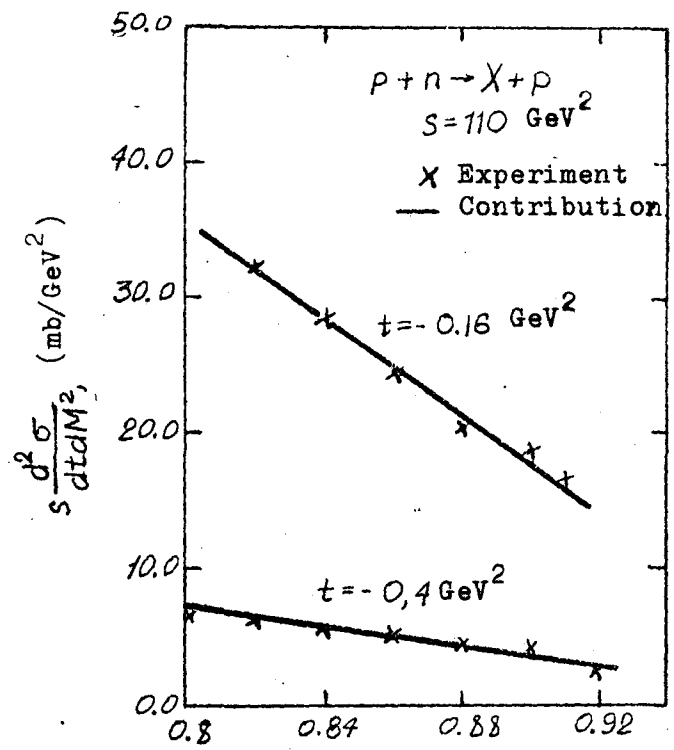

Fig. 3.7. Batavia data for proton spectra in the $p + n \longrightarrow X + p$ reaction at $S = 110$ GeV^2. The straight lines correspond to the contribution of $\pi\pi p$ /60/.

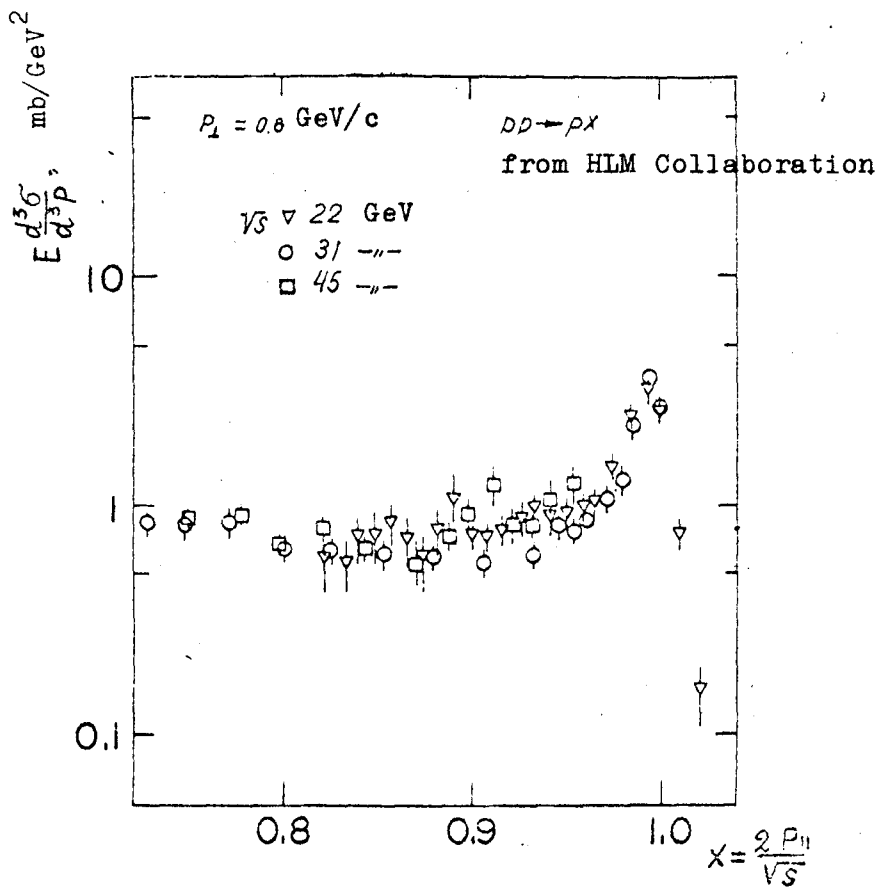

Fig. 3.8. Inclusive cross-sections of protons in the $pp \to pX$ reaction at $P_\perp$ = 0.8 GeV/c for 3 ISR energies /61/.

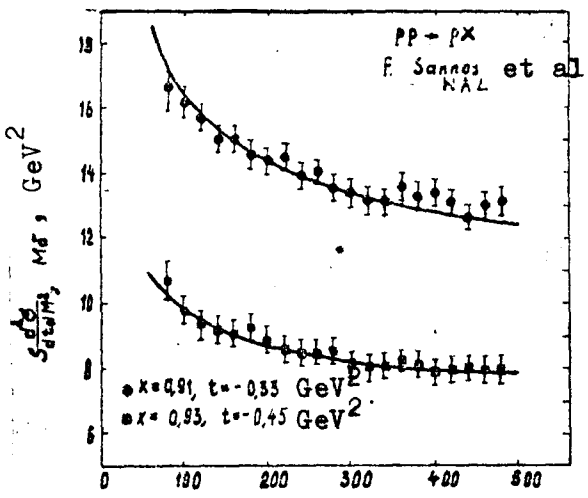

a)

Group: Rutgers-Imperial College

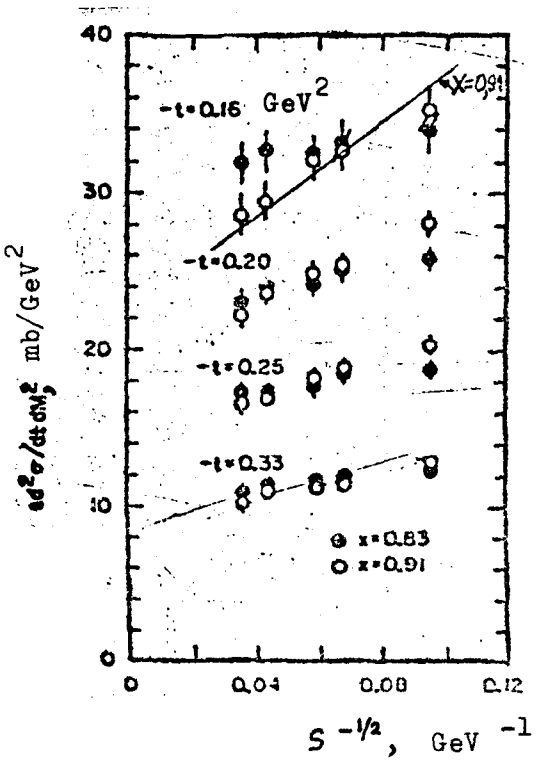

b)

Fig. 3.9. Proton spectra at fixed X, t as a function of energy /55/. The curves show the results of the analysis of /62/. The curves were normalized within the limits of the general normalization error quoted by the authors of /55/.

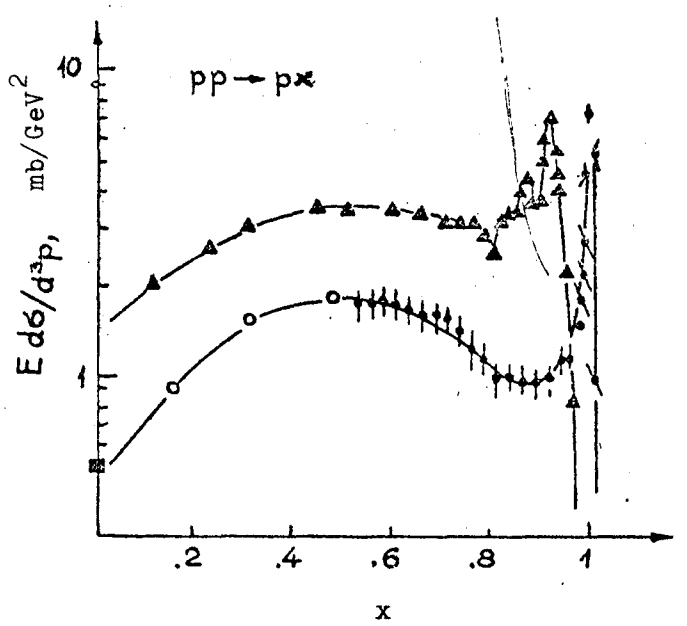

▲ Allaby et al.
$\sqrt{s}$ = 6.7 GeV, $p_\perp$ = 0.6 GeV/c

● CHLM Coll. ○ BC Coll.
$\sqrt{s}$ = 30, $p_\perp$ = 0.72 GeV/c

Fig. 3.10. Comparison of proton spectra as functions of X at $\sqrt{s}$ = 30 GeV [56] (ISR) and at $\sqrt{s}$ = 6.7 GeV [63] (PS, CERN).

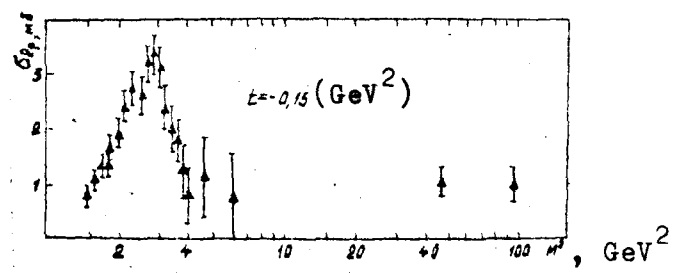

Fig. 3.11. Total interaction cross-section of a proton with a pomeron at t = -0.15 GeV^2 /62/.

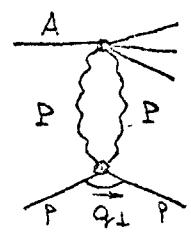

Fig. 3.12.

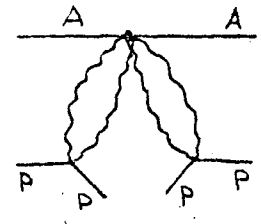

Fig. 3.13.

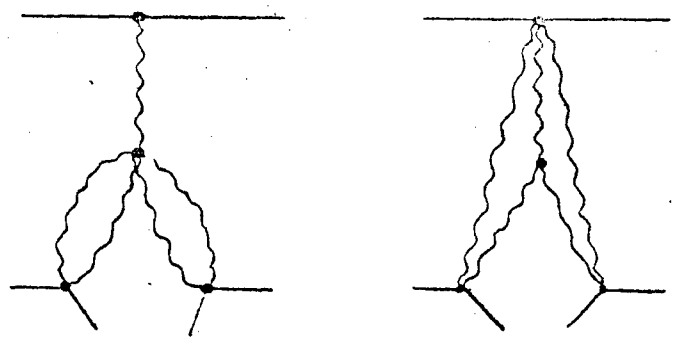

Fig. 3.14.

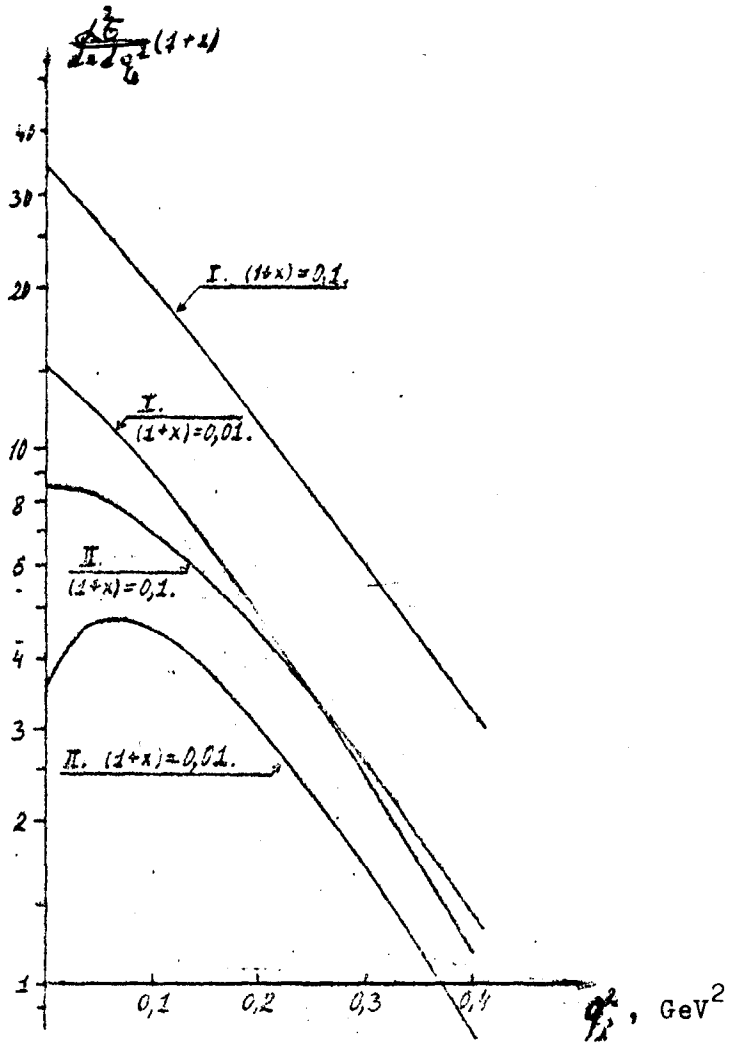

Fig. 3.15. Expected behaviour of the value $(1+X)\frac{d\sigma^2}{dx\,dq_t^2}$ in the three.Reggeon region ($X \longrightarrow -1$) in a model which takes into account the exchange of pomeron (Fig. 3.36) and two-pomeron cut (Fig. 3.14a, b, formula (3.12)). The curves I are calculated on the assumption that the relative contribution of the cut d = 1; curves II: d = 1/2.

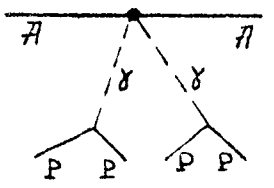

Fig. 3.16.

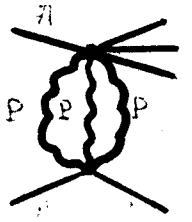

Fig. 4.1.

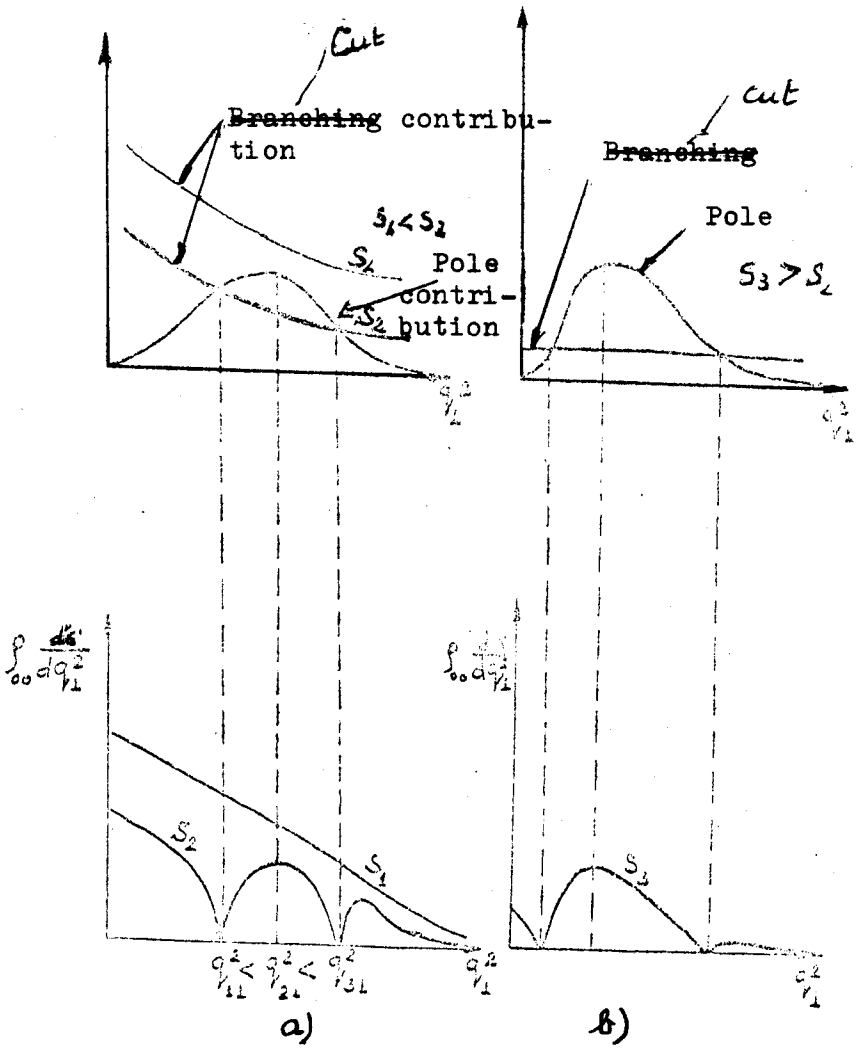
Cut
Branching contribution
$s_1 < s_2$
s_1
Pole
contribution
s_2
$q^2_{\gamma_1}$
cut
Branching
Pole
$s_3 > s_2$
$\int_0^\infty \frac{d\sigma}{dq^2_{\gamma_1}}$
s_2
s_1
$q^2_{\gamma_{11}} < q^2_{\gamma_{21}} < q^2_{\gamma_{31}}$
a)
b)

Fig. 4.2.

a)

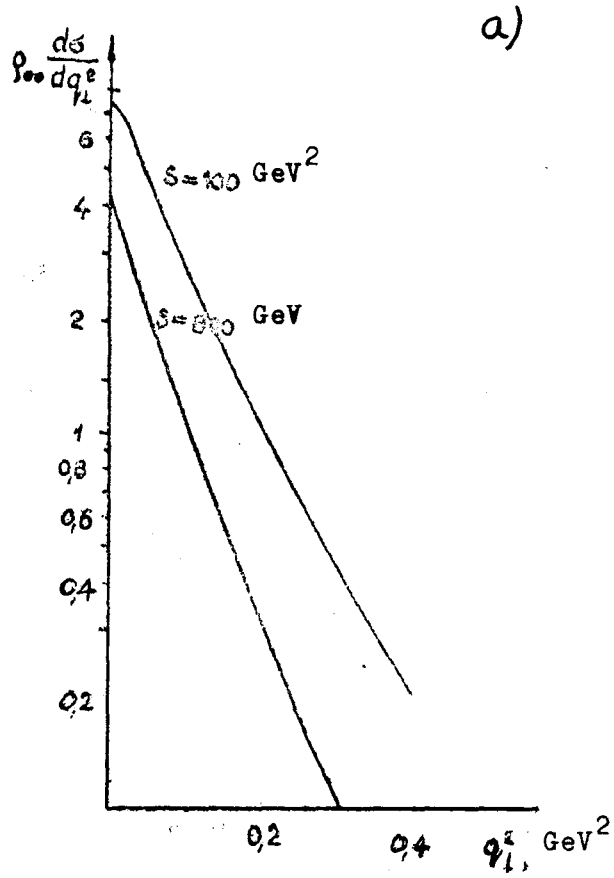
$\rho_\infty \frac{d\sigma}{dq_1^2}$
6
4
2
1
0,8
0,6
0,4
0,2
S=100 GeV^2
S=400 GeV
0,2
0,4
q_1^2, GeV^2

b)

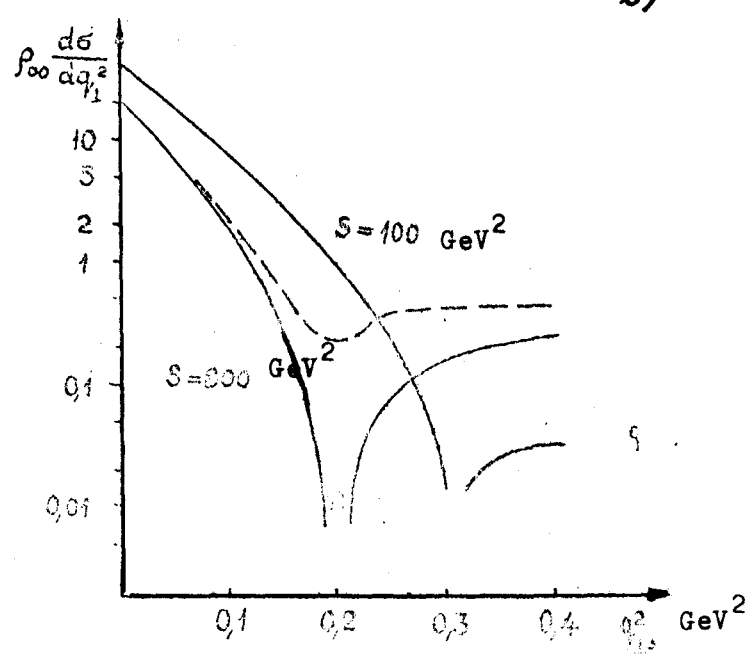
$\rho_\infty \frac{d\sigma}{dq_1^2}$
10
5
2
1
0,1
0,01
S=100 GeV^2
S=400 GeV^2
0,1
0,2
0,3
0,4
GeV^2

Fig. 4.3a, b.

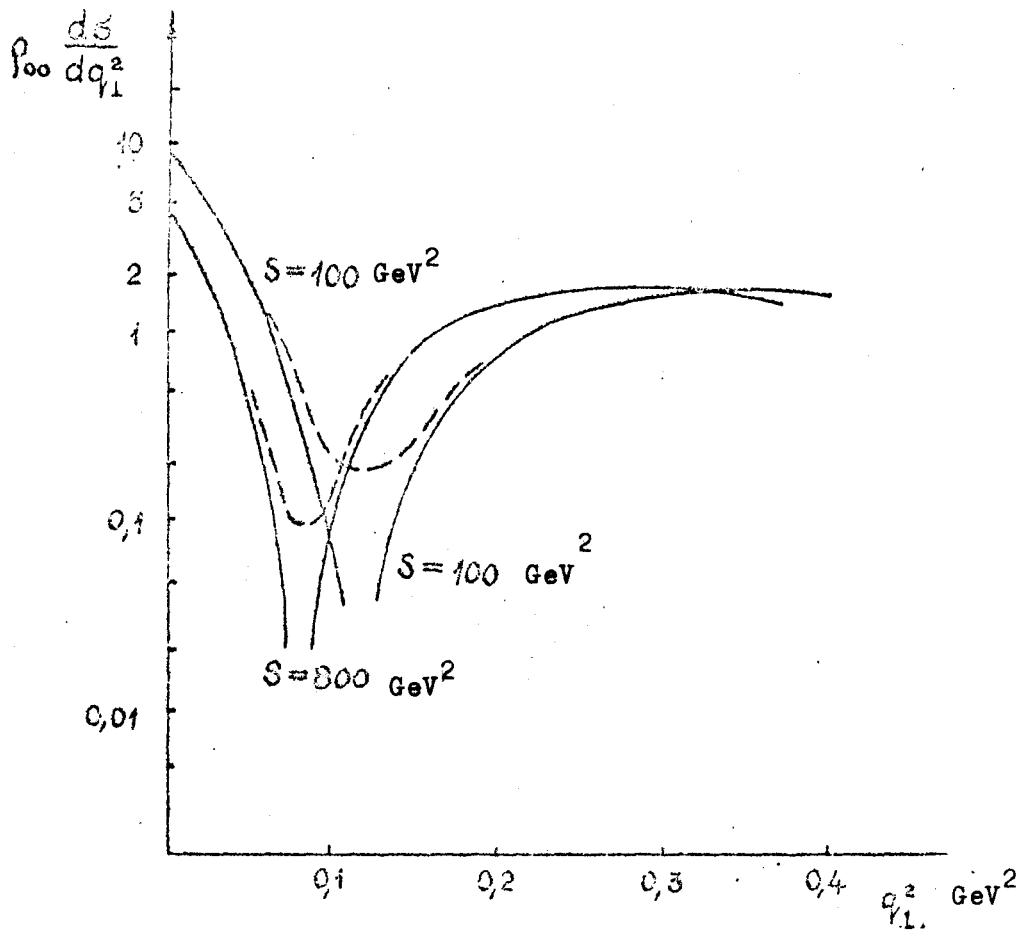

Fig. 4.3. Expected dependence on q_1^2 of an element of the density matrix $\rho_{00}\frac{d\sigma}{dq^2 y_4}$ (in the system of S-channel helicity) for the reaction $\pi + He \to A_1 + {}^4He$ in a model which takes into account the exchange of a pomeron, and two-pomeron cut (4.2.);
a) relative value of the cut contribution d = 1;
b) d = 1/2; c) d = 1/2.
The continuous lines correspond to the contributions only of the imaginary part of the production amplitude A_1 in the cross-sections.
The dashed lines represent the expected $\rho_{00}\frac{d\sigma}{dq_1^2}$ taking into account both the imaginary and real parts of the amplitude.

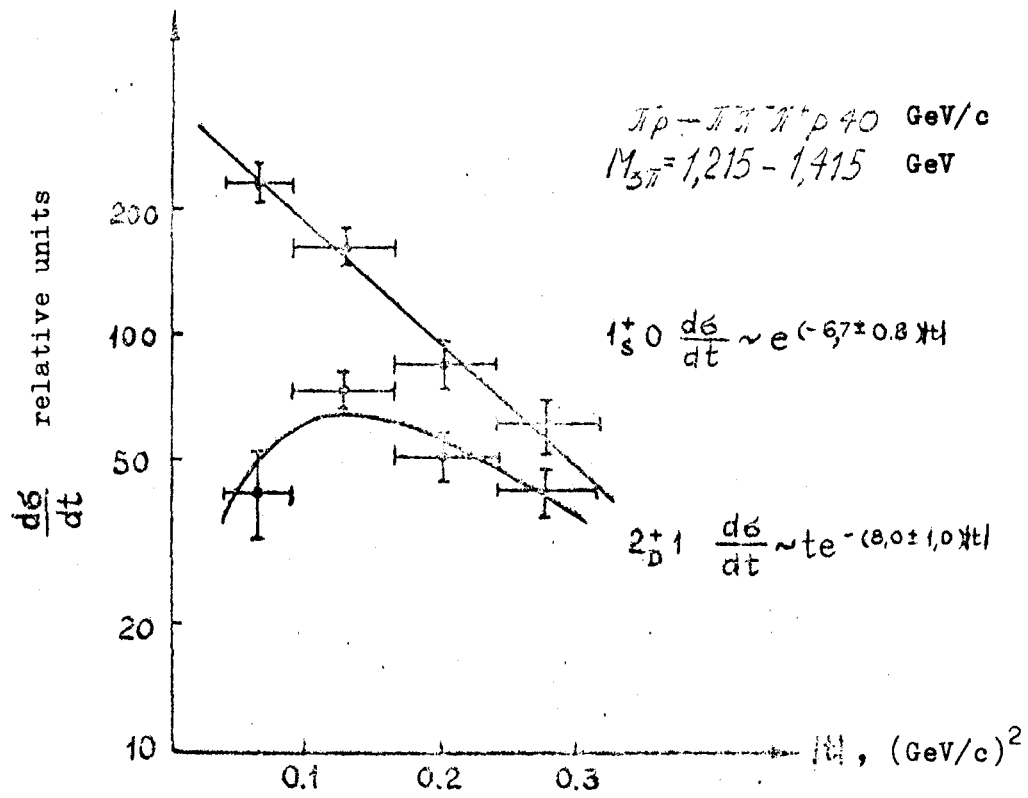

Fig. 4.4. Differential corss-sections of the diffraction excitation of a pion in the system of 3-X π - mesons with quantum figures $1^+_S\ 0(A_1)$ and $2^+_b\ 1(A_2)$ /67/.

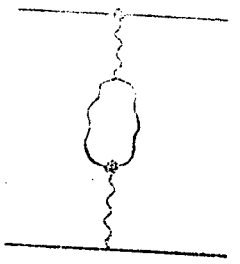

Fig. 4.5.

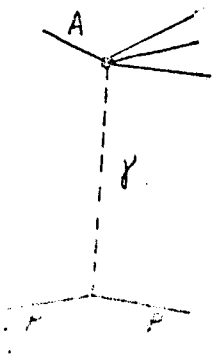

Fig. 4.6.

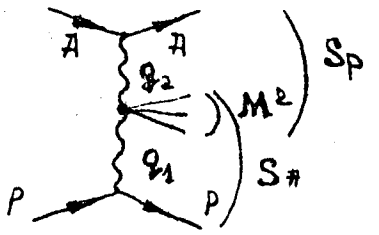

Fig. 5.1.

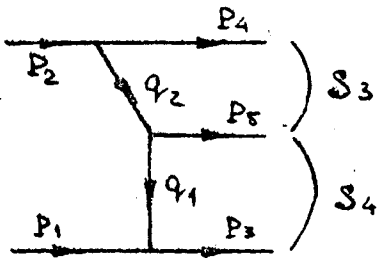

Fig. 5.2.

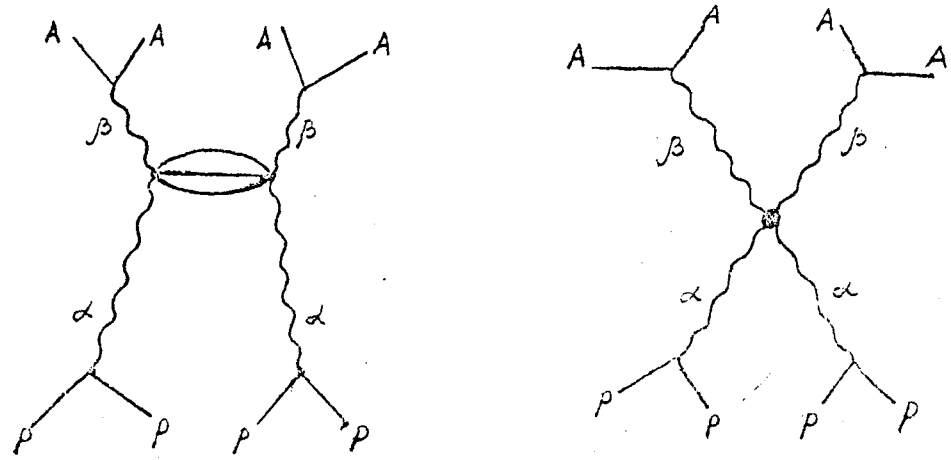

Fig. 5.3.

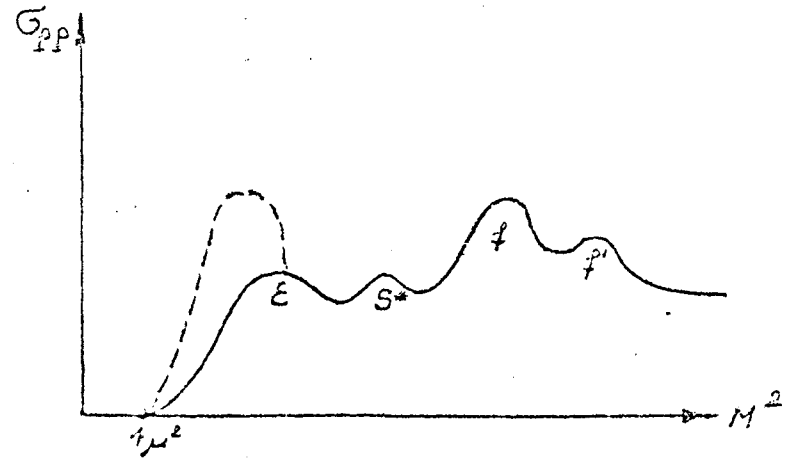

Fig. 5.4.

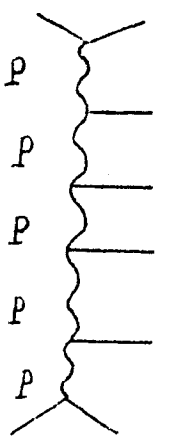

Fig. 5.5.

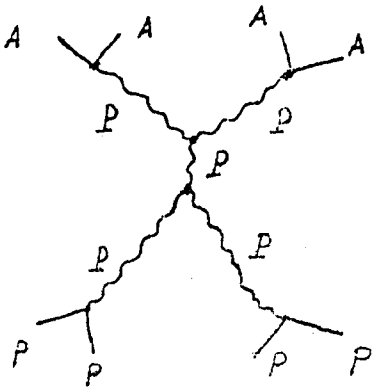

Fig. 5.6.

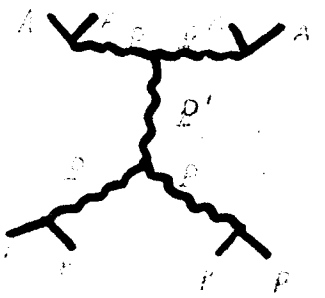

Fig. 5.7.

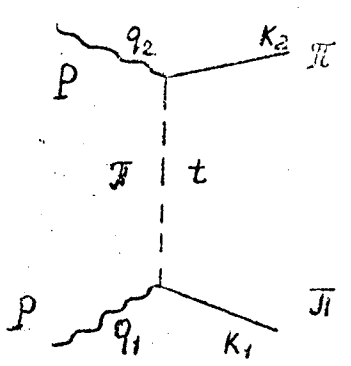

Fig. 5.8.

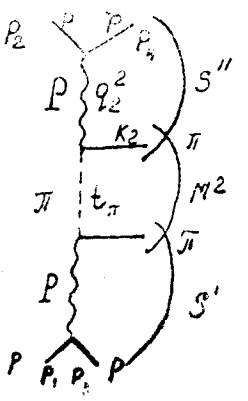

Fig. 5.9.

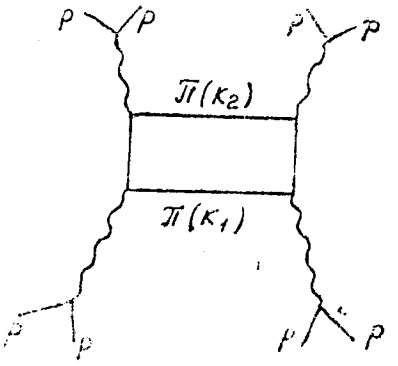

Fig. 5.10.

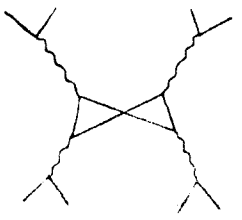

Fig. 5.11.

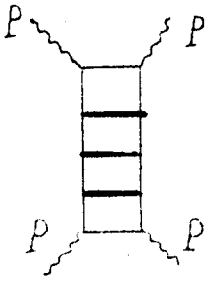

Fig. 5.12.

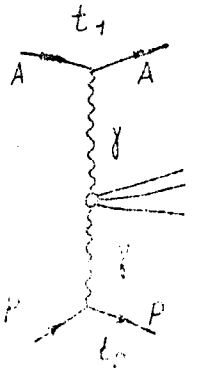

Fig. 5.13.

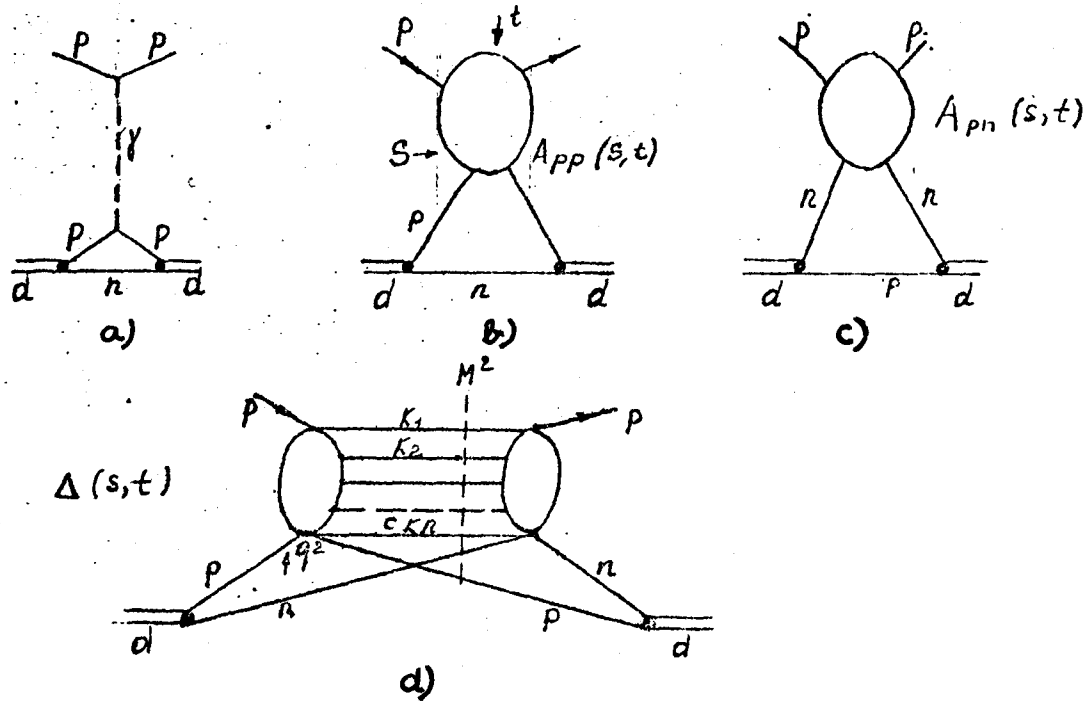
p
p
γ
p
p
d
n
d
a)
p
t
S
$A_{pp}(s,t)$
p
d
n
d
b)
p
p
$A_{pn}(s,t)$
n
n
d
p
d
c)
M^2
$\Delta(s,t)$
p
p
K_1
K_2
c.K.n.
q^2
p
n
n
p
d
d
d)

Fig. 6.1.

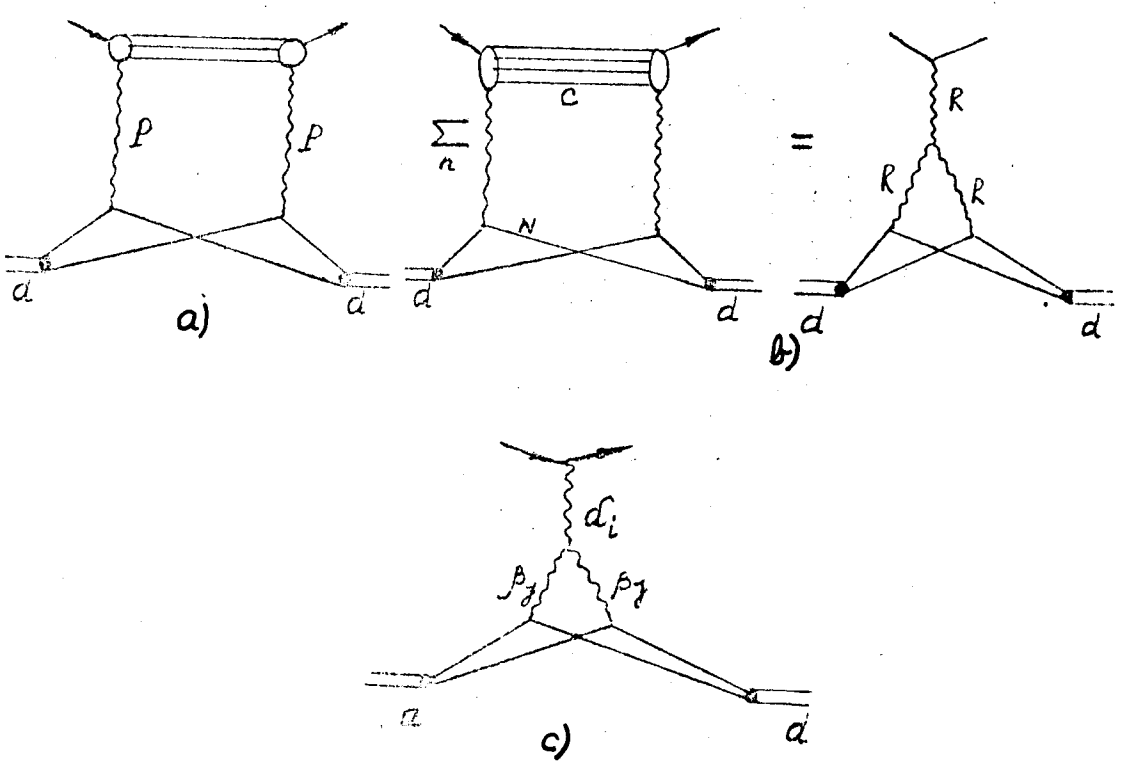

Fig. 6.2.

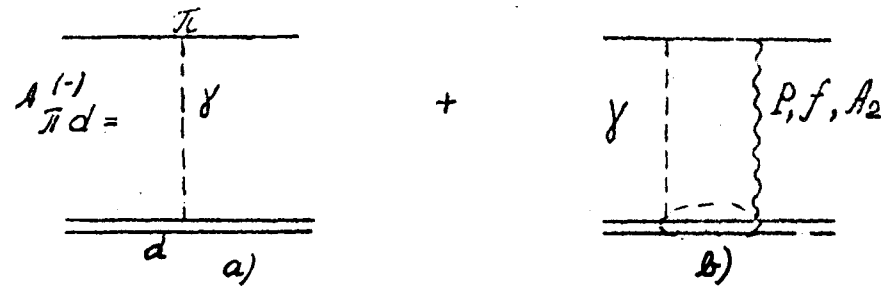

Fig. 6.3.

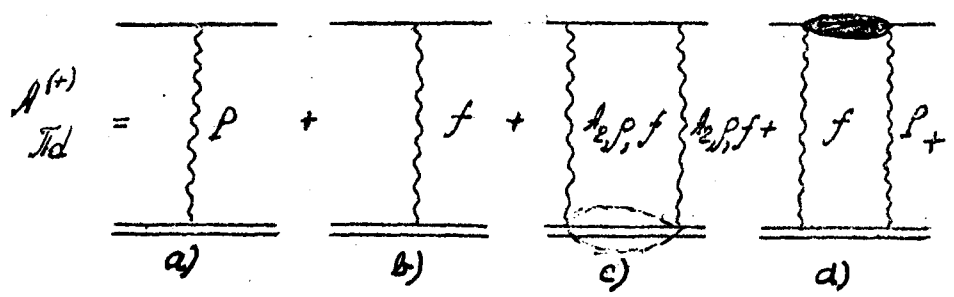

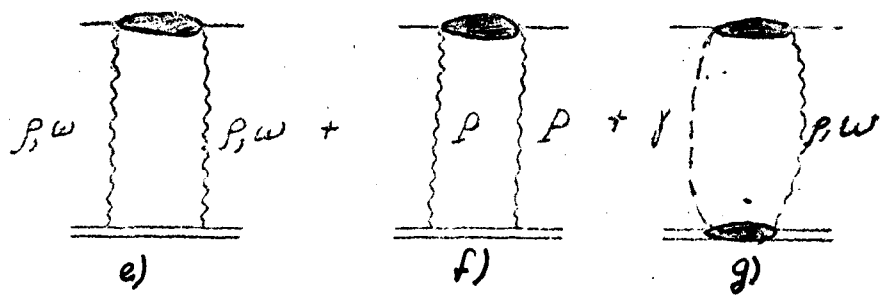

Fig. 6.4.

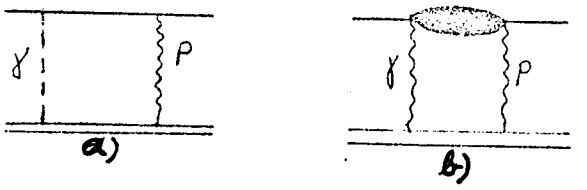

Fig. 6.5.

References

1. A.A. Vorob'ev et al. Preprint FTI-429, Leningrad, 1972.

2. V.N. Gribov. "Questions of Elementary Particle Physics", Erevan, pp. 178, 204 and 373, 1962.
   K.A. Ter-Martirosyan. "Interaction at high energy", Preprint ITEP-417, 1967.
   V.N. Gribov. Lectures on the theory of complex moments, Khar'kov, FTI AN SSSR, 1970.

3. I.T. Dyatlov. Material for the Fifth Winter School of the FTI on Nuclear Theory and High Energy Physics, Part I, p. 94, Leningrad, 1970.
   K.A. Ter-Martirosyan. Material for the Sixth Winter School of the FTI on Nuclear Theory and High Energy Physics, Part II, p.334, Leningrad, 1971.

4. V.N. Gribov. Material for the Eighth Winter School of the LNPI on Nuclear Physics and Elementary Particles, Part II, p. 5, Leningrad, 1973.

5. A.A. Ansel'm. Loc. cit. p. 37.

6. R.P. Feyman. "Proton - Hadron Interactions", W.A. Benjamin, Inc. 1972.

7. D.R.O. Morrison. "Review of quasi two-body reactions", ITP-71--66E, Kiev, 1971.

8. Yu.M. Antipov et al. Nucl. Phys., B57, 333 (1973).

9. D.W.G.S. Leith, SLAC-PUB-1141, October 1972.

10. V.A. Kudryavtsev, E.M. Levin, A.A. Shchipalin. Ya. F., 9, 1274, 10, 148 (1969).

11. G.Giacomelli. "Rapporteur's talk at the 16-th International Conference on High-Energy Physics", Batavia, September 1972.

12. V.N. Gribov. ZhETF, 53, 654 (1967).

13. V.N. Gribov. Ya. F., 5, 197 (1967).

14. V.N. Gribov, A.A. Migdal. Ya. F., 8, 1002, 1213 (1968).

15. Ya.I. Azimov, V.A. Khoze. Material for the 8-th Winter School of the LNPI on Nuclear Physics and Elementary Particles, Part II, 101, Leningrad, 1973.

16. K.A. Ter-Martirosyan. "Binary reactions of hadrons at high energies", p.466, Dubna, 1972.

17. V. Bartenev et al. Preprint NAL-PUB-73/73-EXP. 7100. 036., Phys. Rev. Lett., (to be publ.).

18. A.B. Kajdalov. Ya. F., 10, 619 (1969).

19. E.N. Levin. UFN, III, 29 (1973). Material for the Fifth Winter School of FTI on Nuclear Physics and High-Energy Physics, Part I, 114, Leningrad, 1970.

20. A.B. Kajdalov, B.M. Karnakov. Ya. F., 7, 1147 (1968).
M.H. Ross, P.S. Henyey, G.L. Kane. Nucl. Phys., B23, 269 (1972).

21. V.A. Abramovskij, O.V. Kancheli. ZhETF (Letters), 15, 559 (1972).

22. V.A. Abramovskij, V.N. Gribov, O.V. Kancheli. Ya. F., 18, 595 (1973).

23. M. Jacob. Preprint TH-1683-CERN, 1973, TH-1570-CERN, 1972, TH-1639-CERN, 1973.

24. K.A. Ter-Martirosyan. Phys. Lett., 44B, 377 (1973).

25. E.M. Levin, M.G. Ryskin. ZhETF (Letters), 18, 654 (1973).

26. V.A. Abramovskij, O.V. Kancheli, S.G. Matinyan. Phys. Lett., 36B, 565 (1971).

27. V.N. Gribov. Ya. F., 17, 603 (1973).

28. K.A. Ter-Martirosyan. ZhETF, 44, 341 (1963).
K.A. Verdiev, O.V. Kancheli, S.G. Matinyan, A.M. Popova, K.A. Ter-Martirosyan. ZhETF, 46, 1700 (1964).

29. V.N. Gribov, I.Ya. Pomeranchuk, K.A. Ter-Martirosyan. Phys. Lett., 9, 369 (1964), 12, 153 (1964).

30. G.G. Beznogikh et al. Phys. Lett., 39B, 411 (1972).

31. U. Amaldi et al. Phys. Lett., 43B, 231 (1973).

32. G.G. Beznogikh et al. Nucl. Phys., B54, 97 (1973).

33. K.J. Foley et al. Phys. Rev. Lett., 19, 857 (1967).

34. J.R. Campbell et al. Nucl. Phys., (to be publ.), CERN/D.Ph/II/ Phys. 73-21.

35. U. Amaldi. Rapporteur's talk at the 2-nd Aix-en-Provence Intern. Conf. on Elementary Particles, September 1973.

36. K.A. Ter-Martirosyan. Material for the Sixth Winter School on Nuclear Theory and on High-Energy Physics, Part I, p. 155, Leningrad (1971).

37. V.B. Kopeliovich, Ya. F. 18, 406 (1973).

38. A.A. Vorob'ev et al. Phys. Lett., 41B, 639 (1972).

39. G. Barbiellini et al. Phys. Lett., 39B, 663 (1972).

40. E.M. Levin, L.L. Frankfurt, UFN, 94, 243 (1968).

41. L.L. Frankfurt. Material for the 4th Winter School on Nuclear Theory and High Energy Physics, Part I, p. 226, Leningrad, 1969.

42. C.N. Brown et al. Phys. Rev. Lett., 26, 991 (1971).

43. A.A. Ansel'm, V.N. Gribov. Phys. Lett., 40B, 487 (1972).

44. K.A. Ter-Martirosyan. Phys. Lett., 41B, 621 (1972).

45. A.R. Dzierba et al. Phys. Rev., 70, 725 (1973).

46. R.A. Carrigan. Phys. Rev. Lett., 24, 168 (1970).

47. E.L. Berger, G.C. Fox. Nucl. Phys., B26, 1 (1971).
G.E. Hita. Rev. Mod. Phys., 41, 669 (1969).
P.D.B. Collins. Phys. Rept., 1C, N4 (1971).
D.V. Shirkov. UFN, 102, 98 (1970).
G. Gidal. Preprint LBL-352, September 1971.

48. L. Caneschi, A. Pignotti. Phys. Rev. Lett., 22, 1219 (1969).

49. A. Capella, Min-Shih Chen. Preprint SLAC-PUB-1252, May 1973.
D. Amati, L. Caneschi, M. Ciafaloni. Preprint CERN-TH-1676, 1973.

50. A.B. Kajdalov, V.A. Khoze, Yu.F. Pirogov, N.L. Ter-Isaakyan. Phys. Lett., 45B, 493 (1973).
A.B. Kajdalov. Material for the 8th Winter School of the LNPI on Nuclear and Elementary Particle Physics, Part II, p. 83, Leningrad, 1973.

51. C. Quigg, L.L. Wang. Phys. Lett., 43B, 314 (1973).

52. M.G. Albrow et al. Nucl. Phys., B51, 388 (1973), B54, 6 (1973).

53. T.C. Sens. Invited report to the Conference on Recent Advances in Particle Physics, USA, 1973.

54. M.G. Albrow et al. CERN Preprint, September 1973, Submitted to Nucl. Phys.

55. F. Sannes et al. Phys. Rev. Lett., 30, 766 (1973).
K. Abe et al. Paper submitted to the APS Meeting, Berkeley, 1973.

56. L. Föa. Rapporteur's talk at the 2-nd Aix-en-Provence Int. Conf. on Elementary Particles, Aix-en-Provence, 1973.

57. F.C. Winkelman et al. Preprint LBL-2113, 1973.

58. S.J. Barish et al. Preprint AHL/HEP-7338, 1973.

59. K.G. Boreskov, A.B. Kajdalov, L.A. Ponomarev. Lectures to the ITEF School of Physics, 1973.

60. M. Bishari. Preprint LBL-2066, UC-34d, 1973.

61. E.L. Berger. Preprint CERN TH-1737-CERN.
M. Jacob. Lecture at 1973 CERN/JINR School of Physics, 1973.

62. A.B. Kajdalov, Yu.F. Pirogov, N.L. Ter-Isaakyan, V.A. Khoze. Letters to the ZhETF, 17, 626 (1973).

63. J.V. Allaby et al. Nucl. Phys., B52, 316 (1973).

64. H.D.I. Abarbanel, V.N. Gribov, O.V. Kancheli. Preprint NAL-THY-76, August 1972.
H.D.I. Abarbanel, S.D. Ellis, M.V. Green, A. Zee. Preprint NAL-THY, April 1972.

65. G. Ascoli et al. Phys. Rev. Lett., 26, 929 (1971).

66. J.W. Lamsa et al. Nucl. Phys., B37, 364 (1972).
J.V. Beaupre et al. Nucl. Phys., B47, 51 (1972).

67. Yu.M. Antipov et al. Nucl. Phys., B63, 153 (1973).

68. F.Halzen, C. Michael. Phys. Lett., 36B, 367 (1972).
A. de Lesquen et al. Phys. Lett., 40B, 277 (1972).
G. Cozzika et al. Phys. Lett., 40B, 281 (1972).

69. V.N. Bolotov et al. Ya. F. 18, 1046 (1973).

70. B.Bartenev et al. (to be published).

71. J.V. Allaby et al. Nucl. Phys., B52, 316 (1973).
E.W. Anderson et al. Phys. Rev. Lett., 16, 855 (1966).
R.M. Edelstein et al. Phys. Rev., 5D, 1073 (1972).

72. A.A. Migdal, A.M. Polyakov, K.L. Ter-Martirosyan. "Theory of interacting pomeron", Preprint L.D. Landau Inst. for Theor. Phys., Ya. F. (in course of publication), 1974.

73. H.D.I. Abarbanel, G.F. Chew, M.L. Goldberger, L.M. Saunders. Phys. Rev. Lett., 26, 937 (1971).

74. A.B. Kajdalov. Lectures at the First School of Physics of ITEF, 1973.

75. K.A. Ter-Martirosyan. Report to the Second International Conference on High Energy Physics, Geneva, 1962, ZhETF, 44, 341 (1963).
T.W.B. Kibble. Phys. Rev., 131, 2282 (1963).

76. D.Z. Freedman, C.E. Jones, F.E. Low, J.E. Joung. Phys. Rev. Lett., 26, 1197 (1971).
K.A. Ter-Martirosyan, Yu.M. Shabel'skij. Letters to the Zh. E.T.F.,15, 154 (1972).

77. R. Lipes, G. Zweig, W. Robertson. Phys. Rev. Lett., 22, 433, (1969).

78. J.V. Beaupre et al. Nucl. Phys., B46, 1 (1972).

79. U. Idschok et al. Nucl. Phys., B53, 282 (1973).

80. V. Blobel et al. Preprint DESY 73/37, August 1973.

81. M. Derrick et al. Submitted to Phys. Rev. Lett., 1974.

82. A.B. Kajdalov, K.A. Ter-Martirosyan. Nucl. Phys. (to be publ.), 1974.

83. K.G. Boreskov, A.B. Kajdalov et al. Ya. F., 15, 361 (1972); 17, 1285 (1973).

84. K.G. Boreskov, A.B. Kajdalov, L.A. Ponomarev. Lectures to the First School of Physics of the ITEF, 1973.

85. R.J. Glauber. Phys. Rev., 100, 242 (1955).

86. V.N. Gribov. ZhETF, 88, 892 (1968).

87. O.V. Kancheli, S.G. Matinyan. Ya. F., 11, 1305 (1970).

88. V.V. Anisovich. Material for the Eighth Winter School of the LINP on Nuclear and Elementary Particle Physics, Part I, p. 51, Leningrad, 1973.

89. J. Pumplin, M. Ross. Phys. Rev. Lett., 21, 1778 (1968).

90. V.N. Gribov, E.M. Levin. Ya. F., (in course of publication), 1974.

91. V.B. Kopeliovich. Ya. F., 18, 408 (1973).
A.A. Kondratyuk, V.B. Kopeliovich. Ya. F., 13, 600 (1971).

92. V.M. Kolybasov, M.S. Marinov. UFN, 109, 137 (1973).

93. H. Bethe. Ann. Phys., (N.Y.), 3, 190 (1958).

94. G.B. West, D.R. Yennie. Phys. Rev., 172, 1413 (1968).

******